



**CHEMISTRY OF GEOTHERMAL FLUIDS  
DURING PRODUCTION AND DISPOSAL:  
CALCITE SCALING IN YANGBAJING,  
SVARTSENGI AND HVERAGERDI**

**Yu Heping**

**Geothermal Training Programme  
Reykjavík, Iceland  
Report 17, 1987**

Report 17, 1987

CHEMISTRY OF GEOTHERMAL FLUID DURING PRODUCTION AND  
DISPOSAL: CALCITE SCALING IN YANGBAJING, SVARTSENGI  
AND HVERAGERDI

Yu Heping  
UNU Geothermal Training Programme  
National Energy Authority  
Grensásvegur 9  
108 Reykjavík  
ICELAND

Permanent Address:  
Bureau of Industry and Electric Power of  
Xizang (Tibet) Autonomous Region  
Lhasa, Tibet  
PEOPLE'S REPUBLIC OF CHINA



## ABSTRACT

Problems associated with the chemical behaviour of geothermal fluids in production and disposal processes have constituted technical and economical barriers to the development and utilization of geothermal energy resources in many countries. One of these problems is mineral scaling when the fluids become supersaturated due to changes in physical and chemical conditions. The thermodynamics of calcite scaling in water-dominated geothermal wells are reviewed. Two conceptual mechanisms for calcite deposition are discussed. The handling methods for calcite scaling in production wells are summarized. The WATCH computer program which models the chemical behaviour of geothermal fluids is used for interpreting data from the Yangbajing, Svartsengi and Hveragerði geothermal areas and for predicting their calcite scaling potential. The results show that calcite deposition is most severe for the geothermal fluid which has the highest ionic strength and the lowest reservoir temperature. Sampling equipment and procedures for geothermal wells and chemical analysis methods are outlined as used for wells in Svartsengi and Hveragerði. Finally, the problems related to chemistry and tracer testing in geothermal injection are reviewed.



## TABLE OF CONTENTS

ABSTRACT . . . . .	iii
TABLE OF CONTENTS . . . . .	v
LIST OF TABLES . . . . .	vii
LIST OF FIGURES . . . . .	viii
1. INTRODUCTION . . . . .	1
2. PROCESSES AND PROPERTIES . . . . .	3
2.1. Geothermal Power Processes . . . . .	3
2.2. Physical Properties . . . . .	3
2.2.1. Pressure in Wellbore . . . . .	4
2.2.2. Steam Fraction . . . . .	8
2.3. Two Phase Flow Regimes . . . . .	8
2.4. Chemistry . . . . .	10
3. SAMPLING AND CHEMICAL ANALYSIS . . . . .	13
3.1. Sampling of Water-Dominated Wells . . . . .	13
3.2. Chemical Analysis Techniques . . . . .	15
4. THERMODYNAMICS AND KINETICS OF CALCITE SCALING . . . . .	19
4.1. System Studied . . . . .	19
4.2. Thermodynamics . . . . .	20
4.2.1. Equilibrium Consideration . . . . .	20
4.2.2. Effect of Ion-Strength . . . . .	25
4.2.3. Effect of Steam Loss . . . . .	26
4.2.4. Calculation of pH of Geothermal Fluid . . . . .	26
4.2.5. Effect of Degassing . . . . .	28
4.2.6. Effect of Temperature and $P_{CO_2}$ . . . . .	29
4.3. Kinetics . . . . .	30
4.3.1. General . . . . .	30
4.3.2. Deposition Models . . . . .	32

5. THE CHEMICAL EQUILIBRIUM PROGRAM WATCH . . . . .	38
5.1. Introduction . . . . .	38
5.2. Program Description . . . . .	38
5.3. Yangbajing, Svartsengi and Hveragerði Fields .	39
5.4. Chemical Data Treatment . . . . .	40
5.5. Result . . . . .	43
6. HANDLING OF CALCITE SCALING IN WELLBORE . . . . .	44
6.1. Mechanical Removal . . . . .	44
6.2. Pressure Manipulation . . . . .	45
6.3. Partial Pressure Control . . . . .	45
6.4. pH Manipulation . . . . .	46
6.5. Inhibitors . . . . .	46
6.6. Others . . . . .	47
7. FLUID INJECTION . . . . .	48
7.1. Fluid/Formation Compatibility . . . . .	48
7.2. Precipitation Avoidance and Acceleration . . .	49
7.3. Chemical Monitoring and Tracer Testing . . . .	51
8. CONCLUSIONS . . . . .	54
ACKNOWLEDGEMENT . . . . .	56
NOMENCLATURE . . . . .	57
REFERENCES . . . . .	59
APPENDIX 1 Computer Output for Separated Samples From Wells ZK-309, ZK-311, ZK-324, NLFI-1 and SG-8	64
APPENDIX 2.1 Computer Output for Downhole Sample of Well ZK-323 . . . . .	83
APPENDIX 2.2 Computer Output for Calibration of the Downhole Sample from Well ZK-323 . . . . .	87
APPENDIX 2.3 Computer Output for the Calibrated Downhole Sample . . . . .	89

## LIST OF TABLES

Table 2.1	Chemical Composition of Typical Geothermal Waters . . . . .	92
Table 2.2	Summary of the Chemical Equilibria Controlling the Composition of Geothermal Fluid . .	93
Table 2.3	Equations Describing the Temperature Dependence of Cation/Proton Ratios and Undissociated Weak Acid Concentrations in Geothermal Well Discharge . . . . .	94
Table 3.1	Analysis of Geothermal Waters with AAS . . .	95
Table 4.1	Equations Expressing the Temperature Dependence of Equilibrium Constants in CaO-CO <sub>2</sub> -H <sub>2</sub> O System . . . . .	96
Table 4.2	Ionic Strength of Typical Geothermal Waters .	97
Table 4.3	Aqueous Species for Proton Mass Balance and Alkalinity Equations . . . . .	98
Table 5.1	Schematic Layout of the Function of WATCH Program . . . . .	99
Table 5.2	Input Data for WATCH Program . . . . .	100
Table 7.1	Effect of Process Parameters on Scale Formation . . . . .	101
Table 7.2	Factors affecting Silica Deposition Kinetics	102

## LIST OF FIGURES

Figure 1.1	Output Decay due to Scaling in Well, Svartsengi. . . . .	103
Figure 1.2	Formation of Calcite Deposition in Well 4 in Svartsengi . . . . .	104
Figure 2.1	Schematic Flow Diagram of Double Flashing System in Yangbajing Power Plant . . . . .	105
Figure 2.2	Flow Diagram of Svartsengi Power Plant (Björnsson and Albertsson, 1985) . . . . .	106
Figure 2.3	Flow Patterns of Vertical Two Phase Flow . . . . .	107
Figure 2.4	Flow Pattern Map for Vertical Two Phase Flow . . . . .	108
Figure 2.5	Flow Regimes in Horizontal Two Phase Flow . . . . .	109
Figure 2.6	Flow Pattern Map of Baker as Modified by Scott . . . . .	110
Figure 2.7	Relationship of the Product of Calcium and Carbonate Ion Concentrations with Temperature and Sodium Concentration in Equilibrium Reservoir Conditions . . . . .	111
Figure 2.8	Concentration Ranges for Elements in Geothermal Water . . . . .	112
Figure 3.1	Small Separator for Sampling of Geothermal Well . . . . .	113
Figure 3.2	Collection of Water Phase . . . . .	114
Figure 3.3	Collection of Condensate and Gases . . . . .	115
Figure 3.4	Collection of Vapor Phase into NaOH Solution . . . . .	116
Figure 3.5	Flow Chart for Comprehensive Sampling and Analysis of Geothermal Fluid . . . . .	117
Figure 3.6	Positions of Sampling Points on Surface Piping . . . . .	118
Figure 4.1	Aragonite-Calcite Phase Transition Diagram . . . . .	119
Figure 4.2	Stability Relations in $\text{Ca}^{2+}$ - $\text{Mg}^{2+}$ - $\text{CO}_2$ - $\text{H}_2\text{O}$ System . . . . .	120
Figure 4.3	Effect of Salt Concentration on Henry's Law Constant . . . . .	121
Figure 4.4	Fraction of Carbonate, Bicarbonate, Carbonic Acid and $\text{CO}_2$ Present as a Function of pH at 100°C . . . . .	122
Figure 4.5	Loss of Carbon Dioxide as Flash Progresses . . . . .	123

Figure 4.6	Solubility of Calcite in Water up to 300#C at Various Partial Pressures of Carbon Dioxide . . .	124
Figure 4.7	Plot of Free Energy of Precipitation vs Crystal Size Illustrating Nucleation and Growth . . .	125
Figure 4.8	Schematic Representation of Concentration in Solution as a Function of Radial Distance . . . . .	126
Figure 5.1	Difference Between Function and Output Values vs Gas Solubility Mutilplication Factor . . .	127
Figure 5.2	Calcite Activity Product for Samples from Yangbajing Geothermal Field . . . . .	128
Figure 5.3	Calcite Activity Product for Samples from Svartsengi Geothermal Field . . . . .	129
Figure 5.4	Calcite Activity Product for Samples from Hveragerði Geothermal Field . . . . .	130
Figure 5.5	Comparison of Calcite Activity Product for Samples from Yangbajing, Svartsengi and Hveragerði Geothermal Fields . . . . .	131
Figure 5.6	Ratio of Calcite Activity and Solubility Products for Samples from Yangbajing, Svartsengi and Hveragerði Geothermal Fields . . . . .	132
Figure 5.7	Difference of Calcite Solubility and Activity Products for Samples from Yangbajing, Svartsengi and Hveragerði Geothermal Fields . . . . .	133
Figure 6.1	Mechanical Cleaning Equipment in Yangbajing	134
Figure 6.2	Reaming of Scale in Svartsengi . . . . .	135
Figure 6.3	Sketch of a Plant for P <sub>CO2</sub> Control . . . . .	136
Figure 7.1	Types of Wellbore Impairment Caused by Suspended Solids . . . . .	137
Figure 7.2	Silica Solubility as a Function of pH . . . . .	138
Figure 7.3	Effect of Lime Treatment on Silica . . . . .	139
Figure 7.4	Metal Sulfides Solubility in Water as a Function of pH . . . . .	140
Figure 7.5	Solubility of Sulfides in Solution as a Function of Temperature . . . . .	141
Figure 7.6	Iodide Breakthrough Curve in Well 6, Svartsengi . . . . .	142



## 1. INTRODUCTION

The chemical behaviour of geothermal fluids is an important factor associated with its utilization. One of the most serious problems in exploiting water-dominated geothermal reservoir is the precipitation of various mineral scales due to changes in process chemistry and physics. Scaling in production and injection wells can significantly reduce flow-rates (Figure 1.1) and even block the wells. Flow-tests in Miravalles, Costa Rica, illustrated the time behaviour of wells suffering from wellbore deposition. At early time the decrease in output flow rate and well-head pressure is slow but at late time it becomes rapid (Granados and Gudmundsson, 1985). Deposition of minerals on energy production plant equipments and pipelines can cause costly downtime for removal and affect the heat transfer effectiveness. Scaling in major fissures in wells may result in a irreparable decay in flow.

There are three main types of scales from geothermal fluid that have been recognized. Calcium carbonate (mainly calcite) is encountered when flashing happens within geothermal wells. Siliceous compounds are confined mainly to spent brine discharged to atmosphere. Sulfates and sulfides are observed in the form of many phases usually well crystallized in production processes.

Geothermal reservoir fluids in Yangbajing (Xizang, China), Svartsengi and Hveragerði (Iceland) are invariably just saturated with respect to calcite under reservoir conditions. During the exploiting of those fluids, calcite scale forms in production wellbores. Thus, frequent or periodic cleaning of the wellbore is needed to maintain the output. Knowledge of calcite scaling is very important for managing this problem effectively.

In the literature, the thermodynamic aspects of calcite scaling have been studied extensively and some possible ways

to control this scaling have been suggested and tested in geothermal fields in which the problem appears. But information on kinetics is very limited, and so is the economics of handling.

Location and tendency of calcite deposition in a geothermal well can be measured by caliper logging (Figure 1.2) or estimated by computer modelling. This will make it easy for management and operation.

The credibility and usefulness of chemical data for chemical models depends on the sampling and analytical methods and the care taken in the collection and analysis of samples.

After eleven years of development and utilization of geothermal resources in Yangbajing, drawdown in the reservoir and the pollution associated with large scale exploitation are becoming serious problems. Injection of the spent brine can maintain the output of geothermal reservoir and prevent environmental effect. Fluid chemical behaviour and tracer testing can play important roles in successful geothermal injection.

Those all above are the some targets of my project work at UNU Geothermal Training Programme. The training included introduction courses, engineering and geochemical lectures, field excursion and sampling, literature search and data interpretation. This report is the final part of the training.

## **2. PROCESSES AND PROPERTIES**

### **2.1. Geothermal Power Processes**

The practical cycles used for geothermal energy extraction plants are various due to the nature of the resources, utilization purposes, technical and economical considerations etc.

Figure 2.1 shows a conceptual diagram of double flash geothermal power generation cycle in Yangbajing. Figure 2.2 is the flow diagram of combined thermal and electric power production cycle in Svartsengi (Björnsson and Albertsson, 1985).

In a geothermal multi-purpose power cycle, the temperature may vary from as high as 350°C in the reservoir to values approaching 15°C in disposal lines, and the pressure may ranges from 300 to 0.08 bar, while the chemical composition of the geo-fluids varies from almost pure water or steam to hot brine with 360,000 ppm of total dissolved solids. Thus, chemical behaviour of geothermal fluids are very site-specific with its thermodynamic conditions and fluid chemistry (Corsi, 1987).

### **2.2. Physical Properties**

Since geothermal brine are abundant of sodium chloride with smaller amounts of calcium, silica and potassium (Table 2.1), its physical parameters can be predicted from a knowledge of pure water and sodium chloride solutions, modified approximately according to the concentrations of other ions by using the term "equivalent NaCl content" with sufficient accuracy (Wahl, 1977). The "equivalent NaCl content" is the amount of NaCl in solution which gives the same effect on the properties as the amount of all salts combined (Michaelides, 1981). This assumption is supported by "quantity effect of salts" in aquatic solution. Non-condensable gases dissolved

in the fluid is an important factor affecting phase change. Release of gases such as CO<sub>2</sub>, H<sub>2</sub>S, H<sub>2</sub> and NH<sub>3</sub> results in boiling of geothermal brine at a higher pressure, or by lowering the flashing depth in a two phase flowing well.

Calcite scaling is promoted by boiling of geothermal fluid. Among the physical properties, pressure and enthalpy are the two most important factors affecting the boiling.

### 2.2.1. Pressure in Wellbore

When the vapour pressure of a geothermal fluid is equal to the external pressure acting on the fluid, flashing takes place. Flashing of geothermal brine inside a well leads to two-phase flow, i.e. water and vapor mixture. The salts present in the brine are nonvolatile and hence the produced vapour is free of salts. It contains steam and non-condensable gases such as CO<sub>2</sub>, H<sub>2</sub>S, NH<sub>3</sub>, N<sub>2</sub> and H<sub>2</sub>. The vapour pressure can be considered the sum of the saturation pressure of the fluid at a given temperature and gas partial pressures. Since CO<sub>2</sub> is usually the major constituent of the non-condensable gases, it is often assumed for simplicity that the vapor phase is a mixture of steam and CO<sub>2</sub>. Based on this assumption, we have

$$P_v = P_s + \sum P_{gi} \approx P_s + P_{CO_2} \quad (2.1)$$

The saturation pressure of an aqueous salt solution at temperature, T(°K), can be expressed by Raoult's Law.

$$P_s = P_w * (1 - X_{sa}) = P_w - \Delta P \quad (2.2)$$

The pure water saturation pressure, P<sub>w</sub>, is given by the following simplified correction (Michaelides, 1981):

$$P_w = \exp(0.21913 * 10^{-6} * t^3 - 0.17816 * 10^{-3} * t^2 + 0.653665 * 10^{-1} * t - 4.96087) \quad (2.3)$$

Treating steam as an ideal gas and calibrating this model by experiment, the decrease in steam pressure,  $\Delta P$ , due to a salt of mole fraction,  $X_{sa}$ , can then be derived:

$$\Delta P = 1.8RT/(V_V - V_1) * m_{sa} / 55.56 * 10^{-2} \quad (2.4)$$

The constant 1.8 is derived empirically and is related to the fact that the salt is ionized in the solution (Michaelides, 1981).

The partial pressure of  $CO_2$  has been studied by Sutton (1976):

$$P_{CO_2} = w_{CO_2} * x / \alpha(T) \quad (2.5)$$

where

$$\alpha(T) = [5.4 - 3.5 * (T/100) + 1.2 * (T/100)^2] * 10^{-4} \quad (2.6)$$

and  $w_{CO_2}$  is the weight percent in the vapor phase.  $P_{CO_2}$  can also be expressed in terms of Henry's Law, which is discussed in Part 4.

The pressure at any point in a wellbore has been described by Parlaktuna (1985):

$$P = P_{wf} - dP_t \quad (2.7)$$

The total pressure drop is made up of frictional, acceleration and potential pressure drops.

$$dP_t = dP_f + dP_a + dP_p \quad (2.8)$$

$$dP_f = (\rho f v^2 / 2d) * dZ * 10^{-5} \quad (2.9)$$

$$dP_a = \rho v * dv * 10^{-5} \quad (2.10)$$

$$dP_p = \rho g * dZ * 10^{-5} \quad (2.11)$$

The friction factor  $f$  is given by modified Colebrook equation as

$$f = \{[-2\log(\epsilon/3.7d) + (7/Re)^{0.9}]^2\}^{-1} \quad (2.12)$$

where, the Reynolds Number is given as

$$Re = \rho v d / \mu \quad (2.13)$$

The density of liquid water is determined by Whal (1977) to follow the correction:

$$\rho_l = \rho_w + [(1 + 1.6E-6 * t^2) * 5844 m_{sa} / (1000 + 58.44 m_{sa})] * 10^3 \quad (2.14)$$

where the pure water density form Keenan and Keyes (1951) was used:

$$\rho_w = [(1 + dt'^{1/3} + et) / (v_c + at'^{1/3} + bt' + ct'^4)] * 10^3 \quad (2.15)$$

where  $t' = 374.11 - t$  for  $t$  in  $^{\circ}C$

$$v_c = 3.1975 \text{ cm}^3/\text{g}$$

$$a = -0.3151548$$

$$b = -1.203374 * 10^{-3}$$

$$c = 7.48908 * 10^{-13}$$

$$d = 0.1342489$$

$$e = -3.946263 * 10^{-3}$$

The density correlation for the vapour phase suggested by Michaelides (1981) is as follows:

$$\rho_v = 100P / (-0.1296 * 10^{-2} * t^2 + 0.6325t + 121.05) \quad (2.16)$$

The density of a two phase mixture obeys the ideal mixing rule.

$$\rho = \alpha \rho_v + (1 - \alpha) \rho_l \quad (2.17)$$

The bottom hole flowing pressure for high flow-rate geothermal wells can be written as:

$$P_{wf} = P_a - CW^2 \quad (2.18)$$

when turbulence is the dominant factor in friction loss (Parlaktuna, 1985). In Equation (2.18), reservoir pressure can be measured in a well during shutdown, and C can be obtained by using a wellbore simulator to match the deliverability measurements of a well since the wellhead pressure is given by

$$P_{wh} = P_{wf} - \Delta P_t = P_a - CW^2 - \Delta P_t \quad (2.19)$$

When  $P_v = P$ , flashing occurs. In water phase region,  $dP_c = 0$ , so

$$P_v = P_s + P_{CO_2} = P = P_{wf} - (\rho f v^2 / 2d * \Delta Z - g \rho \Delta Z) * 10^{-5}$$

Then the flashing or boiling depth from wellhead is given

$$D_f = D_a - [(P_{wf} - P_s - P_{CO_2}) / (\rho f v^2 / 2d + \rho g)] * 10^5 \quad (2.20)$$

In practice, calcite deposit may occur in the first 20-25 meters above the first boiling point ( $D_f$ ) (Granados, 1985). The deposition shape may taper off from this point and become almost zero (Figure 1.2). In Equation (2.20) only the wellhead pressure is a parameter related to operation directly. Therefore deposition can be controlled to occur at a chosen level.

### 2.2.2. Steam Fraction

In the process of adiabatic flashing in a geothermal well-bore, the following heat balance relationships applies:

$$H_o = H_l + H_v$$

i.e.

$$h_o = h_l * (1-x) + h_v * x \quad (2.21a)$$

where  $h_o$  is the enthalpy of initial liquid prior to flashing,  $h_l$  and  $h_v$  are the enthalpy of coexisting water and steam after boiling. Based on the salt solution enthalpy equation given by Wahl (1977), and taking  $T_o = 0$ , the following results:

$$h_l = h_w * [1 - 58.44m_{sa} / (1000 + 58.44m_{sa})] + T * 11.688m_{sa} / (1000 + 58.44m_{sa}) \quad (2.22)$$

The correction for the enthalpy of vapor phase recommended by Michaelides (1981) is

$$h_v = -0.81275 * 10^{-2} * t^2 + 3.65228t + 2388.4 \quad (2.23)$$

The steam fraction can be given by

$$x = (h_o - h_l) / (h_v - h_l)$$
$$x = (h_o - h_l) / L \quad (4.21)$$

where  $L$  is the evaporative heat.

### 2.3. Two Phase Flow Regimes

Flowing properties of two phase geothermal fluids can affect geothermal sampling and mineral precipitation. For vertical flow five regimes can be defined as showed in Figure 2.3

(Hetsroni, 1982). The general-flow-pattern map (Figure 2.4) of Hewitt and Roberts (1969) can be recommended for determining the vertical flow regimes. On this map, the plotting coordinates are the superficial momentum fluxes of the respective phase, i.e.  $\rho_l v_l^2$  and  $\rho_v v_v^2$ .

Flow regimes in horizontal flow tend to be somewhat more complex than those in vertical flow. This result from that the gravitational force act normal to the direction of the flow and makes the liquid phase tend to accumulate at the bottom of the channel. The flow patterns are illustrated in Figure 2.5 (Hetsroni, 1982). The best know generalized flow-pattern map for horizontal flow is the Baker Diagram modified by Scott (1963). The coordinates of the Baker Diagram (Figure 2.6) are

$$B_X = 2.105*(1-x)/x*\rho_v^{1/2}/\rho_l^{0.166}*\mu^{1/3}/\sigma \quad (3.24)$$

$$B_Y = 2.752Wx/(d^2*\sqrt{(\rho_l\rho_v)}) \quad (3.25)$$

where the correlation equation of viscosity can be developed as (Michaelides, 1981):

$$\log[\mu(t,m)/\mu_w(t)] = A(m)+B(m)*\log[\mu_w(t)/\mu_w(20)] \quad (2.26)$$

with pure water viscosity,  $\mu_w(t)$ , is given by the expression:

$$\log[\mu_w(t)/\mu_w(20)] = [(20-t)/(96+t)]* [1.2378-1.303*10^{-3}*(20-t)+3.06*10^{-6}*(20-t)^2+2.55*10^{-8}*(20-t)^3] \quad (2.27)$$

with  $\mu_w(20) = 1002 \mu \text{ Pa s}$ .

A and B are functions of molality.

$$A(m) = 0.3324*10^{-1}*m+0.3624*10^{-2}*m^2-0.1879*10^{-3}*m^3 \quad (2.28)$$

$$B(m) = -0.3961*10^{-1}*m+0.102*10^{-2}*m^2-0.702*10^{-3}*m^3 \quad (2.29)$$

The surface tension correction is given by (Wahl, 1977) as:

$$\sigma = \sigma_w * [1 + 22.7916 m_{sa} / (1000 + 58.44 m_{sa})] + 1.4856 * 10^3 * m_{sa}^2 / (1000 + 58.44 m_{sa})^2 * 10^{-3} \quad (2.30)$$

with

$$\sigma_w = 0.0755 * (t_c - t)^{0.776} * 10^{-3} \quad (2.31)$$

#### 2.4. Chemistry

A hydrothermal or geothermal system is where water currents circulate in the crust of the earth. It may be heated by convection of water from magma. High temperatures at shallow depth are commonly the result of convective flow. Convection may occur because of the heating and consequent thermal expansion of water at depth. Hot water of low density tends to rise and be replaced by cooler water of higher density (Gudmundsson, 1986). As the water circulates through the rock structure by this convection, it dissolves, leaches and precipitates minerals to form an equilibrium hot brine solution with the reservoir rocks at certain temperature and pressure.

The composition of a geothermal reservoir brine is controlled by mineral equilibria. Some of them are listed in Table 2.2. The pH of the brine is determined by acid-base equilibria and reactions involving alumino-silicates. In general, the pH of carbonate-type geothermal waters tends to be between 6.0 and 6.5 or close thereto because of the buffering action of the carbonate reactions (Wahl, 1977), which is discussed in Part 4.

It is not known which minerals control carbon dioxide concentrations in high temperature waters (>200°C). Conceivably, the assemblage involved is zoisite (epidote)-prehnite-quartz-calcite (Arnorsson et al., 1982).

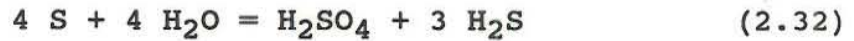
Calcite is a prominent secondary mineral in reservoir rocks. In geothermal reservoir, the product of carbonate and calcium ion concentrations is a fixed quantity as a function of temperature due to equilibrium with calcite. It is strongly dependant on pH, which in turn is dependent on the equilibria reactions between the alumino-silicates and sodium in the absence of dominating sulfate chemistry. Thus the product of the calcium and carbonate concentrations will be related to the sodium concentration and temperature as shown in Figure 2.7 (Wahl, 1977).

The concentration of potassium in geothermal brine is determined by ion exchange equilibria between sodium and potassium with the alumino-silicates. The molecular ratio of sodium to potassium is fixed at a given temperature (Ellis and Mahon, 1977).

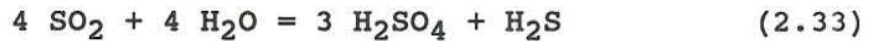
The distribution of major cations and hydrogen ion is governed by temperature dependent ionic exchange equilibria (Table 2.3), so the ratio  $\sqrt{(\text{Ca})/\text{H}}$  is approximately fixed at a given temperature, variable concentrations of the other major cations, Na, K and Mg, which may cause some scatter in the  $\sqrt{(\text{Ca})/\text{H}}$  ratio. The absolute concentrations of Ca, H and other major cations are in turn mostly governed by the supply of the incompatible element chlorine (Arnorsson, 1978; Arnorsson et al., 1983).

At high temperature (180°C to 225°C), silica concentration correspond the solubility of quartz. At lower temperatures other silica species such as chalcedony, cristobalite, or amorphous silica may control dissolved silica (Fournier, 1977).

The presence of sulfur deposits and rock through which the hot water is permeating will give rise to the formation of hydrogen sulfide and sulfuric acid:



In geologically active volcanic regions, sulfur dioxide if present also gives rise to the formation of sulfuric acid through reaction with warm water as follows:



The acid developed from this reaction will override the buffering reactions with the alumino-silicates in controlling the pH (Wahl, 1977).

Ammonia is found in geothermal waters that have come in contact with organic matters.

The concentrations of the various constituents in geothermal brine are shown in Figure 2.8 and in Table 2.1 are shown the chemical compositions for typical wells and hot springs in various geothermal fields.

The measured chemical properties of geothermal fluids at surface temperature and pressure are different from those of deep geothermal brine because of steam loss, gas separation, mineral precipitation and the temperature dependence of homogeneous equilibria. Methods for calculating the geothermal reservoir water composition from analysis made under surface condition are discussed in the following parts.

### 3. SAMPLING AND CHEMICAL ANALYSIS

#### 3.1. Sampling of Water-Dominated Wells

The collection of representative samples from a geothermal well discharging steam and water is a complex procedure. High temperature water (150°C to 350°C) from deep levels can partially flash into steam-water mixture as pressures decrease toward the wellhead, and discharge into the atmosphere at velocities approaching the speed of sound with an explosion of the volume. Thus, special methods and care should be taken for sampling geothermal wells (Ellis and Mahon, 1977). It is necessary to sample each phase separately, at a known pressure, which should be the same as the pressure of the pipe or vessel being sampled. The subsequent combination of the analysis of the separate phases is discussed in Part 5.

The methods used for sampling a geothermal well depend on the surface pipework. Representative sampling of steam, gas and water from wells is made using one or more of the following techniques:

1. Down-hole direct collection.
2. Separator collection, that is, samples of steam, water and gas are collected under pressure from sampling points at the wellhead and on the surface pipes separately.
3. Discharging collection. Steam, water and gas samples are collected from the vertical silencer at atmospheric pressure and boiling point.

The sampling procedure and cautions for separator collection are described in detail by Olafsson (1987). Figure 3.1 shows a small separator for sampling and Figures 3.2, 3.3 and 3.4 are a series of sampling sketches. Figure 3.5 is a flow chart

for sampling and analysis. During the sampling, flow through the separator is controlled by the three main valves, i.e. fluid inlet valve, water phase outlet valve and vapor outlet valve.

In order to obtain representative samples, great care has to be taken to select the sampling points and to adjust the three control valves.

Tests have shown that the optimum location of a sampling point is about 1.5 meter from the T-joint on surface discharging piping (Figure 3.6). At this point the flow is free from interference from the T-joint, and the water and steam phases are still in thermodynamic equilibrium (Olafsson, 1987).

Flow patterns in horizontal piping can affect the representativeness of the samples. For slug or plug flow, since the alternating pulses of water and steam exist, the inlet valve of the separator should be adjusted a little closed instead of fully open to create a relative bigger volume of the separator. For stratified and wavy flow, water and steam samples can be taken from the top and bottom sampling points on the horizontal pipe, separately, without using a separator (Arnorsson, 1987a).

Boiling of sampling fluid in the separator should always be avoided. This can be done by adjusting the valves carefully, while looking at the pressure gauge at the top of the separator. The pressure should not fall down more than 0.1 kPa/cm<sup>2</sup> during the collection (Olafsson, 1987).

During the whole sampling, from the preparation until ending, it is necessary to have a check list or a uniform record form for apparatus and samples. And they should be fully used!

### 3.2. Chemical Analysis Techniques

The analytical techniques (Figure 3.5) for determining the major constituents in geothermal waters can be outlined in the following. For detail on some subjects, please refer to Ellis and Mahon (1977).

#### 1. Atomic Absorption Spectrophotometry

Alkali metals, boron, calcium, magnesium, iron, aluminum, SiO<sub>2</sub> in acid and near neutral pH thermal waters can be determined by this method (Table 3.1).

#### 2. Emission Flame Photometry

It can accurately determine sodium (5893Å, 2000ppm), potassium (7665Å, 250ppm), lithium (6708Å, 25ppm), rubidium (7800Å, 5ppm) and cesium (8521Å, 5ppm).

#### 3. Gas Analyzer and Gas Chromatograph

Residual gases e.g. H<sub>2</sub>, N<sub>2</sub>, CH<sub>4</sub> and NH<sub>3</sub> can be analyzed by standard PVT gas analysis equipments.

4. Ion Chromatograph is used for measuring Cl<sup>-</sup> and SO<sub>4</sub><sup>2-</sup>.

#### 5. Spectrographic Analysis and Spectrophotometry

Many heavy metals and rare earth metals can be extracted by chloroform with mixed solution of diethyl dithiocarbamate, oxine and dithizone at pH 3, 5, 7 and 9. That catchall concentrate is later analyzed spectrographically.

A rapid assessment of the trace metals present in waters can be made by spectrographic analysis of residue obtained by evaporation.

Cu, Pb, Zn, Ag, W, Ni and Cd can be concentrated by one of

two techniques, (1) absorption onto Chelex-100 cation exchange resin and elution with 2N nitric acid; (2) extraction with a benzene solution of mixed diethyl and pyrrolidine dithiocarbamic acid. The concentrate obtained by both methods are evaporate to dryness, and later dissolved for analysis by atomic absorption spectrophotometry.

Sulfate in water is reacted with barium cremate to form insoluble barium sulfate to liberate cremate ions, which are measured photometrically.

Ionic silica formed by digestion with alkali is reacted with an acid solution (pH 1.2-1.5) of ammonium molybdate in the presence of oxalic acid, producing the yellow silicomolybdic acid. The concentration (50-200ppm) can be measured by comparing the absorbance against a standard calibration curve.

## 6. Ion Selective Electrode

A fluoride specific ion electrode gives a direct reading of fluoride contained in samples buffeted with a citrate-citric acid buffer.

Ammonium concentration can also be read directly on a specific ion meter using calibration curve.

## 7. Titration

a. Acid-Base Titration. The total carbon dioxide in solution can be determined by titrating this solution from a pH of 8.25 to pH 3.8 with standard acid (0.1N HCl).

b. Redox Titration. In acid solution, total hydrogen sulfide is quantitatively oxidized to sulfur by iodine. Excess iodine is back titrated with sodium thiosulfate, using sodium starchglycollate as indicator.

I<sup>-</sup> in a buffered is oxidized to I<sub>2</sub> with Br<sub>2</sub> water. Excess Br<sub>2</sub> is removed by addition of KI. Total I<sub>2</sub> liberated is titrated by Na<sub>2</sub>S<sub>2</sub>O<sub>3</sub> to obtain I<sup>-</sup> in original sample. I<sup>-</sup> and Br<sup>-</sup> in a second aliquot of the sample are oxidized to I<sub>2</sub> and Br<sub>2</sub> with hypochlorite, the excess hypochlorite then being decomposed. I<sub>2</sub> liberated from both I<sup>-</sup> and Br<sup>-</sup> which produced by addition of KI is titrated with Na<sub>2</sub>S<sub>2</sub>O<sub>3</sub>. Br<sup>-</sup> is obtained from the difference between the two titration.

c. Direct Titration. F<sup>-</sup> in solution at pH 3.5 is titrated with thorium nitrate in the presence of the indicator chromazurol-S.

Cl<sup>-</sup> is titrated against standard AgNO<sub>3</sub> solution using potassium cremate as indicator (Mohr Method).

Total H<sub>2</sub>S is determined by titration with Hg(CH<sub>3</sub>COO)<sub>2</sub>.

d. Potentiometric Method. Cl<sup>-</sup> in a supporting sulfuric acid electrolyte is titrated with standard AgNO<sub>3</sub>, The end point being detected by a silver electrode and a reference mercurous sulfate electrode in association with a standard expanding-scale pH meter.

e. EDTA Titration. Standard EDTA is used to titrate Ca<sup>2+</sup> at pH 13 with cal-red indicator, and Ca<sup>2+</sup> plus Mg<sup>2+</sup> are titrated at pH 10 with solochrome black as indicator. Mg<sup>2+</sup> is obtained by difference.

8. Distillation. Ammonia is distilled from an alkaline buffeted solution, and an aliquot of the distillate is examined by colorimetry using the Nessler reaction.

9. Dissolved O<sub>2</sub> is measured with a Chemet test kit based on reaction with rhodazine D.

10. A measured volume of geothermal fluid is evaporated and the dry residue is weighted to indicate the total amount of

mineral matter in water.

11. Conductivity and salinity are measured by conductivity meter.

12. pH is measured by pH meter with a glass electrode.

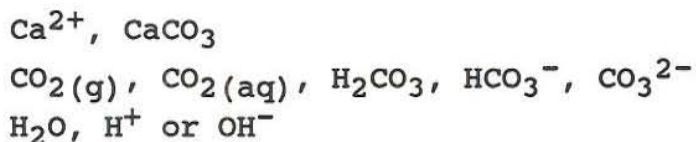
13. Gonfiantini (1975) reviewed the specialized techniques required for the analysis of stable isotopes in the samples.

## 4. THERMODYNAMICS AND KINETICS OF CALCITE SCALING

### 4.1. System Studied

In order to approach the nature of calcite scaling effectively, the following is assumed for simulating the behaviour of geothermal fluids in the calcite deposition section of a wellbore (from flashing depth to either the end of deposition or until wellhead).

1. Chemical equilibria between the following constituents are considered:



2. Thermodynamic equilibrium of each reaction is approached in the system. From this assumption, some remarks can be derived. (a) The degassing factor of fluid during flashing is unity (=1) because volatile constituents are sufficiently transferred into steam to establish equilibrium. (b) Calcite is the only stable scale of calcium carbonate in high temperature and high pressure geothermal wells. Aragonite and  $\text{CaCO}_3 \cdot 6\text{H}_2\text{O}$  are transferred to calcite (Figure 4.1). Precipitation of  $\text{CaSO}_4$ ,  $\text{MgCO}_3$  and  $\text{Mg}_x\text{Ca}_{(1-x)}\text{CO}_3$  are omitted.

3. The reservoir and wellbore performances are assumed constant in the period of study. The well is a water-dominated well. The production process is adiabatic and one step flashing take place in the wellbore.

4. The effect of erosion due to flowing on calcite scaling is not considered.

Based on the above assumptions, the maximum calcite precipitation potential or rate can be reached in the wellbore.

## 4.2. Thermodynamics

### 4.2.1. Equilibrium Consideration

The geothermal fluid chemistry following flashing can be summarized in the following principle chemical reactions:

#### Carbon Dioxide in Solution

At interfaces of a vapor-liquid system, carbon dioxide gas is associated with dissolved carbon dioxide.



Taking consideration of a degassing factor,  $b$ , according to Henry's Law the fugacity of carbon dioxide is

$$f_{\text{CO}_2} = b \cdot \gamma \cdot K_H^\circ \cdot X \quad (4.2a)$$

where  $b$  is a value in the range of 0 to 1, In thermodynamic equilibrium  $b = 1$ .

If Henry's Law coefficient for saline solutions is

$$K_H = \gamma \cdot K_H^\circ \quad (4.3)$$

Putting Equation (4.3) into Equation (4.2a) and using  $b = 1$

$$f_{\text{CO}_2} = K_H \cdot X \quad (4.2)$$

Increasing the salinity of a solution increases the Henry's Law coefficient (Fig. 4.3). Since salt out coefficient,  $k$ , for carbon dioxide in sodium chloride solution, are generally of the Steshenow type (Fournier, 1985):

$$k = (1/m_{\text{sa}}) \cdot \log(K_H/K_H^\circ) \quad (4.4)$$

Rearranging Equation (4.4),

$$K_H = 10^{(kmsa)} * K^*_H \quad (4.4a)$$

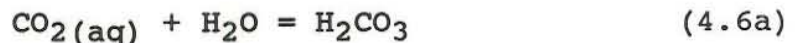
Comparing Equation (4.4a) with Equation (4.3),

$$\gamma = 10^{(kmsa)} \quad (4.5)$$

Because the fugacity coefficient for carbon dioxide in dilute aqueous solution at temperature below about 330°C are near unity (Ellis and Golding, 1963),  $f_{CO_2}$  in Equation (4.2) can be replaced by the partial pressure of carbon dioxide with little error.

$$P_{CO_2} \approx K_H * X \quad (4.2b)$$

In the liquid phase, the total carbon dioxide can be distributed between  $CO_2(aq)$ ,  $H_2CO_3$ ,  $HCO_3^-$  and  $CO_3^{2-}$  with the following equilibrium reactions:



The equilibrium constants are, respectively,

$$K'_0 = [H_2CO_3] / [CO_2(aq)] \quad (4.9a)$$

$$K_1 = [HCO_3^-] * [H^+] / [H_2CO_3^*] \quad (4.10)$$

$$K_2 = [CO_3^{2-}] * [H^+] / [HCO_3^-] \quad (4.11)$$

Ionization equilibria in dissolved carbonate system are established very rapidly. Somewhat slower is the attainment of the equilibrium of Reaction (4.6a) with the reaction rate constants (Stumm and Morgan, 1970):

$$k_+ = 4.37 \cdot 10^{-2} \quad \text{s}^{-1}$$

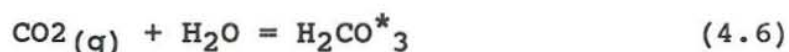
$$k_- = 19.2 \quad \text{s}^{-1}$$

at 298°K and 0.5 ionic strength.

By tradition a distinction is not made between  $\text{CO}_2(\text{aq})$  and  $\text{H}_2\text{CO}_3$ . They are reported as  $\text{H}_2\text{CO}^*_3$ .

$$[\text{H}_2\text{CO}^*_3] = [\text{CO}_2(\text{aq})] + [\text{H}_2\text{CO}_3] \quad (4.12)$$

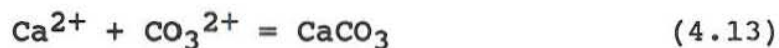
Combining Reaction (4.6a) with Reaction (4.1), the net reaction is general written:



$$K_0 = [\text{H}_2\text{CO}^*_3] / f_{\text{CO}_2} \quad (4.9)$$

#### Calcite in Aqueous Solution

The simplest reaction representing the precipitation of calcite in solution can be written,



for which the solubility product is

$$K_C = [\text{Ca}^{2+}] * [\text{CO}_3^{2-}] / [\text{CaCO}_3] \quad (4.14a)$$

In the above formula, the activity of solid calcite is unity if there is no significant substitution of other cations such as  $\text{Mg}^{2+}$ ,  $\text{Fe}^{3+}$  or  $\text{Mn}^{2+}$  for calcium in the solid. Then

$$K_C = [\text{Ca}^{2+}] * [\text{CO}_3^{2-}] \quad (4.14)$$

Table 4.1 summaries the equations expressing each coefficient i.e.  $K_H^0$ ,  $k$ ,  $K_0$ ,  $K_1$ ,  $K_2$  and  $K_C$  as a function of temperature (Fournier, 1985).

From Equations (4.9), (4.10), (4.11) and (4.14), we can derive

$$[\text{H}_2\text{CO}_3^*] = K_O * f_{\text{CO}_2} \quad (4.15)$$

$$[\text{HCO}_3^-] = K_O * K_1 * f_{\text{CO}_2} / [\text{H}^+] \quad (4.16)$$

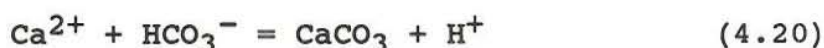
$$[\text{CO}_3^{2-}] = K_O * K_1 * K_2 * f_{\text{CO}_2} / [\text{H}^+]^2 \quad (4.17)$$

$$[\text{Ca}^{2+}] = K_C * [\text{H}^+]^2 / (K_O * K_1 * K_2 * f_{\text{CO}_2}) \quad (4.18)$$

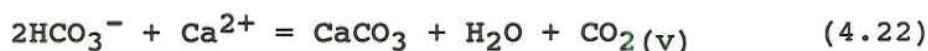
In the  $\text{CO}_2\text{-H}_2\text{O}$  system, the total carbon species in solution can be expressed in the mass balance equation

$$[\text{CO}_{2\text{total}}] = [\text{H}_2\text{CO}_3^*] + [\text{HCO}_3^-] + [\text{CO}_3^{2-}] \quad (4.19)$$

This is usually what is given in chemical analysis. Figure 4.5 indicates the fraction of carbonate, bicarbonate, carbonic acid and  $\text{CO}_2(\text{aq})$  present as a function of pH in a solution at  $100^\circ\text{C}$ . Since very little  $\text{CO}_3^{2-}$  presents in most acidic geothermal fluid, precipitation of calcite is commonly expressed in terms of the following reactions with corresponding equilibrium formula (Henry and Brown, 1985):



$$K_C / K_2 = [\text{Ca}^{2+}] * [\text{HCO}_3^-] / [\text{H}^+] \quad (4.21)$$



$$K_C K_1 K_O / K_2 = [\text{Ca}^{2+}] [\text{HCO}_3^-]^2 / f_{\text{CO}_2} \quad (4.23)$$

or

$$-\log K = -226.43 + 6552.81/T + 89.084 * \log T - 0.0746 * T \quad (4.23a)$$

Equation (4.23a) is valid in a temperature range of  $100^\circ\text{C}$ - $300^\circ\text{C}$ .

By using the above equations with equation

$$[H^+][OH^-] = K_w = 10^{-14} \quad (4.24)$$

the mass balance and the charge balance equations we can do the chemical equilibrium calculations in CaO-H<sub>2</sub>O-CO<sub>2</sub> system. For this system the charge balance is

$$2[Ca^{2+}] + [H^+] = [HCO_3^-] + 2[CO_3^{2-}] + [OH^-] \quad (4.25)$$

### Activity Product of Calcite

For a fluid the activity product of calcite is defined as

$$Q = [Ca^{2+}][CO_3^{2-}] \quad (4.26)$$

This equation is useful mainly for testing whether a given solution is under-saturated, saturated or supersaturated in respect to calcite by comparing with Equation (4.14) with definition of supersaturation ratio

$$\Omega = Q/K_c \quad (4.27)$$

The geothermal fluid chemistry obtained from chemical analysis is usually given by molality. They can be conveniently changed into activity by using following equation.

$$[i] = \gamma_i m_i \quad (4.28)$$

Taking Equation (4.28) into Equation (4.26), the activity product of calcite can be expressed

$$Q = \gamma_{Ca^{2+}} \gamma_{CO_3^{2-}} m_{Ca^{2+}} m_{CO_3^{2-}} \quad (4.29)$$

Most high-temperature geothermal fluids are closed to calcite saturation (as mentioned in Part 2.4). During flashing, the

fluids rapidly become supersaturated with mineral scales due to following mechanisms leading to increase of the corresponding activity product  $Q$ .

- a. Loss of steam from the liquid phase increases chemical concentration of remaining solutes and ionic strength.
- b. Evaporation in adiabatic process leads to temperature drop of the fluid.
- c. Loss of stable gases such as  $CO_2$  and  $H_2S$  increases the pH of fluid and reduces the gas contents in the remaining fluid.

#### 4.2.2. Effect of Ion-Strength

The ionic strength of a aqueous solution is defined by the equation

$$I = 1/2 * \sum m_i z_i^2 \quad (4.30)$$

In Table 4.2, the ionic strengths of representative sets of world-wide geothermal systems are shown.

Activity coefficient for solution with ion strength less than 2 molal can be calculated using an extended form of the Debey - Hückel equation.

$$-\log \gamma_i = AZ_i^2 I^{1/2} / (1 + a_i B I^{1/2}) + bI \quad (4.31)$$

The equations for A and B factors are in Table 4.1. For  $Na^+$ ,  $HS^-$ ,  $H_3SiO_4^-$ ,  $H_2BO_3^-$ ,  $SO_4^{2-}$ ,  $HSO_4^-$  and  $OH^-$ ,  $a$  is 4.0, in common,  $NH_4^+$ , 2.5;  $K^+$ , 3.0;  $HCO_3^-$  and  $CO_3^{2-}$ , 4.5;  $Li^+$  and  $Ca^{2+}$ , 6.0;  $Mg^{2+}$ , 8.0 and  $H^+$ , 9.0 (Fournier, 1985).

For high temperature calculations the following approximate values are quite satisfactory (Henley and Brown, 1985).

$$\begin{aligned}
\gamma_{H^+} &= 0.8, \\
\gamma_{Ca^{2+}} &= 0.3, \\
\gamma_{K^+} &= \gamma_{Cl^-} = \\
\gamma_{HCO_3^-} &= \gamma_{H_3SiO_4^-} = \\
\gamma_{HS^-} &= \gamma_{BO_2^-} = \\
\gamma_{Na^+} &= 0.7.
\end{aligned}$$

#### 4.2.3. Effect of Steam Loss

Flashing affects the composition of the brine in two ways. One is the simple concentration of the brine as a result of remove of water. The other is change of fluid chemistry resulting from remove of certain constituents such as CO<sub>2</sub>, H<sub>2</sub>S and NH<sub>3</sub> leading to the increase of pH and reduction of dissolved gases in the brine and reestablishment of the equilibria.

After boiling, the chemistry of the remained liquid phase is expressed by using the steam fraction.

For non-volatile constitutes

$$m_i = m_i^0 / (1-x) \quad (4.33)$$

For volatile constituents

$$m_i = (m_i^0 - m_v * x) / (1-x) \quad (4.34)$$

#### 4.2.4. Calculation of pH of Geothermal Fluid

Since the pH of geothermal brine are determined by acid-base equilibria and reactions involving alumino-silicates (as mentioned in Part 2.4), by taking account of all H<sup>+</sup> species and effects of dissolved gases, Reed and Spycher (1984) calculated in situs pH and distribution of aqueous species in a homogeneous equilibrium system at high temperature, based

on chemical analyses and pH/25°C measurement of quenched high temperature water.

The distribution of species, molalities of species whose compositions are described as containing H<sup>+</sup> are summed to obtain total molalities of "ionizable hydrogen",

$$N_{H^+}^+ = m_{H^+} + \sum \nu_{H^+j} * m_j \quad (4.35)$$

$N_{H^+}^+$  is independent of temperature.

For a geothermal water, Equation (4.35) contains a term for each of the 57 species listed in Table 4.2. The numerical values for the coefficients,  $\nu_{H^+j}$ , of Equation (4.35) are also list in that table.

If the solution under consideration produced a vapor phase, i.e. boiled, it is necessary first to calculate  $N_{H^+}^+$  in the remaining solute without concerning the gases released, rename the value of  $N_{H^+}^+$  calculated as  $N_{H^+}^{aq}$  referring to the remaining aqueous phase alone. Then using the known quantity and composition of gases calculate the moles of components in vapor phase of corresponding steam and add to the moles of aqueous phase components by using steam fraction. For example, for a gas which includes H<sub>2</sub>O, CO<sub>2</sub>, HCl, H<sub>2</sub>S and H<sub>2</sub>, we have

$$N_{H^+}^+ = N_{H^+}^{aq} * (1-x) + (2n_{CO_2} + n_{HCl} + n_{H_2S} - 1/4 * n_{H_2}) * x \quad (4.36)$$

A simplistic calculation provides a useful approximation of pH (Henley and Brown, 1985). Considering the Equation (4.7) and logK<sub>1</sub> in Table 4.1. Calculating  $m_{HCO_3^-}$ ,  $m_{H_2CO_3^*}$  based on water sample analysis at laboratory temperature. Then recalculating those two species in the fluid at reservoir temperature before boiling through Equation (4.34). Since

$$\log K_1 = \log m_{HCO_3^-} + \log \gamma_{HCO_3^-} + \log [H^+] - \log m_{H_2CO_3^*} \quad (4.37)$$

we can substitute values to obtain pH.

#### 4.2.5. Effect of Degassing

When flashing is first initiated, the ratio of CO<sub>2</sub> to steam in the vapor phase tends to be relatively large because most of the carbon dioxide initially dissolved in the liquid passes quickly into the gas phase (Figure 4.7), while only a small amount of water changes to steam. With continued boiling, the mole fraction of CO<sub>2</sub> in the vapor phase steadily decreases because little additional CO<sub>2</sub> is available to partition into the vapor phase, while the fraction of water that is converted to steam increases at a relatively constant rate. As the temperature of the ascending vapor water mixture decreases, the volume of the vapor phase increases due to the decrease in hydrostatic load. The net effect is a drastic decrease in the partial pressure of CO<sub>2</sub> as a boiling fluid ascends toward the earth's surface (Fournier, 1985).

Degassing of CO<sub>2</sub> from the fluid result in changing of total CO<sub>2</sub> content, and increasing pH leading to distribution change of carbon species in fluid. For one step flashing, without calcite precipitation (although fluid is supersaturated) and that thermodynamic equilibrium is reached, the total moles of carbon bearing species is expressed

$$n_{\text{total}} = n_{\text{H}_2\text{CO}_3^*} + n_{\text{HCO}_3^-} + n_{\text{CO}_3^{2-}} + n_{\text{CO}_2\text{g}} \quad (4.38)$$

Using the distribution coefficient (Table 4.1),

$$\begin{aligned} K_D &= m_{\text{CO}_2(\text{aq})} / m_{\text{CO}_2(\text{g})} \\ &= [n_{\text{CO}_2(\text{aq})} / (1-x)] / [n_{\text{CO}_2(\text{g})} / x] \\ &= n_{\text{CO}_2(\text{aq})} / n_{\text{CO}_2(\text{g})} * x / (1-x) \end{aligned} \quad (4.39)$$

and rearranging the above formula

$$n_{\text{CO}_2(\text{g})} = (n_{\text{H}_2\text{CO}_3^*} / K_D) * [x / (1-x)] \quad (4.40)$$

with  $n_{\text{CO}_2(\text{aq})} = n_{\text{H}_2\text{CO}_3^*}$ . Inserting (4.38) into (4.40), for a unit mass fluid changing moles to molality and dividing by  $m_{\text{HCO}_3^-}$

$$\begin{aligned} m_{\text{total}}/m_{\text{HCO}_3^-} &= m_{\text{H}_2\text{CO}_3^*}/m_{\text{HCO}_3^-} \{1+x/ \\ &[K_D^*(1-x)]\} + m_{\text{CO}_3^{2-}}/m_{\text{HCO}_3^-} + 1 \end{aligned} \quad (4.41)$$

Combining Equations (4.10) and (4.11) changing the molalities into activities where required through Equation (4.28) and rearranging

$$\begin{aligned} [\text{HCO}_3^-] &= m_{\text{total}} / ([\text{H}^+] / K_1 * (1+x*(K_D^*(1-x))) \\ &+ 1/\gamma_{\text{HCO}_3^-} + K_2 / ([\text{H}^+] * \gamma_{\text{CO}_3^{2-}}) \end{aligned} \quad (4.42)$$

In a similar manner,  $[\text{CO}_3^{2-}]$  and  $[\text{H}_2\text{CO}_3^*]$  can be obtained.

#### 4.2.6. Effect of Temperature and $P_{\text{CO}_2}$

Differentiating Equation (4.23a), we have

$$d\log K/dT = -3276.405/T^2 - 38.689/T + 0.0746 \quad (4.43)$$

Up to  $T = 573.15^\circ\text{K}$ ,  $d\log K_1/dT = -2.88 \times 10^{-3} < 0$ . Therefore, calcite is more soluble at low temperature than at high temperature (see Figures 5.1 to 5.5 and Appendix). So calcite cannot be deposited from solution by simply cooling down of the fluid temperature at constant concentrations of  $\text{CO}_2$  and other constituents in the fluid.

By using Equations (4.21) and (4.23), we can draw the solubility product curve for calcite as a function of  $P_{\text{CO}_2}$  at given temperature (Figure 4.7).

### 4.3. Kinetics

#### 4.3.1. General

Deposition of solids may occur in the bulk of a solution or on a solid surface. It occurs first by nucleation and is then followed by growth. A distinction between those two processes can be made in terms of Figure 4.8 (Berner, 1981). The rate of deposition may have a contribution from three terms: the formation of nuclei in the bulk of the solution (homogeneous), the formation of nuclei on the surface (heterogeneous), and the formation of deposited on nuclei already-formed either in the solution or on the solid surface (Whal, 1977).

#### Nucleation

As a body precipitating from solution begins to increase in size, it encounters a free energy barrier to further growth. Considering a spherical nucleus of radius  $r$ , the interfacial energy rate between the phase and solution is  $R' \text{cm}^{-2}$ , and as the degree of the supersaturation is increased, the decrease of free energy ( $\Delta G' \text{cm}^{-3}$ ) of nucleation is resulted in by decreasing in the size of the critical nucleus, then the net free energy  $E_n$  associated with the nucleus is

$$E_n = 4\pi r^2 R' - (3/4)\pi r^3 \Delta G' \quad (4.44)$$

setting  $dE_n/dr = 0$ ,

$$E_{no} = 16\pi R'^3 / 3\Delta G'^2 \quad (4.44a)$$

Inserting Equation (4.44a) into the Arrhenius equation

$$k = A(T) * \exp(-E_a/RT) \quad (4.45)$$

the rate of nucleation should be

$$k = A(T) \cdot \exp[(-16\pi R^3)/(3\Delta G^2 RT)] \quad (4.46)$$

(Drever, 1980).

### Growth

Once the critical nucleus has formed, further increase in its size can take place spontaneously with a net decrease in free energy. This process is referred to as crystal growth.

Crystal growth involves the transport of dissolved species to the surface of a crystal and various chemical reactions occurring at surface. The latter includes adsorption, ion exchange, dehydration of ions, formation of two-dimensional nuclei on the surface, diffusion along the surface, ion-pair formation etc. The rate of growth is limited by the slowest step with a whole chain of process. It can be characterized as being controlled either by transport of species to the surface (transport-controlled), by reaction at the surface (surface-reaction-controlled), or by a combination of both processes. A comparison of the three mechanisms is shown in Figure 4.9 (Berner, 1981).

In case of diffusion limited kinetics, the rate of reaction on the grain surface is so rapidly that migration of species in solution to take their place cannot keep pace. As a result concentrations in solution adjacent to the crystal surface fall until they almost reach the equilibrium or saturation level. So there is a concentration gradients existing in diffusion layer. Further growth is limited by the rate at which additional ions can be transported to the crystal surface and the lowest process is that of molecular or ion diffusion.

In the case where the deposition rate is limited by chemical kinetics, ion attachment to the surface is so slow that replenishment of ions in solution near the surface is easily accomplished by molecular diffusion and other transport

process. Concentrations in the near surface zone are little different than those in the bulk solution, and the growth rate is proportional to the drive force for the chemical reaction and is not affected by the hydrodynamic state of the solution.

#### 4.3.2. Deposition Models

##### Mechanisms

Nuclei already exist in geothermal fluid or on wellbore surface. The concern of this study therefor, is with the growth kinetics but not the nucleation kinetics of calcite deposition.

Calcite scaling is site-specific. The mechanisms and rates can be influenced by relevant surface property such as surface area, supersaturation ratio (SR), species which can take part in the reaction path to form "intermediaries" temperature, pressure and flowing properties.

Geothermal fluid chemistry is very complicated and different from one well to another, and it is a high temperature, high pressure, high mass flow and flowing system, the data related to kinetics are few in the literature. According to the distinction between ionic reaction taking place in the bulk of solution and that on the mineral surface, the following mechanistic sequences can be assumed for studying the path and rate by which calcite deposit in geothermal production wells.

##### Mechanism A

Step 1.  $\text{Ca}^{2+}$  reacts with  $\text{HCO}_3^-$  or  $\text{CO}_3^{2-}$  in solution forming a "transfer species" such as  $\text{CaCO}_3^*$ ;

Step 2.  $\text{CaCO}_3^*$  diffuses from boundary interface to mineral grain surface;

Step 3. Adsorption, ion exchange, dehydration and precipitation on mineral surface to form scale.

The rate of ionic reaction is instant because there is little or no energy barrier that must be overcome to form products once the ions are in proximity to one another, especially at high temperature. In this case the whole process rate seems to be controlled by the "big" and "heavy" transient constituent diffusion to the surface to form a crystal. Some of the calcite that has not yet diffused to wellbore surface before being carried out by the fluid from the well, can be derived by using this mechanism.

The rate of deposition caused by mass diffusion will be proportional to the concentration difference. Lasaga(1984) has discussed the concentration gradient in the boundary layer during stable mineral dissolution processes. Assuming deposition has a process just opposite to that of dissolution, the diffusion equation (see Figure 4.9) can be written

$$C(r,t) = C_{\infty} + (C_{eq} - C_{\infty}) \operatorname{erf}[(r/2)(Dt)^{1/2}] \quad (4.47)$$

The flux of species is obtained from

$$\begin{aligned} J &= -D \left( \frac{dC}{dr} \right)_{r=0} \\ &= (C_{\infty} - C_{eq}) * D / (\pi Dt)^{1/2} \end{aligned} \quad (4.48)$$

The consequent increase in the concentration of the same species in the boundary layer is then given by

$$dC/dt = J * A / V \quad (4.49)$$

Assuming  $C_{t=0} = 0$ , and integrating Equation (4.48)

$$C = [(C_{\infty} - C_{eq}) * D^{1/2} * A] / (2V\pi^{1/2}) * t^{1/2} \quad (4.50)$$

The thickness of boundary layer is relatively insensitive to crystal size, crystal density, flowing properties and diffusion coefficient (Nielsen, 1984). It is usually in range of 1 to 5 nm (Lasaga, 1984). Transport to the surface can be accelerated by bulk flow of solution past the growing crystal or by stirring due to reducing of the thickness of the diffusion layer or concentration gradient. Thus, transport-controlled growth is a strong function of the hydrodynamic state of the solution.

The diffusion coefficient of the species in solution is given as

$$D = \lambda^2 * k' T / [(2\pi w k' T)^{1/2} v_f^{1/3}] * \exp(-E_{vap}/3k'T) \quad (4.51)$$

in Lasaga (1981).

#### Mechanism B

Step 1.  $Ca^{2+}$ ,  $HCO_3^-$  and  $CO_3^{2-}$  diffuse to mineral surface;

Step 2. Ions collide and react on surface to form calcite scale;

The two rate-limited possibilities for this mechanism can be explained as follows.

In case of the rate of deposition is controlled by Step 1, the assertion that diffusion of  $HCO_3^-$  or  $CO_3^{2-}$  through the boundary layer is the rate-controlling factor can be made. It is supported by

A. Experimental evidence indicates that the reaction producing scale can be very rapid, occurring in fractions of a second, following the creation of over-saturation condition (Granados, 1983);

B. Calcium ion diffusion is much faster than that of

bicarbonate and carbonate ions owing to (a) the size of un-hydrated calcium ion is much smaller (b) in the early stage of precipitation, concentration ratio of  $\text{Ca}^{2+}/\text{CO}_3^{2-}$  is much higher (see Appendix), though after deposition carbonate ion is more abundant than calcium ion. So no discernable effect of calcium ion concentration on the rate of reaction at earlier stage.

Bicarbonate can effectively increase the rate of diffusion of carbonate through the boundary layer, which can be explained in two terms (Przybylinski, 1987):

A. Bicarbonate combines with calcium on the surface of the crystal to form calcite with Reaction (4.20). As diffusion of hydrogen ion in water is very fast, it can easily diffuse out. This would run in parallel with the referred Reaction (4.14). Although Reaction (4.20) would likely have a rate constant that is lower than Reaction (4.14), but the concentration of bicarbonate is overwhelmingly greater than that of carbonate (see Appendix) in geothermal fluid. The rate of diffusion is proportional to the concentration gradient across the boundary layer. The difference will be proportional to the actual concentrations of each carbonate species. So bicarbonate ion concentration will primarily determine the diffusion rate. Thus, its overall rate may be greater.

B. Bicarbonate ion merely aids the transport of carbonate through the boundary layer. Since hydrogen and hydroxide ions diffuse very rapidly, the surface pH is essentially identical to the bulk pH. Near the surface, carbonate ion is depleted relative to the bulk, whereas calcium is less depleted. The carbonate ion can be replenished by Reaction (4.8) as well as by diffusion. In this case the bicarbonate ion tends to buffer the concentration of carbonate ion.

In the case where the deposition rate is controlled by Step 2, based on a assumption of that the precipitation has the same, but reversed process and reactions as the mechanism of dissolution, for heterogenous kinetics, the precipitation rate of a mineral is given in general by (Lasaga, 1984),

$$dC/dt = A/V \cdot \nu_i \cdot Q^m / K_{eq}^m \cdot K \cdot [H^+]^n \quad (4.52)$$

The Gibbs free energy change of a particular reaction can be

$$\begin{aligned} \Delta G &= \Delta G^\circ + RT \ln Q = \\ RT \ln(Q/K_{eq}) &= RT \ln \Omega \end{aligned} \quad (4.53)$$

therefore

$$dC/dt = A/V \cdot \nu_i \cdot K \cdot [H^+]^n \cdot \exp(m \cdot \Delta G / RT) \quad (4.54)$$

The topography of the mineral surface normally includes "step" and "kink", which are imaginative terms for description. Specie at kink, step and plane surface has higher surface energy in order, because kink has three "sides", in common, step two, and planner only one. During growth, new units of the crystal form at the points where they have the maximum surface area in common with the existing crystal. Thus growth normally takes place at kinks, and the rate of growth may be limited by the rate of nucleation of new kinks and steps (Berner, 1981).

Dislocation of crystalline structure creates a step which can propagate continuously during growth, so the slow process of nucleating a new step is not required. The rate of growth of a mineral is thus sensitive to the number and type of dislocations present.

Kinks, because they are points of high surface energy, are favoured locations for adsorption of species from solution. The adsorbed species may "block" or immobilize the kink, and so have a large effect on rate of growth. Phosphates can

interrupt the growth of calcite scale by means of being adsorbed at the kinks and steps.

Degassing of  $\text{CO}_2$  from geothermal fluid results in the increase of the fluid pH, which leads to an increase in the concentration of carbonate in the  $\text{CO}_2\text{-H}_2\text{O}$  system. That means an increase of the calcite deposition rate. But after the affect of pH on the supersaturation ratio and bicarbonate ion concentration are accounted for, there is no discernable effect of pH on the rate (Przybylinski, 1987). Because hydrogen and hydroxide ions are not species which can join forming a transient species in the kinetics of calcite scaling.

Calcite deposition in the wellbore results in the calcium ion concentration change in the solution, i.e. the concentration distribution. Based on the concentration distribution, we can predict the amount of calcite deposited in the well. This purpose can be approached according to the mechanisms, equilibrium relationships and reactions discussed above.

## **5. THE CHEMICAL EQUILIBRIUM PROGRAM WATCH**

### **5.1. Introduction**

The chemical properties of a geothermal brine are strongly affected by the way the brine is manipulated in the energy extraction plant. Therefore, the chemical properties of the fluid need to be taken into account in the designing and operation of the production and disposal processes. Unfortunately, the properties are quite complicated functions of temperature, pressure and concentration variables of the working fluid. Computer models of geothermal fluid behaviour are needed to predict these properties. The WATCH program is one such computer model for this purpose. It can be used for analyzing the scaling potential in various process options and aiding the selection of the optimal extraction process (Arnorsson et al. 1982). This program was developed by Dr. Stefan Arnorsson and co-workers at the National Energy Authority during the period of 1973 to 1978 (Svavarsson, 1981).

### **5.2. Program Description**

There are two parts of the WATCH program: WATCH1 and WATCH3. The WATCH1 program calculates the chemical behaviour of a fluid on the basis of a chemical analysis of the total flow of a two-phase production well (water, gas and condensate collected at wellhead) (Appendix 1). The WATCH3 program is used for calculations exclusively dealing with the aqueous phase. It is a question of two methods. On the one hand it is assumed that there has been no loss of steam in samples, i.e. the water subjected to analysis is the same as the groundwater (SSTEMP =999). In this case, the program is called WATCH2 in printout (Appendix 2.1 and 2.3). This is valid for cold water, water from down-hole and spring water which has not been boiled. On the other hand, it is realized that the water analyzed has boiled before being sampled, the program is printout as WATCH3 (Appendix 2.2). Then "SSTEMP"

is set equal to the temperature at which the water started boiling (Svavarsson, 1981; Arnorsson et al., 1982).

By combination of the WATCH1 and WATCH3 programs, we can also predict the geothermal fluid chemistry in surface equipment systems. For example, the WATCH1 can be used for calculating the composition of liquid phase in separator and the result can then be put into WATCH3 program to study the effect of further processing.

The WATCH programs calculate only the thermodynamic properties of the fluids but not the kinetics of the reactions. Table 5.1 is a summary of the program function. Table 5.2 is the input data needed for the program (Arnorsson, et al., 1982).

### **5.3. Yangbajing, Svartsengi and Hveragerði Fields**

The Yangbajing field is located at an elevation of 4300 m, about 91 km NW of Lhasa. The structure setting of the area is characterized by a narrow, elongated recent asymmetric graben trending NE-SW. The upper portion of the graben is filled by Quaternary lacustrine and fluviolacustrine sediments of variable thickness from about 300 m in the NW to about 100 m in the SE, whose coarse levels represent the shallow reservoir now being exploited. The temperature distribution measured inside the reservoir is quite uniform, ranging between 150°C and 160°C, with a sharp decrease of temperature at the borders. Higher values (172°C) are recorded in the hot water recharging zone. The fluid chemistry is of the type  $\text{Na}^+\text{-Cl}^-\text{-HCO}_3^-$  with a total dissolved solids of about 2100 mg/l (ENEL-AQUATER, 1985). The calcite scale in the production wells is cleaned by means of daily mechanical removing.

The Svartsengi geothermal field is located in south-west Iceland. It is classified as high-temperature and water-dominated. The reservoir temperature is in the range 235°-

240°C, and the fluids produced are in composition two-thirds seawater and one-third rainwater. The chemical composition of the brine produced from the wells is spatially and temporally uniform, suggesting good fluid mixing with the reservoir (Gudmundsson and Thorhallsson, 1986).

The Hveragerði geothermal field is located about 50 km east of Reykjavik. There are 8 wells of 300-1000 m depth in the area. The maximum temperature measured in those wells is in the range of 180°C-230°C. All the strata are late Quaternary (Zhou, 1980). The hot water is used for direct utilizations. The calcite deposits in the production wells in Svartsengi and Hveragerði areas are reamed by drilling yearly.

#### 5.4. Chemical Data Treatment

In this project work, the chemical analysis results for surface samples from Wells ZK-309, ZK-311 and ZK-324 in Yangbajing, NLFI-1, G-2 and G-4 in Hveragerði, and SG-6, SG-7, SG-8, SG-9 and SG-11 in Svartsengi are interpreted by using the WATCH1 program. The chemical data for down-hole sample of Well ZK-323 in Yangbajing is interpreted by using the WATCH3 program. The temperatures at the bottom of each wells are not known. Based on the statements mentioned in Part 2.4 and general reservoir temperature, the chalcedony geothermometer is selected for the samples from Yangbajing and Hveragerði fields and the quartz geothermometer is used for the samples from the Svartsengi field.

In general, the interpreting procedure used in this project work can be described in the following.

1. Creating WATCH program input data file according to Svavarsson (1981). Setting a series of boiling temperatures in the range from the geochemical reservoir temperature to 90°C and giving the degassing factor as 1.

2. Running the program for calculation.
3. Checking if the input data accepted by the program or has agreeable result with chemical knowledge to make sure of the credibility.
4. Using the computer output (Appendix) to make the curves of calcite activity product of the samples (Figures 5.2 to 5.5).
5. Comparing the activity product with the solubility product by means of difference and ratio (Figures 5.7 and 5.6).
6. Interpreting the above figures.

For the down-hole sample analysis data from Well ZK-323 in Yangbajing, the computer output (Appendix 2.1) shows that calcite is very supersaturated under the reservoir condition. This result is not possible because it does not agree with the real situation, i.e. thermodynamic equilibrium. As there is no background knowledge on the sampling and analysis of the Yangbajing samples, Arnorsson (1987b) suggested a method on the basis of geothermometers (as mentioned in Part 2.4) to calibrate the data roughly. The procedure can be described as follows.

1. Using the chemical analysis result as the input data for WATCH3 program and assuming the sample of deep water has been boiled at a reasonable guessing temperature such as 135°C with a series of degassing factors or gas solubility multiplying factor (GSMF).
2. Selecting chalcedony temperature as reservoir temperature for the computer calculation of above input files. The calculated result is adapted as Appendix 2.2.
3. Using the temperature dependent functions or

geothermometers of  $\log(\text{Na}^+/\text{H}^+)$ ,  $\log(\text{K}^+/\text{H}^+)$ ,  $\log(\sqrt{\text{Ca}^{2+}}/\text{H}^+)$ ,  $\log(\sqrt{\text{Mg}^{2+}}/\text{H}^+)$  and  $\log\text{H}_2\text{CO}_3$  listed in Table 2.3 to calculate out the "function values" at each chalcedony reservoir temperature in the computer outputs.

4. Using the computer output results to calculate the "output values" of the above five ones.

5. Comparing the each "function value" with its corresponding "output value" at each GSMF.

6. Using the differences obtained by the above step to make Figure 5.1.

7. Finding out the GSMF value when the difference is zero in Figure 5.1, which is about 0.1.

8. Using the deep water composition on the computer output sheet when the GSMF is 0.1 to creating a new WATCH3 input data file.

9. Running the WATCH3 program with SSTEMP = 999 to calculating the calibrated data at given boiling temperatures with the degassing factor (GSMF) is 1. The output is as Appendix 2.3.

Since the  $\text{CO}_2$  gas geothermometer is not considered to be applicable below  $200^\circ\text{C}$  because of the effect of the salinity of the parent water on the concentration of  $\text{CO}_2$  in the steam (Arnorsson, 1983), it is understandable that the curve in Figure 5.1 for  $\log\text{H}_2\text{CO}_3$  has a big scatter. But for the others they are suitable quite well.

## 5.5. Result

Figure 5.2 is the activity products of the samples from Yangbajing with one step adiabatic boiling temperature. The calcite deposition potential for separator samples is in the order of ZK-311, ZK-324 and ZK-309. The surface separated sample represents the fluid which has been boiled in the well-bore before sampling, therefore some of the calcite has been deposited out of the fluid during the boiling inside the well. This is why Appendix 1 shows that the activity product of deep waters for calcite is smaller than the solubility products under the reservoir temperature. The sample from ZK-323 is a down-hole collected fluid sample. Calcite has not deposited before sampling. So the scaling potential of this sample is much higher than the others. Figure 5.3 shows the activity product of surface separated samples from wells in Svartsengi. Figure 5.4 is for samples from Hveragerði.

Figure 5.5 is a comparison of the calcite scaling potential for samples from Wells ZK-311, NLFI-1 and SG-8, which has the highest deposition thermodynamic potentials among the interpreted samples in Yangbajing, Hveragerði and Svartsengi, respectively. It shows that the lower reservoir temperature, the higher calcite scaling potential. This statement can be a factor guiding the setting and drilling geothermal production wells (see Part 6.6).

Figure 5.6 is the ratio of activity product and solubility product. Figure 5.7 is the difference between them. They are showing the degree of supersaturation for calcite reaches maximum by one step adiabatic boiling the geofluid at a temperature below the reservoir temperature in the range of 15°F to 60°C. This result is useful for geothermal project design and operation. From Appendix 1 we can also have another conclusion, which is that the higher ionic strength of the fluid, the higher calcite deposition potential.

## 6. HANDLING OF CALCITE SCALING IN WELLBORE

Effective scale handling in geothermal operation is often critical to the success of a project. The methods must be designed and tailored to the site-specific conditions. These conditions dictate the type of managing method that will be feasible, since engineer does not take consideration of technical feasibility only, but also concern economic feasibility, and easy operation and maintenance. Calcium carbonate scaling may be handled by following possibilities based on its thermodynamics and kinetics.

### 6.1. Mechanical Removal

Mechanical removal of calcite scaling in geothermal wells is a most practical method used world wide. In Yangbajing, Xizang, China, a equipment and method shown in Figure 6.1 has been used for several years with satisfactory results. Since calcite scaling in the production wells are very heavy (about 0.2 cm/week during the earlier stage of development), the wells must be cleaned daily by lowering the device down to wellbore to scrape the deposits in order to keep them fully producing. During the operation the well is discharging out of the gathering system through a bi-pass valve to carry the debris out of the well. The weight of the equipment is mainly depended on the flowing pressure of the fluid. In case of Yangbajing, it is normally 80-100 kg. The main problem recorded in this operation is the loss of the equipment and blocks of scales into the well bottom to decrease the output of the well.

In Svartsengi and Hveragerði, Iceland, glands (Figure 6.2) are used for cleaning the wells. The gland allows drill pipes to be entered into the well under full pressure, and the calcite is removed by drilling with a convectional drill bit, while the well is flowing and discharging the drill-cutting. The time required to clean the well is only 2-3 days with a truck-mounted rig. Use of this clean method allows unhindered

operation of the plants and the cost is low (Björnsson and Albertsson, 1985).

## **6.2. Pressure Manipulation**

Calcite scaling is developed by flashing, which is resulted from that the process pressure acting on the fluid drops to be lower than the flashing pressure of the geothermal fluid (as discussed in Part 2.2.1). Pressure manipulation can be achieved quite easily by pumping instead of relying on its nature flow. Utilizing down-hole pumps such as shaft-deep-well-pump, turbo-pump and submerged-pump will drastically decrease or eliminate the in-hole pressure drop to maintain the producing fluid as water phase. Thus, the formation of "pressure sensitive" scaling,  $\text{CaCO}_3$ , can be eliminated in geothermal wellbore, or at least shifted from the wellbore into the more accessible surface equipment where the handling becomes much easier.

Unfortunately, the use of down-hole pumps is restricted somewhat by the fluid temperature and well casing structure. At present, no down-hole pump is guarantee to work at wellbore temperature in excess of approximately  $190^\circ\text{C}$  (Corsi, 1987).

## **6.3. Partial Pressure Control**

This control is a potential calcite prevention method. By re-injecting some of the produced carbon dioxide back into the producing well according to the scheme of Figure 6.3 can maintain a high  $\text{CO}_2$  particle pressure, which in turn maintain the dissolved carbon dioxide content in geothermal fluid artificially to keep the carbonic species equilibria. Experiments on this method were carried out in the USA (Kuwada, 1982), but it appears valid only for fluid with low  $\text{CO}_2$  content (as mentioned in Part 2.2).

#### 6.4. pH Manipulation

On-line manipulation of the geothermal fluid pH is another potentially way to avoid scaling. However, the cost of a such process is often overlooked. Adding hydrogen chloride solution to a geothermal fluid in order to decrease the pH below a certain value at which no calcite scaling can form may be technically but not economic feasibility, since excessively large amounts of acid are required to obtain even fairly a small decrease of pH due to many geothermal fluids have an extremely large flow-rate and buffer capacity.

Off-line acidification of geothermal wells within calcite scale has been used in some geothermal fields. But care should be taken, since well casing and other equipments can be corroded by acidic solution when lack of a sufficiently stable inhibitor, which is capable of maintaining its properties at high temperature for a period of time long enough to allow the complete removal of calcite.

#### 6.5. Inhibitors

The utilization of scale inhibitors seems like a promising method of combatting scaling problems. A lot of studies have been carried out on this subject. Inorganic phosphates are able to prevent precipitation of almost insoluble compound if added to the over-saturated  $\text{CaCO}_3$  solution in small quantities. The proposed mechanism suggests that the phosphate maintain in solution large quantities of  $\text{CaCO}_3$  while it begins to crystallize. Practically phosphates do not prevent the initial nucleation, but maintain microscopic the size of crystalline nuclei preventing them to grow (as discussed in Part 4.3). The main drawback of that treatment is the possible precipitation of calcium phosphate with the consequence of further encrustation. Therefore, organic phosphorous has been developed. In organic compounds, phosphorus links to the carbonic atom and hence calcium phosphate can be avoided.

## 6.6. Others

If a sudden increase in diameter of the well (i.e. a liner hanger) is present, calcite scaling may be promoted due to the similar mechanism of pressure drop. Therefore, transitions in the casing diameter should either be avoid or located at a safe distance above or below the predicted flashing zone. It is likely that the scaling rate can be reduced but not eliminated by having a uniform diameter from the bottom to the wellhead. The use of the techniques of cementing through portholes provides a smooth pipe of a single diameter from the reservoir to the wellhead to approach this purpose and also carry the production with less pressure loss (Granados, 1983). Operating the well at a relatively high wellhead pressure, thereby ensuring flashing above the casing-liner joint can also be minimizing deposition of scale.

Increased well casing diameter has reduced frequency of calcite cleaning in Svartsengi field in Iceland, if combining mechanical cleaning and well design improvement with good organization may provide the less costly method that can be applied in the field (Gudmundsson, 1983).

It is common that wells form scale in the wellbore when they are located peripherically with respect to hotter regions of a reservoir. Since hotter source has a less calcite scaling environment (as discussed in Part 4.2.6 and Part 5), therefore the possibility of sitting wells on and/or deepening wells to hotter region is worth consideration (Granados, 1983).

## 7. FLUID INJECTION

### 7.1. Fluid/Formation Compatibility

The successful development of a geothermal reservoir will require injection of heat-depleted brine to improve reservoir longevity and to minimize environmental damage. To maintain injectability, the spent brine must be compatible with the receiving formation, i.e. geological strata. Process chemistry of geothermal fluids is one of the very important factor to influence this brine/formation compatibility. It is discussed and reviewed in detail by Kindle et al. (1984).

In general terms, formation/fluid incompatibility can arise from particulate plugging due to precipitation, clay swelling and dispersing, and influencing of rock-solution equilibria in hydrothermal system of the injected fluid. To diagnose injection problems in this area, information on geological and hydrological characteristics of the receiving formation and data on the injection composition, temperature, and suspended solids content of the fluid are required.

Particulate plugging is the most common type of impairment experienced in geothermal injection wells. It can arise from four processes that have been described by Barkman and Davidson (1972) and shown in Figure 7.1.

- \* Formation of a filter cake on the wellbore face;
- \* Particle invasion into the rock formation, which reduces available pore space or forms an internal filter cake;
- \* Well filling;
- \* Well casing perforation plugging.

Particulate plugging in geothermal systems is often a

combination of the mechanisms outlined above. Experiences show that particles less than 0.45  $\mu\text{m}$  in diameter generally pass through the formation without causing impairment, particles greater than 10  $\mu\text{m}$  in diameter generally accumulate in the wellbore or are retained on the surface and form a filter cake, and particles with diameter between those can invade the formation and cause impairment depending on the formation and fluid properties (Kindle et al., 1984).

In order to avoid particulate plugging, a spent geothermal fluid should be treated by means of either or combined following processes before injection.

- \* Precipitation avoidance or control;
- \* Liquid/solid separation: chemical coagulation/flocculation, sedimentation, filtration, gas flotation;
- \* Purification treatments: reverse osmosis and ion exchange.

Permeability can also be impaired when gas bubbles enter and are entrained in the fluid stream. These bubbles can lodge in pore spaces and plug the formation, but this type of plugging can frequently be remedied by back flushing.

## **7.2. Precipitation Avoidance and Acceleration**

Many brine, particularly those from high-temperature reservoir, undergo severe chemical disequilibrium during the energy extraction process because of temperature and/or pressure changes. As the brine regains equilibrium, precipitates form that can plug the injection process (Table 7.1).

Based on the knowledge of thermodynamics and kinetics of silica, calcite, sulfide and sulfate scales precipitation, process parameters (temperature and pressure) and additives

(acid, inhibitor, carbon dioxide, lime and water) can be used to control scaling before and during the injection process.

When it is uneconomic to prevent precipitation, it may be possible to design a process so that scale formation occurs at all location and in a form that can be manipulated at minimal cost. Among these techniques is the use of crystallizer, crystallizer-separator, reactor clarifier and fluidized bed, and aging the brine in a tank or pond. They control the location of geothermal scaling to surface vessels and keep the injection well usable. They will be most usable for silica, silicate and sulfide scales that have moderate to slow kinetics. Calcite scale, with its rapid kinetics, will probably form in a pipe before reaching a vessel.

During a disposal process, the most universal problem is caused by silica polymerization. Factors that depress the speed of silica precipitation include: decreased temperature, decreased supersaturation ratio, the absence of fluoride ion catalyst, and lowering the pH. Maintaining silica supersaturation ratio below 2 or maintaining high temperature give some opportunity for controlling precipitation at the pH ranges normally. Lowering the pH by one unit slows the kinetics by a factor of 10, and on the other hand, by raising the pH with lime (CaO) addition flocculate the silica (Figures 7.2 and 7.3). As the fluid becomes very acid (pH about 3), the kinetics slows and the presence of fluoride catalyst can maintain the precipitation rate even in the face of further pH drops. Since silica equilibrium solubility increase with temperature, which partially offsets temperature-based kinetic factors, the net effect is that the maximum rate of silica precipitation should occur when the brine is 25°C to 50°C below the temperature for saturation at a given amorphous silica concentration (Table 7.2).

Calcite precipitation is typically a production problem, although it may result from the injection of surface or incompatible waters are involved (as discussed in Part 4).

Sulfide scale frequently occur in conjunction with other scales, although as techniques are used to control these other scales (Figures 7.4 and 7.5), sulfide precipitates become more noticeable as geothermal scales on their own basis. The sulfide chemistry is more complicated and less understood than the silica and calcite chemistry, and it deserves more investigation.

Sulfate scales are a similar problem where incompatible waters are involved.

### **7.3. Chemical Monitoring and Tracer Testing**

Data from sampling and analyzing spent fluid in injection treatment process can be used to identify or understand chemical problems arising from injecting altered or foreign water into a geothermal reservoir by geochemical modeling. The geochemical models can calculated the tendency of the brine to scale in process condition and help in the optimization of critical design of disposal process.

Injection would support reservoir pressure and eliminated surface disposal of spent brine and condensate of geothermal power plant, but it could lead to cold water fingering from injection well to production wells. If large flow-rate of cold water injected into reservoir reaches to production zone rapidly without heated up by heat source to reservoir temperature, it would result from the cooling down of aquifer or even kill the reservoir. Thus, understanding the cold water traveling paths and speed are most important during the whole injection process. Tracer monitoring of well interference is a useful tools for this purpose.

Tracer selection and testing data interpretation are very important two aspects in tracer testing. Factors governing tracer selection are as follows.

- \* High thermal stability in geothermal reservoir;

- \* No interference with other chemicals in water-rock interactions in geothermal formation;
- \* Suitable adsorption-de-adsorption characteristics;
- \* Low background concentration in original geothermal fluid;
- \* High sensitivity in analysis;
- \* Excellent and easy instrument and method for detectability;
- \* Cheap to use, i.e. low price and high activity at low concentration etc.

A test in Svartsengi, Iceland showed that Iodide seems to be a good choice for use in tracer surveys of high temperature geothermal field, at least much better than rhodamine WT dye (Gudmundsson and Hauksson, 1985). Fluorescent dye has also been used in a few geothermal tracer tests at low-to-moderate temperatures (Gudmundsson et al. 1983).

A tracer breakthrough curve (Figure 7.6) shows the concentration of tracer with time. It provides a record of what happens underground when a fluid flows between two or more geothermal wells. Tracer testing provides three main pieces of information (Gudmundsson and Hauksson, 1985).

The first is the arrival time of the peak concentration. It indicates the mean speed of movement of flow in reservoir. Rapid tracer movement implies a high degree of fracturing or high permeability in the reservoir, and may suggest that the thermally swept volume of reservoir rock will be small.

The second parameter is the total tracer recovery. A production well that receives more of the injected water than others is more likely to suffer temperature decline as a

result. The relative recoveries in several production wells can be useful for comparison between wells.

The third one is to analyze the shape of breakthrough curve. it requires the uses of a tracer flow model between the injection and production wells. This procedure is still under development, but shows possibilities for the estimation of fracture characteristics. An estimate of fracture aperture may be useful for calculating the rate of local thermal depletion along the flow path.

## 8. CONCLUSIONS

Geothermal fluids are usually just saturated with respect to calcium carbonate under the water-dominated reservoir conditions. During the exploitation of the fluids, large calcite scale is often developed upon boiling in the production wells due to the concentrating and degassing of the liquid phase, which leads to the reestablishment of the chemical equilibrium in CaO-CO<sub>2</sub>-H<sub>2</sub>O system, and extreme mass flow rate. The lower in reservoir temperature and the higher of ionic strength the fluid, the more severe of the calcite deposition problem.

The degree of calcite supersaturation for a unflashed reservoir fluid reaches a maximum when cooled by 10°C to 60°C through a adiabatic boiling. But simply cooling of the fluid owing to heat losses, i.e. thermal conductivity and/or diffusivity from the fluid to the environment can not cause calcite deposition from the fluid in a general temperature range. Since calcite is formed by ionic reactions in the system, deposition of calcite takes place much faster than the geothermal process operation time. Deposition of calcite in geothermal production well may be mainly controlled by the diffusion mechanism.

Mechanical removal of calcite scale in low enthalpy and high scaling potential production wells as those in Yangbajing and reaming of that in high enthalpy wells as in Svartsengi seem like the practical ways for handling at present. Although the former method is easy for operation, it needs more labor. But that is not a economical problem in Tibet. Using inhibitors is a promising way but it is still under development.

Chemistry can contribute important effects on the successes of geothermal depleted fluid injection. Chemical monitoring and tracer survey can play significant roles in the injection process decision and operation.

The chemical behaviour of geothermal fluids can be estimated by chemical equilibrium process modelling at a certain extent. The usefulness of the input chemical data depends on the sampling and analytical methods and the care taken in the collection and analysis of the sample.

## ACKNOWLEDGEMENT

The author would like to thank his advisor, Dr. Jon-Steinar Gudmundsson, the director of the UNU Geothermal Training Programme for running the whole training and supervising this project with invaluable comments on the report. I am also indebted to Professor Stefán Arnórsson and Dr. Sigurður R. Gíslason, of the University of Iceland, for geochemical lectures and using the WATCH program, and Mr. Hjörtur Þráinsson for help with computer drawing. Many individuals who has involved in this training and project work are acknowledged.

The chemical analysis data interpreted by WATCH program are from ENEL-AQUATER (1985) with the permission from Mr. Zhang Zhenguo, the national project director of UN Project No. CPR 81/011, for Yangbajing field. The Svartsengi and Hveragerði chemical data are from the files of the National Energy Authority.

This training is supported by the People's Government of Xizang Autonomous Region, PRC and the National Energy Authority of Iceland. It is executed by the UNU Geothermal Training Programme in Iceland.

## NOMENCLATURE

- A: Area in Part 4,  $m^2$
- b: Degassing Factor
- C: Concentration in Part 4, Mole/kg
- C: Turbulence Factor in Part 2,  $\text{bar}/(\text{kg}/\text{s})^2$
- D: Depth, m
- d: Diameter, m
- D: Diffusion Factor in Part 4,  $\text{cm}^2/\text{s}$
- f: Friction factor
- G: Gibbs free Energy
- g: Acceleration of Gravity,  $\text{m}/\text{s}^2$
- H: Energy, kJ
- h: Enthalpy, kJ/kg
- I: Ionic Strength
- J: Flux of Mass Transfer
- K: Coefficient
- k: Coefficient
- L: Latent heat, kJ/kg
- m: Molality, mole/kg
- n: Mole Number
- P: Pressure, bar
- Q: Activity Product
- R: Universal gas constant,  $8.314 \text{ kJ}/(\text{kg}^\circ\text{K})$
- r: radial distance
- T: Temperature,  $^\circ\text{K}$
- t: Temperature in Part 2,  $^\circ\text{C}$
- t: Time in Part 4, s
- V: Specific Volume in Part 2,  $\text{m}^3/\text{kg}$
- $V_f$ : Molar Volume,  $\text{cm}^3/\text{mole}$
- V: Volume,  $\text{m}^3$
- v: Velocity, m/s
- W: Flow rate, kg/s
- w: Weight percent
- w: molar weight in Equation (4.51)
- X: Mole fraction
- x: Mass fraction
- Z: Length, m

$Z_i$ : Charges of Species  $i$   
 $[i]$ : activity of species  $i$   
 $\mu$ : Dynamic viscosity,  $\text{Ns/m}^2$   
 $\sigma$ : Surface Tension,  $\text{N/m}$   
 $\alpha$ : Void Fraction  
 $\rho$ : density,  $\text{kg/m}^3$   
 $\varepsilon$ : Absolute roughness factor,  $\text{m}$   
 $\gamma$ : correction factor for  $K_H^0$  in sanility solution  
 $\gamma_i$ : activity coefficient of species  $i$   
 $\nu_i$ : stoichiometric constant  
 $\lambda$ : jump distance,  $\text{cm}$   
erf: error function

## REFERENCES

- Arnorsson, S., (1978): "Precipitation of Calcite from Flashed Geothermal Waters in Iceland," *Contrib. Mineral Petrol.* vol. 66, pp. 21-28.
- Arnorsson, S., Sigurdsson, S. and Svavarsson, H., (1982): "The Chemistry of Geothermal Waters in Iceland, I: Calculation of Aqueous Speciation from 0°C to 370°C," *Geochim. Cosmochim. Acta*, vol. 46, pp. 1513-1532.
- Arnorsson, S., Gunnlaugsson, E. and Svavarsson, H., (1983a): "The Chemistry of Geothermal Waters in Iceland, II: Mineral Equilibria and Independent Variables Controlling Water Compositions," *Geochim. Cosmochim. Acta*, vol. 47, pp. 547-566.
- Arnorsson, S., Gunnlaugsson, E. and Svavarsson, H., (1983b): "The Chemistry of Geothermal Waters in Iceland, III: Chemical Geothermometry in Geothermal Investigations," *Geochim. Cosmochim. Acta*, vol. 47, pp. 567-577.
- Arnorsson, S., (1987a): Personal Communication.
- Arnorsson, S., (1987b): Personal Communication.
- Barkman, J. H. and Davidson, D. H., (1972): "Measuring Water Quality and Predicting Well Impairment," *Trans. AIME*
- Berner, R. A., (1981): "Kinetics of Weathering and Digenesis," *Reviews in Mineralogy*, vol. 8, pp.111-134.
- Björnsson, G. and Albertsson, A., (1985): "The Power Plant at Svartsengi, Development and Experience." GRC Annual Meeting, Kona, Hawaii, pp. 427-442.

- Corsi, R., (1987): "Engineering Aspects of CaCO<sub>3</sub> and SiO<sub>2</sub> Scaling," NATO Advanced Study Institute, Geothermal Reservoir Engineering, Antalya, Turkey, July 1-10.
- Drever, J. I., (1980): "The Geochemistry of Nature Water." pp. 118-119.
- Ellis, A. J. and Golding, R. M., (1963): "The Solubility of Carbon Dioxide above 100°C in Water and in Sodium Chloride Solutions," American Journal of Science, vol. 261, pp. 47-61.
- Ellis, A. J. and Mahon, W. A. J., (1977): "Chemistry and Geothermal Systems," Academic Press, New York.
- ENEL-AQUATER(ENI), (1985): "Reservoir and Production Engineering Study Of the Yangbajing Geothermal Field in Tibet," Draft Final Report, UN Project No. CPR 81/011.
- Fournier, R. O., (1977): "Chemical Geothermometers and Mixing Models for Geothermal Systems," Geothermics, vol. 5, pp. 41-50.
- Fournier, R. O., (1985): "Carbonate Transport and Deposition in the Epithermal Environment," Reviews in Economic Geology, vol. 2, pp. 63-72.
- Granados, E., (1983): "Calcium Carbonate Deposition in Geothermal Wellbores, Miravalles Geothermal Field, Costa Rica," Stanford Geothermal Programme, Stanford University, SGP-TR-67.
- Granados, E. and Gudmundsson, J. S., (1985): "Production Testing in Miravalles Geothermal Field, Costa, Rica," Geothermics, vol. 14. pp. 517-524.

- Gonfiantini, R. (ed.) (1975): "Proc. Int. At. Energy Agency Advisory Group Meeting Appl." Nucl. Tech. Geothermal Stud., Pisa, Italy.
- Gudmundsson, J. S., Johnson, S. E., Horne, R. N., Jackson, P. B. and Culver, G. G., (1983): "Double Tracer Testing in Klamath Falls, Oregon," Proc. Ninth Workshop Geoth. Reservoir Engineering, Report SGP-TR-74, Stanford Geothermal Program.
- Gudmundsson, J. S. and Hauksson, T., (1985): "Tracer Survey in Svartsengi Field 1984," Geothermal Resources Council, TRANSACTIONS, vol. 9, Part II. pp.307-315.
- Gudmundsson, J. S., (1983): "Geothermal Electric Power in Iceland: Development in Perspective," Energy, vol. 8, pp.491-513.
- Gudmundsson, J. S., (1986): "Composite Model of Geothermal Reservoirs," Geothermal Resources Council Bulletin, pp. 3-10.
- Gudmundsson, J. S. and Thorhallsson, S., (1986): "The Svartsengi Reservoir in Iceland," Geothermics, vol. 15, pp. 3-15.
- Henley, R. W. and Brown, K. L., (1985): "A Practical Guide to the Thermodynamics of Geothermal Fluids and Hydrothermal Ore Deposits," Reviews in Economic Geology, vol. 2, pp.25-45.
- Hetsroni, G., (1982): "Handbook of Multiphase Systems," pp. 2-15 to 2-26. Hemisphere Publishing Corporation.
- Hewitt, G. F. and Robert, D. N., (1969): "Studies of Two Phase Flow Patterns by Simultaneous X-ray and Flash Photography," Rept. AERE-M2159, UKAEA, Harwell.

- Keenan, J. H. and Keyes, F. G., (1951): "Thermodynamic Properties of Steam," Wiley, New York.
- Kindle, C. H., Mercer, B. W., Elmore, R. P., Blair, S. C. and Myers, D. A., (1984): "Geothermal Injection Treatment: Process Chemistry, Field Experiences, and Design Options," Battelle, PNL-4767.
- Kuwada, J. T., (1982): "Field Demonstration of the EFP System for Carbonate Scale Control," Geothermal Resources Council Bulletin, Sept.-Oct. pp. 3-9.
- Lasaga, A. C., (1981): "Transition State Theory," Reviews in Mineralogy, vol. 8, pp.135-170.
- Lasaga, A. C., (1984): "Chemical Kinetics of Water-Rock Interactions," J. of Geophysical Research, vol. 89, pp.4009-4025.
- Michaelides, E. E., (1981): "Thermodynamic Properties of Geothermal Fluids," Geothermal Resources Council, TRANSACTIONS, vol. 5, pp. 361-364.
- Nielsen, A. E., (1984): "Electrolyte Crystal Growth Mechanisms," J. Crystal Growth, vol. 67, pp. 289-310.
- Olafsson, M., (1987): "Handbook of Collecting Water and Gas Samples," OS-87021/JHD-03, in Icelandic.
- Parlaktuna, M., (1985): "Two Phase Wellbore Simulator and Analysis of Reinjection Data from Svartsengi, Iceland," UNU Geothermal Training Programme, Report 1985-7.
- Przybylinski, J. L., (1987): "The Role of Bicarbonate Ion in Calcite Formation," SPE Production Engineering, vol. 2, pp. 63-67.

- Reed, M. and Spycher, N., (1984): "Calculation of pH and Mineral Equilibria in Hydrothermal Waters with Application to Geothermometry and Studies of Boiling and Dilution," *Geochim. Cosmochim. Acta*, vol. 48, pp. 1479-1492.
- Scott, D. S., (1963): "Properties of Co-Current Gas-Liquid Flow," *Advances in Chemical Engineering*, vol. 4, pp. 119-277.
- Stumm, W. and Morgan J. J., (1970): "Aquatic Chemistry: An Introduction Emphasizing Chemical Equilibria in Nature Waters," Wiley, New York.
- Sutton, F. M., (1976): "Pressure Temperature Curves for a Two Phase Mixture of Water and Carbon Dioxide," *N. Z. J. Sci.* vol. 19, pp. 297-301.
- Svavarsson, H., (1981): "The WATCH1 and WATCH3 Programs, A Guide for Users." National Energy Authority, Report OS81007.
- Whal, E. F., (1977): "Geothermal Energy Utilization," Wiley, New York.
- Zhou, X. X., (1980): "Interpretation of Subsurface Temperature Measurements in the Mosfellssveit and Ölfusdalur Geothermal Areas. SW-Iceland," UNU Geothermal Training Programme, Report 1980-7.

**APPENDIX 1 Computer Output for Separated Samples From  
Wells ZK-309, ZK-311, ZK-324, NLFI-1 and SG-8**

REP.VBJ.001                      YANGDAJING ZX-324                      TIBET

PROGRAM WATCH1.

WATER SAMPLE (PPM)		GAS (VOL.%)		REFERENCE TEMP.	DEGREES C	.0 (CHA)
PH/DEG.C	8.25/20.0	CO2	99.00	SAMPLING PRESSURE	BARS ABS.	0.1
SiO2	254.00	H2S	.68	DISCHARGE ENTHALPY	WJGUL/EG	.704 (CALCULATED)
NA	395.00	H2	.03	DISCHARGE	EG/SEC.	.0
K	48.50	O2	.00	MEASURED TEMPERATURE	DEGREES C	.0
CA	2.00	CH4	.01	RESISTIVITY/TEMP.	OHMM/DEG.C	.0/ .0
MG	.110	N2	.27	EH/TEMP.	MV/DEG.C	.000/ .0
CO2	196.56	He	0.006			
SO4	48.00					
H2S	12.40					
CL	521.00					
F	10.60	LITERS GAS PER KG				
DISS.SOLIDS	.00	CONDENSATE/DEG.C	5.28/20.0	MEASURED DOWNHOLE TEMP.	DEGREES C/METERS	FLUID INFLOW DEPTH (METERS)
AL	.2500					
B	58.8000	CONDENSATE (PPM)				
FE	.6100	PH/DEG.C	5.98/20.0			
NH3	.3200	CO2	17.28			
Li	9.4	H2S	14.90			
Ba	0.15	NA	16.90			
Br	1.7					
		CONDENSATE WITH NaOH (PPM)				
		CO2	.00			
		H2S	.00			
IONIC STRENGTH =	.02064	IONIC BALANCE :		CATIONS (MOL.EQ.)	.01948338	
				ANIONS (MOL.EQ.)	.02161527	
				DIFFERENCE (%)	-15.62	

DEEP WATER (PPM)		DEEP STEAM (PPM)		GAS PRESSURES (BARS ABS.)	
SiO2	239.03	CO2	750.33	CO2	.176E+01
NA	371.69	H2S	15.56	H2S	.144E-01
K	40.75	H2	.01	H2	.400E+02
CA	1.88	O2	.00	O2	.000E+00
MG	.104	CH4	.03	CH4	.270E+02
SO4	45.17	N2	.98	N2	.549E+01
CL	490.21	NH3	.30	NH3	.125E-04
F	9.98			H2O	.702E+01
DISS.S.	.00			TOTAL	.896E+01
AL	.2352				
B	55.3249			H2O (%)	.00
FE	.5740			BOILING PORTION	.00

SAMPLE = SEP.700.000

ACTIVITY COEFFICIENTS IN DEEP WATER

H+	.850	HSO4-	.831	FE++	.489	FECL+	.823
OH-	.819	F-	.819	FE+++	.236	AL+++	.236
H3SIO4-	.823	CL-	.816	FECH+	.829	ALOH++	.431
H2SIO4--	.481	NA+	.823	FE(OH)3-	.829	AL(OH)2+	.831
H2BO3-	.812	K+	.816	FE(OH)4--	.475	AL(OH)4-	.826
HCO3-	.823	CA++	.489	FEOR++	.475	ALSO4+	.826
CO3--	.468	MG++	.514	FE(OH)2+	.831	AL(SO4)2-	.826
HS-	.819	CAHCO3+	.835	FE(OH)4-	.831	ALF2+	.481
S--	.475	MGHCO3+	.823	FESO4+	.829	ALF4-	.826
HSO4-	.826	CAOH+	.835	FECL++	.475	ALF5--	.468
SO4--	.461	MGOH+	.838	FECL2+	.829	ALF6---	.182
NASO4-	.831	NH4+	.812	FECL4-	.823		

CHEMICAL COMPONENTS IN DEEP WATER (PPM AND LOG MOLE)

H+ (ACT.)	.00	-6.272	MG++	.07	-5.545	FE(OH)3	.09	-6.099
OH-	.12	-5.141	NACL	4.53	-4.110	FE(OH)4-	.07	-6.249
H4SIO4	380.65	-2.402	ECL	.18	-5.624	FECL+	.08	-6.058
H3SIO4-	1.47	-4.812	NASO4-	3.66	-4.513	FECL2	.00	-14.011
H2SIO4--	.00	-9.278	ESO4-	1.46	-4.967	FECL++	.00	-18.209
NAH3SIO4	.27	-5.640	CASO4	.35	-5.585	FECL2+	.00	-19.642
H3BO3	315.58	-2.292	MGSO4	.14	-5.946	FECL3	.00	-22.038
H2BO3-	.84	-4.857	CAC03	.02	-6.616	FECL4-	.00	-24.893
H2CO3	781.72	-1.900	MGCC03	.00	-8.385	FESO4	.03	-6.639
HCO3-	270.11	-2.354	CAHCO3+	1.95	-4.716	FESO4+	.00	-17.751
CO3--	.03	-6.264	MGRCO3+	.02	-6.581	AL+++	.00	-17.246
H2S	10.84	-3.497	CAOH+	.00	-8.109	ALOH++	.00	-11.969
HS-	4.57	-3.860	MGOH+	.00	-7.971	AL(OH)2+	.00	-7.350
S--	.00	-12.843	NH4OH	.27	-5.108	AL(OH)3	.64	-5.063
H2SO4	.00	-13.601	NH4+	.18	-5.005	AL(OH)4-	.04	-6.394
HSO4-	.11	-5.953	FE++	.28	-5.301	ALSO4+	.00	-17.328
SO4--	40.69	-3.373	FE+++	.00	-20.244	AL(SO4)2-	.00	-18.646
HF	.14	-5.154	FEOR+	.20	-5.563	ALF2+	.00	-9.639
F-	9.84	-3.286	FE(OH)2	.01	-7.102	ALF3	.00	-8.440
CL-	487.35	-1.862	FE(OH)3-	.00	-9.602	ALF4-	.00	-9.024
NA+	369.15	-1.794	FE(OH)4--	.00	-15.433	ALF5--	.00	-10.738
K+	43.24	-2.956	FE(OH)++	.00	-13.678	ALF6---	.00	-13.635
CA++	1.00	-4.604	FE(OH)2+	.00	-8.641			

IONIC STRENGTH = .01895      IONIC BALANCE :      CATIONS (MOL.EQ.) .01726122  
 ANIONS (MOL.EQ.) .01971595  
 DIFFERENCE (%) -13.28

CHEMICAL GEOTHERMOMETERS DEGREES C      1000/T DEGREES KELVIN = 2.28

QUARTZ      185.8  
 CHALCEDONY      165.1  
 NAR      218.8

OXIDATION POTENTIAL (VOLTS) :      EH H2S= -.391      EH CH4= -.421      EH H2= -.444      EH NH3= -.415

LOG SOLUBILITY PRODUCTS OF MINERALS IN DEEP WATER

	TEOR.	CALC.		TEOR.	CALC.		TEOR.	CALC.
ADULARIA	-15.333	-15.394	ALBITE LOW	-14.769	-14.229	ANALCIME	-11.963	-11.826
ANHYDRITE	-6.613	-8.625	CALCITE	-10.725	-11.509	CHALCEDONY	-2.402	-2.402
MG-CHLORITE	-80.359	-89.485	FLUORITE	-10.597	-11.660	DOBTHITE	-2.002	-1.102
LAUMONTITE	-25.068	-24.810	MICROCLINE	-16.323	-15.394	MAGNETITE	-24.549	-18.271
CA-MONTMOR.	-75.345	-67.031	K-MONTMOR.	-35.935	-34.103	MG-MONTMOR.	-76.727	-67.950
NA-MONTMOR.	-36.112	-32.337	MUSCOVITE	-18.609	-15.224	PREHNITE	-35.793	-37.778
PYRRHOTITE	-66.841	-47.038	PYRITE	-100.948	-54.531	QUARTZ	-2.577	-2.402
WAIKAITITE	-23.824	-24.810	WOLLASTONITE	9.119	5.225	ZOISITE	-35.520	-37.693
EPIDOTE	-38.824	-38.880	MARCASITE	-80.947	-54.531			

=====

LOG DISTRIBUTION COEFFICIENTS CO2 =-3.20 H2S =-3.71 GAS SOLUBILITY MULTIPLYING FACTOR 1.00

DEEP WATER (PPM)				DEEP STEAM (PPM)		GAS PRESSURES (BARR ABS.)	
SiO2	246.70	CO2	181.20	CO2	18477.29	CO2	.320E+01
NA	383.62	H2S	8.07	H2S	248.54	H2S	.820E+01
K	45.16	H2	.00	H2	.25	H2	.107E+04
CA	1.94	O2	.00	O2	.00	O2	.000E+00
MG	.107	CH4	.00	CH4	.93	CH4	.499E+01
SO4	15.62	N2	.00	N2	31.44	N2	.961E+04
CL	505.95	NH3	.22	NH3	2.81	NH3	.142E+04
F	10.30					H2O	.476E+03
DISS.S.	.00					TOTAL	.480E+01
AL	.2423						
B	57.1012			H2O (%)	3.11		
FE	.5925			BOILING PORTION	.03		

ACTIVITY COEFFICIENTS IN DEEP WATER

H+	.854	HSO4-	.836	FE++	.500	FECL+	.828
OH-	.924	F-	.824	FE+++	.247	AL+++	.247
H3SiO4-	.828	CL-	.821	PROH+	.834	ALOH++	.492
H2SiO4--	.492	NA+	.828	FE(OH)3-	.834	AL(OH)2+	.836
H2BO3-	.817	K+	.821	FE(OH)4--	.486	AL(OH)4-	.831
HCO3-	.828	CA++	.500	PROH++	.486	ALSO4+	.831
CO3--	.479	MO++	.525	FE(OH)2+	.836	AL(SO4)2-	.831
HS-	.824	CAHCO3+	.839	FE(OH)4-	.836	ALP++	.492
S--	.486	MGHCO3+	.828	FEBO4+	.834	ALP2+	.836
HSO4-	.831	CAOH+	.839	FECL++	.486	ALP4-	.831
SO4--	.472	MGOH+	.842	FECL2+	.834	ALP5--	.479
NA2SO4-	.836	NH4+	.817	FECL4-	.828	ALP6---	.192

CHEMICAL COMPONENTS IN DEEP WATER (PPM AND LOG MOLE)

H+ (ACT.)	.00	-7.768	MO++	.07	-5.535	FE(OH)3	.06	-6.261
OH-	2.80	-3.783	NACL	4.26	-4.137	FE(OH)4-	1.14	-5.038
H4SiO4	346.98	-2.443	ZCL	.15	-5.694	FECL+	.90	-8.145
H3SiO4-	40.95	-3.366	NA2SO4-	3.32	-4.554	FECL2	.00	-16.298
H2SiO4--	.05	-6.311	HSO4-	1.30	-5.018	FECL++	.00	-22.250
MAH3SiO4	7.64	-4.189	CASO4	.31	-5.638	FECL2+	.00	-23.678
H3BO3	500.44	-2.310	MGSO4	.12	-6.009	FECL3	.00	-26.113
H2BO3-	25.74	-3.374	CACO3	.55	-5.280	FECL4-	.00	-29.035
H2CO3	16.48	-3.576	MGCO3	.01	-6.981	FEBO4	.00	-8.041
HCO3-	232.75	-2.419	CAHCO3+	1.35	-4.874	FEBO4+	.00	-21.775
CO3--	1.08	-4.743	MGRHCO3+	.02	-6.696	AL+++	.00	-21.326
H2S	.48	-4.850	CAOH+	.01	-6.796	ALOH++	.00	-14.944
HS-	7.36	-3.653	MGOH+	.01	-6.711	AL(OH)2+	.00	-9.186
S--	.00	-11.267	NH4OH	.42	-4.917	AL(OH)3	.20	-5.580
H2SO4	.00	-16.921	NH4+	.02	-6.077	AL(OH)4-	.01	-5.195
HSO4-	.00	-7.649	FE++	.00	-7.269	ALSO4+	.00	-21.517
SO4--	42.70	-3.352	FE+++	.00	-23.989	AL(SO4)2-	.00	-32.879
HF	.00	-6.785	PROH+	.04	-6.259	ALP++	.00	-16.948
F-	10.29	-3.266	FE(OH)2	.02	-6.576	ALP2+	.00	-14.041
CL-	503.29	-1.848	FE(OH)3-	.00	-7.923	ALP3	.00	-13.925
NA+	379.82	-1.782	FE(OH)4--	.00	-12.348	ALP4-	.00	-13.549
K+	44.70	-2.942	FE(OH)++	.00	-16.234	ALP5--	.00	-15.282
CA++	1.08	-4.566	FE(OH)2+	.00	-10.059	ALP6---	.00	-18.215

IONIC STRENGTH = .01973 IONIC BALANCE : CATIONS (MOL.EQ.) .01773999  
 ANIONS (MOL.EQ.) .02073995  
 DIFFERENCE (%) -15.57

OXIDATION POTENTIAL (VOLTS) :      BH H2S= -.511      BH CH4= -.510      BH H2= -.556      BH NH3= -.560

LOG SOLUBILITY PRODUCTS OF MINERALS IN DEEP WATER

	TEOR.	CALC.		TEOR.	CALC.		TEOR.	CALC.
ADULARIA	-15.684	-15.481	ALBITE LOW	-15.067	-14.318	ANALCIME	-12.158	-11.876
ANHYDRITE	-8.366	-8.546	CALCITE	-10.399	-9.930	CHALCEDONY	-2.492	-2.441
MG-CHLORITE	-80.047	-77.594	FLUORITE	-10.561	-11.568	COSENITE	-2.659	-1.249
LAUMONTITE	-25.402	-24.890	MICROCLINE	-16.731	-15.481	MAGNETITE	-15.789	-17.891
CA-MONTMOB.	-75.835	-83.966	K-MONTMOB.	-36.807	-42.577	MG-MONTMOB.	-78.177	-84.924
NA-MONTMOB.	-38.953	-41.413	MUSCOVITE	-18.991	-18.000	PBSHWITE	-15.828	-15.650
PYRRHOTITE	-74.605	-57.694	PYRITE	-111.470	-78.682	QUARTZ	-2.653	-2.480
WAIBAKITE	-23.901	-24.890	WOLLASTONITE	9.469	8.227	ZOISITE	-15.407	-15.309
EPIDOTE	-39.779	-36.298	MARCASITE	-90.765	-78.682			

=====

LOG DISTRIBUTION COEFFICIENTS CO2 =-3.41 H2S =-2.93 GAS SOLUBILITY MULTIPLYING FACTOR 1.00

DEEP WATER (PPM)				DEEP STRAM (PPM)		GAS PRESSURES (BARS ABS.)	
SiO2	257.02	CO2	158.35	CO2	2617.49	CO2	.953E-02
NA	399.66	H2S	8.65	H2S	133.85	H2S	.191E-03
E	47.05	H2	.00	H2	.11	H2	.270E-05
CA	2.02	O2	.00	O2	.00	O2	.000E+00
MG	.111	CH4	.00	CH4	.42	CH4	.120E-05
SO4	46.57	N2	.00	N2	13.99	N2	.243E-04
CL	527.10	NH3	.16	NH3	2.22	NH3	.634E-05
F	10.73					H2O	.370E+01
DISS.S.	.00					TOTAL	.271E+01
AL	.2529						
D	59.4880			H2O (%)	7.00		
FE	.6172			BOILING PORTION	.07		

ACTIVITY COEFFICIENTS IN DEEP WATER

H+	.860	HSO4-	.842	FE++	.514	FECL+	.324
OH-	.831	F-	.831	FE+++	.262	AL+++	.262
H3SiO4-	.834	CL-	.827	FE(OH)+	.840	AL(OH)++	.500
H2SiO4--	.506	NA+	.834	FE(OH)3-	.840	AL(OH)2+	.842
H2BO3-	.824	K+	.827	FE(OH)4--	.501	AL(OH)4-	.827
HCO3-	.834	CA++	.514	FE(OH)++	.501	ALSO4+	.627
CO3--	.494	MG++	.539	FE(OH)2+	.842	AL(SO4)2-	.807
HS-	.831	CAHCO3+	.845	FE(OH)4-	.842	ALF++	.500
S--	.501	MGHCO3+	.834	FE(SO4)+	.840	ALF2+	.842
HSO4-	.837	CAOH+	.845	FECL++	.501	ALF4-	.627
SO4--	.487	MGOH+	.848	FECL2+	.840	ALF5--	.494
NASO4-	.842	NH4+	.824	FECL4-	.834	ALF6---	.205

CHEMICAL COMPONENTS IN DEEP WATER (PPM AND LOG MOLE)

H+ (ACT.)	.00	-8.135	MG++	.08	-5.500	FE(OH)3	.03	-6.467
OH-	3.95	-3.634	NaCl	3.75	-4.193	FE(OH)4-	1.04	-5.076
H4SiO4	319.37	-2.479	ECL	.12	-5.784	FECL+	.00	-7.936
H3SiO4-	78.52	-3.083	NASO4-	2.91	-4.611	FECL2	.00	-18.058
H2SiO4--	.21	-5.680	ESO4-	1.11	-5.087	FECL++	.00	-22.751
NAH3SiO4	14.98	-3.897	CASO4	.27	-5.706	FECL2+	.00	-24.170
H3BO3	282.98	-2.339	MGSO4	.10	-6.085	FECL3	.00	-26.660
H2BO3-	56.35	-3.033	CACO3	.89	-5.050	FECL4-	.00	-29.876
H2CO3	4.73	-4.118	MOCO3	.02	-6.687	FE(SO4)	.00	-8.300
HCO3-	210.90	-2.461	CAHCO3+	.90	-5.049	FE(SO4)+	.00	-22.249
CO3--	2.84	-4.325	MGHCO3+	.81	-6.780	AL+++	.00	-21.873
H2S	.16	-5.337	CAOH+	.01	-6.701	AL(OH)++	.00	-15.445
HS-	6.30	-3.720	MGOH+	.01	-6.650	AL(OH)2+	.00	-9.803
S--	.00	-11.150	NH4OH	.30	-5.663	AL(OH)3	.07	-6.049
H2SO4	.00	-18.099	NH4+	.01	-6.264	AL(OH)4-	.81	-5.072
HSO4-	.00	-8.278	FE++	.01	-6.886	ALSO4+	.00	-22.001
SO4--	45.16	-3.328	FE+++	.00	-24.108	AL(SO4)2-	.00	-23.410
HF	.00	-7.333	FE(OH)+	.11	-5.821	ALF++	.00	-17.825
F-	10.73	-3.248	FE(OH)2	.06	-6.188	ALF2+	.00	-14.767
CL-	524.77	-1.820	FE(OH)3-	.00	-7.632	ALF3	.00	-11.774
NA+	394.70	-1.765	FE(OH)4--	.00	-11.847	ALF4-	.00	-14.850
E+	46.06	-2.923	FE(OH)++	.00	-16.389	ALF5--	.00	-16.184
CA++	1.22	-4.516	FE(OH)2+	.00	-10.323	ALF6---	.00	-19.866

IONIC STRENGTH = .02080 IONIC BALANCE : CATIONS (MOL.EQ.) .01844097  
 ANIONS (MOL.EQ.) .02205440  
 DIFFERENCE (%) -17.85

OXIDATION POTENTIAL (VOLTS) : BH H2S= -1.505 BH CH4= -1.499 BH H2= -1.501 BH NH3= -1.554

LOG SOLUBILITY PRODUCTS OF MINERALS IN DEEP WATER

	THEOR.	CALC.		THEOR.	CALC.		THEOR.	CALC.
ADULARIA	-16.196	-15.546	ALBITE LOW	-15.559	-14.385	ANALCIME	-12.512	-11.907
ANHYDRITE	-6.951	-8.445	CALCITE	-9.992	-9.436	CHALCEDONY	-2.521	-2.479
MG-CHLORITE	-79.901	-76.206	FLUORITE	-10.532	-11.467	COETHITE	-3.508	-1.436
LAUMONTITE	-25.983	-24.930	MICROCLINE	-17.376	-15.546	MAGNETITE	-27.385	-17.475
CA-MONTMOR.	-79.557	-86.232	K-MONTMOR.	-38.347	-43.719	MG-MONTMOR.	-80.832	-87.197
NA-MONTMOR.	-38.446	-42.559	MUSCOVITE	-19.675	-18.328	PREHNITE	-36.045	-34.685
PYRRHOTITE	-84.760	-63.308	PYRITE	-125.505	-87.754	QUARTZ	-2.807	-2.479
WAIKAKITE	-24.116	-24.930	WOLLASTONITE	9.971	8.987	ZOISITE	-35.435	-36.075
EPIDOTE	-41.227	-36.121	MARCASITE	-103.789	-87.754			

LOG DISTRIBUTION COEFFICIENTS CO2 =-3.63 H2S =-3.16 GAS SOLUBILITY MULTIPLYING FACTOR 1.00

DEEP WATER (PPM)				DEEP STREAM (PPM)		GAS PRESSURES (BARB ABS.)	
SiO2	267.49	CO2	148.78	CO2	5603.60	CO2	.340E-02
NA	415.94	H2S	5.45	H2S	100.43	H2S	.760E-04
K	46.96	H2	.00	H2	.07	H2	.942E-06
CA	2.11	O2	.00	O2	.00	O2	.000E-00
MG	.116	CH4	.00	CH4	.27	CH4	.440E-06
SO4	50.54	N2	.00	N2	9.21	N2	.848E-05
CL	548.57	NH3	.12	NH3	1.84	NH3	.278E-05
F	11.16					H2O	.143E+01
DISS.S.	.00					TOTAL	.144E+01
AL	.2532						
B	61.9109			H2O (%)	10.64		
FE	.6424			BOILING PORTION	.11		

ACTIVITY COEFFICIENTS IN DEEP WATER

H+	.865	KSO4-	.848	FE++	.529	FECL+	.840
OH-	.837	F-	.837	FE+++	.277	AL+++	.277
H3SiO4-	.840	CL-	.834	FEOH+	.846	ALOH++	.521
H2SiO4--	.521	NA+	.840	FE(OH)3-	.846	AL(OH)2+	.846
H2BO3-	.830	K+	.834	FE(OH)4--	.515	AL(OH)4-	.840
HCO3-	.840	CA++	.529	FEOH++	.515	ALSO4+	.840
CO3--	.508	MG++	.553	FE(OH)2+	.848	AL(SO4)2-	.840
HS-	.837	CAHCO3+	.851	FE(OH)4-	.848	ALF++	.521
S--	.515	MGHCO3+	.840	FE3O4+	.846	ALF2+	.846
HSO4-	.843	CAOH+	.851	FECL++	.515	ALF4-	.840
SO4--	.501	MGOH+	.854	FECL2+	.846	ALF5--	.506
NASO4-	.848	NH4+	.830	FECL4-	.840	ALF6---	.219

CHEMICAL COMPONENTS IN DEEP WATER (PPM AND LOG MOLE)

H+ (ACT.)	.00	-8.389	MG++	.08	-5.462	FE(OH)3	.02	-6.758
OH-	3.87	-3.643	NaCl	3.02	-4.287	FE(OH)4-	.03	-5.296
H4SiO4	301.29	-2.504	KCl	.10	-5.872	FECL+	.00	-7.500
H3SiO4-	107.65	-2.946	NASO4-	2.55	-4.669	FECL2	.00	-12.089
H2SiO4--	.46	-5.308	KSO4-	.95	-5.155	FECL++	.00	-22.929
MAH3SiO4	21.27	-3.744	CASO4	.23	-5.774	FECL2+	.00	-24.337
H3BO3	262.42	-2.372	MUSO4	.08	-6.171	FECL3	.00	-26.687
H2BO3-	90.21	-2.829	CACOO3	1.10	-4.960	FECL4-	.00	-30.094
H2CO3	1.93	-4.506	MGOO3	.03	-6.506	FE3O4	.00	-7.167
HCO3-	197.71	-2.489	CAHCO3+	.60	-5.225	FE3O4+	.00	-23.391
CO3--	5.52	-4.037	MGHCO3+	.01	-6.842	AL+++	.00	-21.550
H2S	.07	-5.587	CAOH+	.01	-6.766	ALOH++	.00	-15.608
HS-	5.22	-3.802	MGOH+	.01	-6.728	AL(OH)2+	.00	-16.201
S--	.00	-11.178	NH4OH	.23	-5.191	AL(OH)3	.03	-5.424
H2SO4	.00	-19.085	NH4+	.01	-6.295	AL(OH)4-	.89	-5.029
HSO4-	.00	-8.789	FE++	.03	-6.317	ALSO4+	.00	-22.016
SO4--	47.58	-3.305	FE+++	.00	-23.911	AL(SO4)2-	.00	-23.478
HF	.00	-7.763	FEOH+	.32	-5.383	ALF++	.00	-17.595
F-	11.16	-3.231	FE(OH)2	.12	-5.866	ALF2+	.00	-15.622
CL-	548.69	-1.812	FE(OH)3-	.00	-7.599	ALF3	.00	-14.099
NA+	410.12	-1.749	FE(OH)4--	.00	-11.763	ALF4-	.00	-14.820
K+	46.64	-2.905	FE(OH)++	.00	-16.340	ALF5--	.00	-16.554
CA++	1.35	-4.471	FE(OH)2+	.00	-10.304	ALF6---	.00	-19.279

IONIC STRENGTH = .02193 IONIC BALANCE : CATIONS (MOL.EQ.) .01916958  
 ANIONS (MOL.EQ.) .02044803  
 DIFFERENCE (%) -20.09

=====

OXIDATION POTENTIAL (VOLTS) :    EH H2S= -0.486    EH CH4= -0.477    EH H2= -0.554    EH NH3= -0.534

## LOG SOLUBILITY PRODUCTS OF MINERALS IN DEEP WATER

	THEOR.	CALC.		THEOR.	CALC.		THEOR.	CALC.
ADULARIA	-16.847	-15.561	ALBITE LOW	-16.143	-14.421	ANALCIME	-12.945	-11.807
ANHYDRITE	-5.750	-8.353	CALCITE	-9.614	-9.079	CHALCEDONY	-2.764	-2.504
MG-CHLORITE	-80.081	-76.042	FLUORITE	-10.528	-11.365	GOETHITE	-4.297	-1.646
LAUMONTITE	-26.736	-24.933	MICROCLINE	-18.155	-15.581	MAGNETITE	-28.936	-17.327
CA-MONTMOR.	-83.280	-86.377	K-MONTMOR.	-40.404	-43.799	MG-MONTMOR.	-64.474	-67.349
NA-MONTMOR.	-40.447	-42.639	MUSCOVITE	-20.593	-18.310	PREHNITE	-26.476	-24.618
PYRRHOTITE	-94.806	-68.188	PYRITE	-139.758	-94.639	QUARTZ	-3.006	-2.504
WAIKAKITE	-24.474	-24.933	WOLLASTONITE	10.525	9.526	ZOISITE	-35.682	-35.983
EPIDOTE	-42.797	-36.264	MARCASITE	-116.925	-94.639			

LOG DISTRIBUTION COEFFICIENTS CO2 =-3.85 H2S =-3.39 GAS SOLUBILITY MULTIPLYING FACTOR 1.00

DEEP WATER (PPM)				DEEP STREAM (PPM)		GAS PRESSURES (DABS ABS.)	
SI02	277.95	CO2	144.00	CO2	4473.90	CO2	.128E+02
NA	432.21	H2S	4.32	H2S	84.50	H2S	.013E+04
K	50.88	H2	.00	H2	.00	H2	.050E+06
CA	2.19	O2	.00	O2	.00	O2	.000E+00
MG	.120	CH4	.00	CH4	.21	CH4	.163E+06
SO4	52.52	N2	.00	N2	7.00	N2	.315E+06
CL	570.04	NH3	.09	NH3	1.58	NH3	.117E+05
F	11.60					H2O	.701E+00
DISS.S.	.00					TOTAL	.702E+00
AL	.2735						
B	64.3338			H2O (%)	14.00		
FE	.6875			BOILING PORTION	.14		

ACTIVITY COEFFICIENTS IN DEEP WATER

H+	.870	KSO4-	.853	FE++	.542	FECL+	.846
OH-	.843	F-	.843	FE+++	.292	AL+++	.292
H3SiO4-	.846	CL-	.839	PROH+	.851	ALOH++	.534
H2SiO4--	.534	NA+	.846	FE(OH)3-	.851	AL(OH)2+	.853
H2BO3-	.836	K+	.839	FE(OH)4--	.529	AL(OH)4-	.849
HCO3-	.846	CA++	.542	PROH++	.529	ALSO4+	.849
CO3--	.522	MG++	.566	FE(OH)2+	.853	AL(SO4)2-	.849
HS-	.843	CAHCO3+	.857	FE(OH)4-	.853	ALF++	.524
S--	.529	MOHCO3+	.846	FE8O4+	.851	ALF2+	.853
H2SO4-	.849	CAOH+	.857	FECL++	.529	ALF4-	.849
SO4--	.515	MOOH+	.859	FECL2+	.851	ALF5--	.522
NASO4-	.853	NH4+	.836	FECL4-	.846	ALF6---	.232

CHEMICAL COMPONENTS IN DEEP WATER (PPM AND LOG MOLE)

H+ (ACT.)	.00	-8.628	MG++	.09	-5.428	FE(OH)3	.01	-7.251
OH-	3.23	-3.721	NaCl	2.16	-4.433	FE(OH)4-	.20	-5.791
H4SiO4	290.25	-2.520	KCl	.08	-5.961	FECL+	.09	-7.382
H3SiO4-	130.23	-2.864	NASO4-	2.23	-4.728	FECL2	.00	-20.467
H2SiO4--	.80	-5.072	KSO4-	.80	-5.226	FECL++	.00	-23.249
NAH3SiO4	26.96	-3.642	CASO4	.20	-5.842	FECL2+	.00	-24.645
H3BO3	236.34	-2.418	MCSO4	.06	-8.279	FECL3	.00	-27.259
H2BO3-	129.50	-2.672	CACOO	1.23	-4.911	FECL4-	.00	-30.496
H2CO3	.89	-4.844	MCCOO	.04	-8.364	FE8O4	.01	-7.400
HCO3-	187.94	-2.511	CAHCO3+	.39	-5.413	FE8O4+	.00	-22.668
CO3--	9.66	-3.793	MOHCO3+	.01	-8.898	AL+++	.00	-21.289
H2S	.03	-5.996	CAOH+	.01	-6.901	ALOH++	.00	-15.639
HS-	4.16	-3.900	MOOH+	.01	-8.866	AL(OH)2+	.00	-10.501
S--	.00	-11.258	NH4OH	.17	-5.311	AL(OH)3	.01	-6.737
H2SO4	.00	-20.017	NH4+	.01	-6.268	AL(OH)4-	.95	-5.092
H2SO4-	.00	-9.281	FE++	.07	-5.921	ALSO4+	.00	-21.863
SO4--	49.96	-3.284	FE+++	.00	-23.861	AL(SO4)2-	.00	-23.368
HF	.00	-8.174	PROH+	.55	-5.121	ALF++	.00	-17.487
F-	11.60	-3.214	FE(OH)2	.13	-5.848	ALF2+	.00	-15.047
CL-	568.89	-1.795	FE(OH)3-	.00	-7.916	ALF3	.00	-14.194
NA+	425.69	-1.732	FE(OH)4--	.00	-12.100	ALF4-	.00	-14.351
K+	50.88	-2.888	FE(OH)++	.00	-16.459	ALF5--	.00	-16.690
CA++	1.48	-4.433	FE(OH)2+	.00	-10.881	ALF6---	.00	-19.345

IONIC STRENGTH = .02315 IONIC BALANCE : CATIONS (MOL.EQ.) .01990849  
 ANIONS (MOL.EQ.) .02493695  
 DIFFERENCE (%) -22.44

=====

OXIDATION POTENTIAL (VOLTS) :    EH H2S= -.462    EH CH4= -.452    EH H2= -.543    EH NH3= -.511

## LOG SOLUBILITY PRODUCTS OF MINERALS IN DEEP WATER

	TEOB.	CALC.		TEOB.	CALC.		TEOB.	CALC.
ADULARIA	-17.632	-15.589	ALBITE LOW	-16.859	-14.431	ANALCIME	-13.478	-11.911
ANHYDRITE	-6.467	-8.271	CALCITE	-9.272	-8.775	CHALCEDONY	-2.922	-2.520
MG-CHLORITE	-80.616	-76.432	FLUORITE	-10.556	-11.276	COBTHITE	-5.041	-2.064
LAUMONTITE	-27.678	-24.910	MICROCLINE	-19.091	-15.589	MAGNETITE	-30.464	-17.907
CA-MONTMOR.	-88.132	-85.509	K-MONTMOR.	-43.045	-43.369	MO-MONTMOR.	-89.231	-86.485
NA-MONTMOR.	-43.022	-42.210	MUSCOVITE	-21.778	-18.129	PREHNITE	-17.142	-14.593
PYRENOTITE	-104.804	-74.498	PYRITE	-154.380	-102.437	QUARTZ	-3.195	-2.520
WAIKANEITE	-24.987	-24.910	WOLLASTONITE	11.140	10.037	ZOISITE	-36.166	-35.330
EPIDOTE	-44.416	-36.744	MARCASITE	-130.306	-102.437			

REP.YBJ.002 YANGBAJING ZE-311 TIBET

PROGRAM WATCH1.

WATER SAMPLE (PPM)		GAS (VOL.%)		REFERENCE TEMP.		DEGREES C		.0 (CRA)	
PH/DEG.C	8.43/20.0	CO2	99.64	SAMPLING PRESSURE	BARS ABS.	3.2			
SiO2	255.00	H2S	.22	DISCHARGE ENTHALPY	MJ/0UL/KG	.705 (CALCULATED)			
NA	400.00	H2	.02	DISCHARGE	KG/SRC.	.3			
K	45.50	O2	.00	MEASURED TEMPERATURE	DEGREES C	.0			
CA	2.20	CH4	.01	RESISTIVITY/TEMP.	OHMM/DEG.C	.0/ .0			
MG	.110	N2	.32	SH/TEMP.	MV/DEG.C	.000/ .0			
CO2	311.04	He	0.0055						
SO4	41.50								
H2S	26.00								
CL	523.00								
F	13.20	LITERS GAS PER KG							
DISS.SOLIDS	.00	CONDENSATE/DEG.C	6.01/20.0	MEASURED DOWNHOLE TEMP.	DEGREES C/METERS			FLUID INFLOW	DEPTH (METERS)
AL	.2100								
P	58.4500	CONDENSATE (PPM)							
FE	.0000	PH/DEG.C	6.65/20.0						
NH3	.0000	CO2	8.64						
Li	9.2	H2S	26.00						
Ba	0	NA	1.20						
Br	1.4								
		CONDENSATE WITH NAOH (PPM)							
		CO2	.00						
		H2S	.00						

IONIC STRENGTH = .02234 IONIC BALANCE : CATIONS (MOL.EQ.) .01863689  
 ANIONS (MOL.EQ.) .02486035  
 DIFFERENCE (%) -28.62

DEEP WATER (PPM)		DEEP STEAM (PPM)		GAS PRESSURES (BARS ABS.)	
SiO2	239.67	CO2	952.27	CO2	.202E+01
NA	375.92	H2S	27.13	H2S	.223E-01
K	42.76	H2	.01	H2	.293E-02
CA	2.07	O2	.00	O2	.000E+00
MG	.103	CH4	.03	CH4	.240E-02
SO4	39.00	N2	1.35	N2	.154E-01
CL	490.54	NH3	.00	NH3	.000E+00
F	10.53			H2O	.703E+01
DISS.S.	.00			TOTAL	.910E+01
AL	.1973				
B	54.9268	H2O (%)			.00
FE	.0000	BOILING PORTION			.00

SAMPLE = ESP.YBJ.002

ACTIVITY COEFFICIENTS IN DEEP WATER

H+	.847	HSO4-	.827	FE++	.479	FECL+	.818
OH-	.814	F-	.814	FE+++	.227	AL+++	.227
H3SIO4-	.818	CL-	.811	FEOH+	.824	ALOH++	.470
H2SIO4--	.470	NA+	.818	FE(OH)3-	.824	AL(OH)2+	.827
H2BO3-	.807	K+	.811	FE(OH)4--	.465	AL(OH)4-	.821
HCO3-	.818	CA++	.479	FEOH++	.465	ALSO4+	.821
CO3--	.457	MG++	.505	FE(OH)2+	.827	AL(SO4)2-	.821
HS-	.814	CAHCO3+	.830	FE(OH)4-	.827	ALF++	.470
S--	.465	MGHCO3+	.818	FESO4+	.824	ALF2+	.827
HSO4-	.821	CAOH+	.830	FECL++	.465	ALF4-	.821
SO4--	.450	MGOH+	.833	FECL2+	.824	ALF5--	.457
NASO4-	.827	NH4+	.807	FECL4-	.818	ALF6---	.173

CHEMICAL COMPONENTS IN DEEP WATER (PPM AND LOG MOLE)

H+ (ACT.)	.00	-6.419	MG++	.07	-5.543	FE(OH)3	.00	.000
OH-	.17	-4.991	NACL	4.53	-4.110	FE(OH)4-	.00	.000
H4SIO4	380.97	-2.402	KCL	.17	-5.639	FECL+	.00	.000
H3SIO4-	2.07	-4.662	NASO4-	3.13	-4.580	FECL2	.00	.000
H2SIO4--	.00	-8.975	ESO4-	1.21	-5.049	FECL++	.00	.000
NAH3SIO4	.38	-5.490	CASO4	.26	-5.717	FECL2+	.00	.000
H3BO3	312.96	-2.296	MGSO4	.11	-6.024	FECL3	.00	.000
H2BO3-	1.18	-4.711	CACCO3	.05	-6.323	FECL4-	.00	.000
H2CO3	896.41	-1.840	MGCCO3	.00	-8.037	FESO4	.00	.000
HCO3-	436.73	-2.145	CAHCO3+	2.74	-4.567	FESO4+	.00	.000
CO3--	.08	-5.901	MGHCO3+	.04	-6.378	AL+++	.00	-17.758
H2S	16.82	-3.307	CAOH+	.00	-8.019	ALOH++	.00	-12.340
HS-	10.00	-3.519	MGOH+	.00	-7.826	AL(OH)2+	.00	-7.579
S--	.00	-12.348	NH4OH	.00	.000	AL(OH)3	.53	-5.166
H2SO4	.00	-13.967	NH4+	.00	.000	AL(OH)4-	.04	-6.329
HSO4-	.07	-6.169	FE++	.00	.000	ALSO4+	.00	-17.926
SO4--	35.28	-3.435	FE+++	.00	.000	AL(SO4)2-	.00	-19.316
HF	.11	-5.278	PEOH+	.00	.000	ALF++	.00	-13.186
F-	10.43	-3.261	FE(OH)2	.00	.000	ALF2+	.00	-10.120
CL-	487.71	-1.861	FE(OH)3-	.00	.000	ALF3	.00	-8.900
NA+	373.46	-1.789	FE(OH)4--	.00	.000	ALF4-	.00	-9.459
K+	42.32	-2.966	FE(OH)++	.00	.000	ALF5--	.00	-11.143
CA++	.89	-4.656	FE(OH)2+	.00	.000	ALF6---	.00	-14.005

IONIC STRENGTH = .02037 IONIC BALANCE : CATIONS (MOL.EQ.) .01740432  
 ANIONS (MOL.EQ.) .02255492  
 DIFFERENCE (%) -25.78

CHEMICAL GEOTHERMOMETERS DEGREES C 1000/T DEGREES KELVIN = 2.28

QUARTZ 185.9  
 CHALCEDONY 165.2  
 NAK 215.2

OXIDATION POTENTIAL (VOLTS) : EH H2S= -.410 EH CH4= -.432 EH H2= -.448 EH NH3= 99.999

LOG SOLUBILITY PRODUCTS OF MINERALS IN DEEP WATER

	TEOR.	CALC.		TEOR.	CALC.		TEOR.	CALC.
ADULARIA	-15.332	-15.484	ALBITE LOW	-14.768	-14.304	ANALCIME	-11.962	-11.902
ANHYDRITE	-6.614	-8.757	CALCITE	-10.726	-11.217	CHALCEDONY	-2.402	-2.402
MG-CHLORITE	-80.361	-87.488	FLUORITE	-10.598	-11.675	GOETHITE	-2.000	99.999
LAUMONTITE	-25.067	-25.026	MICROCLINE	-16.321	-15.484	MAGNETITE	-24.544	99.999
CA-MONTMOR.	-75.342	-69.958	K-MONTMOR.	-35.933	-35.548	MG-MONTMOR.	-75.723	-76.823
NA-MONTMOR.	-36.110	-34.368	MUSCOVITE	-16.698	-15.767	PERHYTE	-35.789	-37.786
PERROTITE	-66.808	99.999	PYRITE	-100.900	99.999	QUARTZ	-2.576	-2.400
WALBARKITE	-23.824	-25.026	WOLLASTONITE	2.117	2.450	SOFSITE	-35.520	-37.901
EPIDOTE	-38.818	99.999	MARCASITE	-80.900	99.999			





23001201088706120050 Svartsengi SG-8 GRINDAVIK

PROGRAM WATCH1.

WATER SAMPLE (PPM)		STEAM SAMPLE				
PH/DEG.C	6.44/23.9	GAS (VOL.%)		REFERENCE TEMP.	DEGREES C	.0 (QTZ)
SiO2	514.80	CO2	96.31			
NA	6993.00	H2S	1.23	SAMPLING PRESSURE	BARS ABS.	16.8
K	1099.00	H2	.07	DISCHARGE ENTHALPY	MJ/EG	1.057 (CALCULATED)
CA	1053.00	O2	.00	DISCHARGE	KG/SEC.	.0
MG	.811	CH4	.05			
CO2	42.20	N2	1.98	MEASURED TEMPERATURE	DEGREES C	.0
SO4	31.64	Ar	0.541	RESISTIVITY/TEMP.	OHMM/DEG.C	.0/ .0
H2S	.69			RH/TEMP.	MV/DEG.C	.000/ .0
CL	13597.00					
F	.14	LITERS GAS PER KG				
DISS.SOLIDS	24352.00	CONDENSATE/DEG.C	1.56/13.8	MEASURED DOWNHOLE TEMP.	DEGREES C/METERS	FLUID INFLOW DEPTH (METERS)
AL	.0000					
B	.0000	CONDENSATE (PPM)				
FE	.0400	PH/DEG.C	4.34/24.4			
NH3	.0000	CO2	1590.00			
Mn	0.3	H2S	40.80			
		NA	9.27			
		CONDENSATE WITH NaOH (PPM)				
		CO2	4220.00			
		H2S	70.00			

IONIC STRENGTH = .40987 IONIC BALANCE : CATIONS (MOL.EQ.) .38342290  
 ANIONS (MOL.EQ.) .38332380  
 DIFFERENCE (%) .03

DEEP WATER (PPM)		DEEP STEAM (PPM)		GAS PRESSURES (BARS ABS.)	
SiO2	467.10	CO2	429.64	CO2	.108E+01
NA	6344.48	H2S	7.12	H2S	.741E-02
K	997.03	H2	.01	H2	.243E-02
CA	955.35	O2	.00	O2	.858E-36
MG	.736	CH4	.05	CH4	.256E-02
SO4	28.71	N2	3.40	N2	.804E-01
CL	12335.00	NH3	.00	NH3	.000E+00
F	.13			H2O	.348E+02
DISS.S.	22093.65			TOTAL	.360E+02
AL	.0000				
B	.0000	H2O (%)			.00
FE	.0363	BOILING PORTION			.00

SAMPLE = 23001201088705120050

ACTIVITY COEFFICIENTS IN DEEP WATER

H+	.635	HSO4-	.544	FE++	.109	FECL+	.495
OH-	.474	F-	.474	FE+++	.021	AL+++	.021
H3SiO4-	.495	CL-	.452	FE(OH)+	.531	ALOH++	.096
H2SiO4--	.096	NA+	.495	FE(OH)3-	.531	AL(OH)2+	.544
H2BO3-	.428	K+	.452	FE(OH)4--	.087	AL(OH)4-	.514
HCO3-	.495	CA++	.109	FE(OH)++	.087	ALSO4+	.514
CO3--	.076	MG++	.155	FE(OH)2+	.544	AL(SO4)2-	.514
HS-	.474	CAHCO3+	.562	FE(OH)4-	.544	ALP++	.096
S--	.087	MGHCO3+	.495	FE(SO4)+	.531	ALP2+	.544
HSO4-	.514	CAOH+	.562	FECL++	.087	ALP4-	.514
SO4--	.065	MGOH+	.577	FECL2+	.531	ALP5--	.076
NASO4-	.544	NH4+	.428	FECL4-	.495	ALP6---	.003

CHEMICAL COMPONENTS IN DEEP WATER (PPM AND LOG MOLE)

H+ (ACT.)	.00	-5.375	MG++	.72	-4.528	FE(OH)3	.05	-6.362
OH-	.07	-5.373	NACL	1436.22	-1.609	FE(OH)4-	.02	-6.729
H4SiO4	746.47	-2.110	KCL	108.16	-2.838	FECL+	.00	-7.693
H3SiO4-	.33	-5.455	NASO4-	5.56	-4.331	FECL2	.00	-10.890
H2SiO4--	.00	-10.747	KSO4-	3.80	-4.551	FECL++	.00	-16.975
NAH3SiO4	.45	-5.422	CASO4	14.43	-3.975	FECL2+	.00	-17.723
H3BO3	.00	.000	MGSO4	.05	-6.386	FECL3	.00	-18.915
H2BO3-	.00	.000	CACOS	.04	-6.401	FECL4-	.00	-20.059
H2CO3	570.60	-2.036	MGCO3	.00	-10.403	FE(SO4)	.00	-11.200
HCO3-	7.30	-3.922	CAHCO3+	44.84	-3.353	FE(SO4)+	.00	-19.512
CO3--	.00	-8.847	MGHCO3+	.00	-7.255	AL+++	.00	.000
H2S	6.95	-3.690	CAOH+	.16	-5.562	ALOH++	.00	.000
HS-	.16	-5.320	MGOH+	.00	-6.934	AL(OH)2+	.00	.000
S--	.00	-14.195	NH4OH	.00	.000	AL(OH)3	.00	.000
H2SO4	.00	-11.493	NH4+	.00	.000	AL(OH)4-	.00	.000
HSO4-	.80	-5.083	FE++	.00	-8.234	ALSO4+	.00	.000
SO4--	10.51	-3.961	FE+++	.00	-21.558	AL(SO4)2-	.00	.000
HF	.04	-5.692	FE(OH)+	.00	-8.846	ALP++	.00	.000
F-	.09	-5.311	FE(OH)2	.00	-10.230	ALP2+	.00	.000
CL-	11412.36	-4.492	FE(OH)3-	.00	-11.899	ALP3	.00	.000
NA+	5778.32	-6.600	FE(OH)4--	.00	-17.943	ALP4-	.00	.000
K+	939.21	-1.619	FE(OH)++	.00	-14.501	ALP5--	.00	.000
CA++	933.20	-1.633	FE(OH)2+	.00	-9.024	ALP6---	.00	.000

IONIC STRENGTH = .34578      IONIC BALANCE :      CATIONS (MOL.EQ.) .32243390  
 ANIONS (MOL.EQ.) .32228410  
 DIFFERENCE (%) .05

CHEMICAL GROTHERMOMETERS DEGREES C      1000/T DEGREES KELVIN = 1.94

QUARTZ      242.2  
 CHALCEDONY      999.9  
 NAK      245.8

OXIDATION POTENTIAL (VOLTS) :      EH H2S= -.401      EH CH4= -.463      EH H2= -.416      EH NH3= 99.999

LOG SOLUBILITY PRODUCTS OF MINERALS IN DEEP WATER

	TROR.	CALC.		TROR.	CALC.		TROR.	CALC.
ADULARIA	-14.432	99.999	ALBITE LOW	-13.978	99.999	ANALCINE	-11.524	99.999
ANHYDRITE	-7.963	-7.739	CALCITE	-12.571	-12.560	CHALCEDONY	-2.026	-2.110
MG-CHLORITE	-84.296	99.999	FLUORITE	-10.916	-13.863	GOETHITE	1.846	-1.296
LAUMONTITE	-24.533	99.999	MICROCLINE	-15.125	99.999	MAGNETITE	-17.676	-23.182
CA-MONTMOR.	-72.624	99.999	K-MONTMOR.	-34.033	99.999	MG-MONTMOR.	-74.121	99.999
NA-MONTMOR.	-34.306	99.999	MUSCOVITE	-17.852	99.999	PREHNITE	-37.076	99.999
PYRRHOTITE	-25.401	-49.833	PYRITE	-46.907	-59.476	QUARTZ	-2.139	-2.110
WAIRAKITE	-24.411	99.999	WOLLASTONITE	7.616	6.046	ZOISITE	-37.620	99.999
EPIDOTE	-37.239	99.999	MARCASITE	-29.886	-59.476			



ACTIVITY COEFFICIENTS IN DEEP WATER

H+	.893	ES04-	.883	FE++	.614	FECL+	.879
OH-	.877	F-	.877	FE+++	.362	AL+++	.362
H3SIO4-	.879	CL-	.876	FE0H+	.882	ALOH++	.610
H2SIO4--	.610	NA+	.879	FE(OH)3-	.882	AL(OH)2+	.883
H2B03-	.874	K+	.876	FE(OH)4--	.606	AL(OH)4-	.880
HCO3-	.879	CA++	.614	FE0H++	.606	ALSO4+	.880
CO3--	.602	MG++	.629	FE(OH)2+	.883	AL(SO4)2-	.880
HS-	.877	CAHCO3+	.885	FE(OH)4-	.883	ALP++	.610
S--	.606	MGHCO3+	.879	FE04+	.882	ALP2+	.883
H04-	.880	CAOH+	.885	FECL++	.606	ALP4-	.880
SO4--	.598	MGOH+	.886	FECL2+	.882	ALP5--	.602
NASO4-	.883	NH4+	.874	FECL4-	.879	ALP6---	.320

CHEMICAL COMPONENTS IN DEEP WATER (PPM AND LOG MOL/L)

H+ (ACT.)	.00	-7.229	MG++	.00	-7.314	FE(OH)3	.00	.000
OH-	.96	-4.249	NACL	.56	-5.017	FE(OH)4-	.00	.000
H4SIO4	359.86	-2.427	KCL	.01	-6.776	FECL+	.00	.000
H3SIO4-	11.77	-3.907	NASO4-	1.92	-4.792	FECL2	.00	.000
H2SIO4--	.00	-7.480	ES04-	.45	-5.480	FECL++	.00	.000
NAH3SIO4	1.05	-5.052	CASO4	.53	-5.407	FECL2+	.00	.000
H3B03	.00	.000	MGS04	.00	-7.545	FECL3	.00	.000
H2B03-	.00	.000	CAC03	.12	-5.924	FECL4-	.00	.000
H2CO3	37.06	-3.224	MGC03	.00	-9.454	FE04	.00	.000
HCO3-	117.61	-2.715	CAHCO3+	.99	-5.011	FE04+	.00	.000
CO3--	.11	-5.720	MGHCO3+	.00	-8.643	AL+++	.00	-19.889
H2S	3.60	-3.976	CAOH+	.00	-7.137	ALOH++	.00	-13.684
HS-	13.47	-3.390	MGOH+	.00	-8.789	AL(OH)2+	.00	-8.132
S--	.00	-11.525	NH4OH	.00	.000	AL(OH)3	.93	-4.925
H2SO4	.00	-15.503	NH4+	.00	.000	AL(OH)4-	.54	-5.246
H04-	.01	-6.889	FE++	.00	.000	ALSO4+	.00	-19.744
SO4--	40.69	-3.373	FE+++	.00	.000	AL(SO4)2-	.00	-20.970
HF	.00	-6.945	FE0H+	.00	.000	ALP++	.00	-16.099
F-	1.49	-4.104	FE(OH)2	.00	.000	ALP2+	.00	-13.810
CL-	128.17	-2.442	FE(OH)3-	.00	.000	ALP3	.00	-13.404
NA+	157.18	-2.165	FE(OH)4--	.00	.000	ALP4-	.00	-14.822
K+	10.77	-3.560	FE(OH)++	.00	.000	ALP5--	.00	-17.412
CA++	1.00	-4.602	FE(OH)2+	.00	.000	ALP6---	.00	-21.223

IONIC STRENGTH = .00757      IONIC BALANCE :    CATIONS (MOL.EQ.) .00717245  
 ANIONS (MOL.EQ.) .00706562  
 DIFFERENCE (%)      1.50

CHEMICAL GROTHERMOMETERS DEGREES C      1000/T DEGREES KELVIN = 2.30

QUARTZ      181.8  
 CHALCEDONY      160.9  
 NAK      163.5

OXIDATION POTENTIAL (VOLTS) :    EH H2S= -.482    EH CH4= -.511    EH H2= -.549    EH NH3= 99.999

LOG SOLUBILITY PRODUCTS OF MINERALS IN DEEP WATER

	TEOR.	CALC.		TEOR.	CALC.		TEOR.	CALC.
ADULARIA	-15.419	-15.708	ALBITE LOW	-14.847	-14.312	ANALCIME	-12.016	-11.885
ANHYDRITE	-6.543	-8.410	CALCITE	-10.633	-10.754	CHALCEDONY	-2.427	-2.427
MG-CHLORITE	-80.256	-88.925	FLUORITE	-10.586	-13.136	GORTHITE	-2.191	99.999
LAUMONTITE	-25.153	-24.142	MICROCLINE	-16.430	-15.708	MAGNETITE	-24.898	99.999
CA-MONTMOR.	-75.717	-73.881	E-MONTMOR.	-36.155	-38.151	MG-MONTMOR.	-77.088	-76.583
NA-MONTMOR.	-36.325	-36.755	MUSCOVITE	-18.705	-16.718	PRRHNITE	-35.792	-35.141
PYRRHOTITE	-69.014	99.999	PYRITE	-103.877	99.999	QUARTZ	-2.606	-2.427
WATRARITE	-23.838	-24.142	WOLLASTONITE	9.214	7.218	ZOISITE	-35.477	-35.646
EPIDOTE	-39.075	99.999	MARCASITE	-83.685	99.999			

APPENDIX 2.1 Computer Output for Downhole Sample of  
Well ZK-323



ACTIVITY COEFFICIENTS IN DEEP WATER

H+	.843	KSO4-	.822	FE++	.469	FECL+	.813
OH-	.809	F-	.809	FE+++	.220	AL+++	.220
H3SiO4-	.813	CL-	.805	FEOH+	.820	ALOH++	.461
H2SiO4--	.461	NA+	.813	FE(OH)3-	.820	AL(OH)2+	.822
H2BO3-	.801	K+	.805	FE(OH)4--	.455	AL(OH)4-	.816
HCO3-	.813	CA++	.469	FEOH++	.455	ALSO4+	.816
CO3--	.447	NG++	.497	FE(OH)2+	.822	AL(SO4)2-	.816
HS-	.809	CAHCO3+	.826	FE(OH)4-	.822	ALF++	.461
S--	.455	MGHCO3+	.813	FESO4+	.820	ALF2+	.822
H2SO4-	.816	CAOH+	.826	FECL++	.455	ALF4-	.816
SO4--	.439	NGOH+	.829	FECL2+	.820	ALF5--	.447
NASO4-	.822	NH4+	.801	FECL4-	.813	ALF6---	.164

CHEMICAL COMPONENTS IN DEEP WATER (PPM AND LOG MOLE)

H+ (ACT.)	.00	-7.632	MG++	.27	-4.962	FE(OH)3	.34	-5.495
OH-	2.65	-3.808	NaCl	5.13	-4.057	FE(OH)4-	6.08	-4.309
H4SiO4	361.55	-2.425	KCl	.19	-5.590	FECL+	.00	-7.769
H3SiO4-	32.35	-3.468	NASO4-	2.93	-4.608	FECL2	.00	-15.962
H2SiO4--	.03	-6.551	KSO4-	1.15	-5.072	FECL++	.00	-21.521
NAH3SiO4	6.95	-4.230	CASO4	1.26	-5.032	FECL2+	.00	-22.981
H3BO3	317.04	-2.290	MGSO4	.33	-5.559	FECL3	.00	-25.404
H2BO3-	19.92	-3.485	CACO3	4.41	-4.356	FECL4-	.00	-28.281
H2CO3	49.24	-3.100	MGCO3	.04	-6.277	FESO4	.00	-8.485
HCO3-	424.78	-2.157	CAHCO3+	15.45	-3.816	FESO4+	.00	-21.225
CO3--	1.30	-4.666	MGHCO3+	.12	-5.834	AL+++	.00	-20.471
H2S	.48	-4.854	CAOH+	.05	-6.061	ALOH++	.00	-13.949
HS-	4.87	-3.831	NGOH+	.03	-6.102	AL(OH)2+	.00	-8.077
S--	.00	-11.471	NH4OH	.65	-4.733	AL(OH)3	2.50	-4.494
H2SO4	.00	-16.567	NH4+	.02	-5.926	AL(OH)4-	3.92	-4.384
H2SO4-	.00	-7.521	FE++	.01	-6.957	ALSO4+	.00	-20.773
SO4--	30.01	-3.505	FE+++	.00	-23.454	AL(SO4)2-	.00	-22.264
HF	.01	-6.521	FEOH+	.09	-5.928	ALF++	.00	-15.948
F-	10.80	-3.246	FE(OH)2	.06	-6.181	ALF2+	.00	-12.922
CL-	485.76	-1.863	FE(OH)3-	.00	-7.401	ALF3	.00	-11.722
NA+	444.06	-1.714	FE(OH)4--	.00	-11.876	ALF4-	.00	-12.282
K+	51.32	-2.882	FE(OH)++	.00	-15.621	ALF5--	.00	-13.952
CA++	5.70	-3.847	FE(OH)2+	.00	-9.331	ALF6---	.00	-16.779

IONIC STRENGTH = .02249 IONIC BALANCE : CATIONS (MOL.EQ.) .02109279  
 ANIONS (MOL.EQ.) .02296164  
 DIFFERENCE (%) -8.48

CHEMICAL GROTHERMOMETERS DEGREES C 1000/T DEGREES KELVIN = 2.30

QUARTZ 182.2  
 CHALCEDONY 161.2  
 NAK 217.2

OXIDATION POTENTIAL (VOLTS) : EH H2S= -.519 EH CH4= 99.999 EH H2= 99.999 EH NH3= 99.999

LOG SOLUBILITY PRODUCTS OF MINERALS IN DEEP WATER

	THEOR.	CALC.		THEOR.	CALC.		THEOR.	CALC.
ADULARIA	-15.412	-14.473	ALBITE LOW	-14.840	-13.301	ANALCIME	-12.011	-10.876
ANHYDRITE	-6.549	-8.038	CALCITE	-10.640	-9.191	CHALCEDONY	-2.425	-2.425
MG-CHLORITE	-80.263	-73.247	FLUORITE	-10.587	-10.851	GORTHITE	-2.176	-.495
LAUMONTITE	-25.146	-22.319	MICROCLINE	-16.421	-14.473	MAGNETITE	-24.870	-16.074
CA-MONTMOR.	-75.687	-69.838	K-MONTMOR.	-36.137	-35.807	MG-MONTMOR.	-77.058	-70.928
NA-MONTMOR.	-36.307	-34.635	MUSCOVITE	-18.697	-15.118	PERHWITE	-35.792	-31.869
PYRRHOTITE	-68.838	-51.584	PYRITE	-103.639	-72.837	QUARTZ	-2.603	-2.425
WAIKAITITE	-23.837	-22.319	WOLLASTONITE	9.206	8.665	ZOISITE	-35.480	-32.192
EPIDOTE	-39.053	-32.364	MARCASITE	-83.463	-72.837			

**APPENDIX 2.2 Computer Output for Calibration of the  
Downhole Sample from Well ZK-323**

UNU Geothermal Training Programme

=====

RBP.YBJ.004

YANGBAJING ZK-323

TIBBT

PROGRAM WATCH3.

TEMPERATURE FIXING STEAM LOSS 135.0 DEGREES C

WATER SAMPLE (PPM)

STEAM SAMPLE

PH/DEG.C	7.85/20.0	GAS (VOL.%)	REFERENCE TEMP.	DEGREES C	.0 (CHA)
SiO2	250.00	CO2			
NA	448.00	H2S	SAMPLING PRESSURE	BARS ABS.	
K	51.75	H2	DISCHARGE ENTHALPY	MJ/OL/KG	
CA	14.00	O2	DISCHARGE	KG/SEC.	.0
MG	.400	CH4			
CO2	351.00	N2	MEASURED TEMPERATURE	DEGREES C	.0
SO4	34.35		RESISTIVITY/TEMP.	OHM/DEG.C	.0/ .0
H2S	5.50		BH/TEMP.	MV/DEG.C	.000/ .0
CL	489.00				
F	10.80	LITERS GAS PER KG			
DISS.SOLIDS	.00	CONDENSATE/DEG.C	MEASURED DOWNHOLE TEMP.	FLUID INFLOW	
AL	1.9800		DEGREES C/METERS	DEPTH (METERS)	
B	58.9750				
FE	3.0300	CONDENSATE (PPM)	.0	.0	.0
NH3	.3350	PH/DEG.C	.0	.0	.0
Li	9.93	CO2	.0	.0	.0
Ba	0.415	H2S	.0	.0	.0
Br	1.525	NA	.0	.0	.0

			.0	.0	.0
			.0	.0	.0
			.0	.0	.0
			.0	.0	.0
			.0	.0	.0
			.0	.0	.0
			.0	.0	.0
			.0	.0	.0
			.0	.0	.0
			.0	.0	.0
			.0	.0	.0

IONIC STRENGTH = .02317 IONIC BALANCE : CATIONS (MOL.EQ.) .02161741  
 ANIONS (MOL.EQ.) .02323177  
 DIFFERENCE (%) -7.20

DEEP WATER (PPM)		DEEP STEAM (PPM)		GAS PRESSURES (BARS ABS.)
SiO2	235.68	CO2	687.43	CO2 .116E+00
NA	422.30	H2S	7.15	H2S .462E-03
K	48.78	H2	.00	H2 .000E+00
CA	13.20	O2	.00	O2 .000E+00
MG	.377	CH4	.00	CH4 .000E+00
SO4	32.38	N2	.00	N2 .000E+00
CL	460.91	NH3	.34	NH3 .197E-05
F	10.18			H2O .676E+01
DISS.S.	.00			TOTAL .687E+01
AL	1.8663			
B	55.5867			H2O (%) .00
FE	2.8563			BOILING PORTION .00

GAS SOLUBILITY MULTIPLYING FACTOR : .10

SAMPLE = REP.YBJ.004

ACTIVITY COEFFICIENTS IN DEEP WATER

H+	.845	KSO4-	.825	FE++	.475	FECL+	.816
OH-	.812	F-	.812	FE+++	.225	AL+++	.225
H3SiO4-	.816	CL-	.808	PROH+	.823	ALOH++	.467
H2SiO4--	.467	NA+	.816	FE(OH)3-	.823	AL(OH)2+	.825
H2BO3-	.805	K+	.808	FE(OH)4--	.461	AL(OH)4-	.819
HCO3-	.816	CA++	.475	PROH++	.461	ALSO4+	.819
CO3--	.454	MG++	.502	FE(OH)2+	.825	AL(SO4)2-	.819
HS-	.812	CAHCO3+	.829	FE(OH)4-	.825	ALF++	.467
S--	.461	MGHCO3+	.816	FESO4+	.823	ALF2+	.825
H2SO4-	.819	CAOH+	.829	FECL++	.461	ALF4-	.819
SO4--	.446	MGOH+	.832	FECL2+	.823	ALF5--	.454
NASO4-	.825	NH4+	.805	FECL4-	.816	ALF6---	.169

CHEMICAL COMPONENTS IN DEEP WATER (PPM AND LOG MOLE)

H+ (ACT.)	.00	-5.645	MG++	.27	-4.958	FE(OH)3	.81	-5.118
OH-	.28	-4.777	NaCl	4.70	-4.095	FE(OH)4-	1.54	-4.904
H4SiO4	372.96	-2.411	KCl	.18	-5.621	FECL+	.18	-5.710
H3SiO4-	3.42	-4.444	NASO4-	2.73	-4.640	FECL2	.00	-13.788
H2SiO4--	.00	-8.524	ESO4-	1.07	-5.103	FECL++	.00	-18.303
NAH3SiO4	.70	-5.225	CASO4	1.30	-5.020	FECL2+	.00	-19.779
H3BO3	315.88	-2.292	MGSO4	.34	-5.555	FECL3	.00	-22.215
H2BO3-	2.02	-4.478	CACO3	.50	-5.299	FECL4-	.00	-25.106
H2CO3	514.79	-2.081	MGCO3	.00	-7.236	FESO4	.06	-6.431
HCO3-	435.82	-2.146	CAHCO3+	17.17	-3.770	FESO4+	.00	-17.999
CO3--	.13	-5.663	MGHCO3+	.13	-5.804	AL+++	.00	-17.376
H2S	3.48	-3.990	CAOH+	.01	-7.003	ALOH++	.00	-11.777
HS-	3.56	-3.968	MGOH+	.00	-7.044	AL(OH)2+	.01	-6.832
S--	.00	-12.581	NH4OH	.44	-4.897	AL(OH)3	4.80	-4.211
H2SO4	.00	-14.558	NH4+	.13	-5.139	AL(OH)4-	.71	-5.124
H2SO4-	.03	-6.520	FE++	.70	-4.899	ALSO4+	.00	-17.667
SO4--	28.17	-3.533	FE+++	.00	-20.265	AL(SO4)2-	.00	-19.167
HF	.06	-5.535	PROH+	1.10	-4.820	ALF++	.00	-12.843
F-	10.13	-3.273	FE(OH)2	.09	-6.017	ALF2+	.00	-9.812
CL-	457.91	-1.889	FE(OH)3-	.00	-8.175	ALF3	.00	-8.619
NA+	419.79	-1.739	FE(OH)4--	.00	-13.631	ALF4-	.00	-9.197
K+	48.38	-2.908	FE(OH)++	.00	-13.367	ALF5--	.00	-10.894
CA++	5.80	-3.839	FE(OH)2+	.00	-8.005	ALF6---	.00	-13.762

IONIC STRENGTH = .02117      IONIC BALANCE :      CATIONS (MOL.BQ.) .02002969  
 ANIONS (MOL.BQ.) .02139642  
 DIFFERENCE (%) -6.60

CHEMICAL GROWTH TEMPERATURES DEGREES C      1000/T DEGREES KELVIN = 2.29

QUARTZ      184.4  
 CHALCEDONY      163.6  
 NAK      217.0

OXIDATION POTENTIAL (VOLTS) :      BH H2S= -.426      BH CH4= 99.999      BH H2= 99.999      BH NH3= 99.999

LOG SOLUBILITY PRODUCTS OF MINERALS IN DEEP WATER

	TEOR.	CALC.		TEOR.	CALC.		TEOR.	CALC.
ADULARIA	-15.364	-14.480	ALBITE LOW	-14.797	-13.307	ANALCINE	-11.982	-10.896
ANHYDRITE	-6.587	-8.046	CALCITE	-10.691	-10.168	CHALCEDONY	-2.411	-2.411
MG-CHLORITE	-80.320	-80.957	FLUORITE	-10.593	-10.890	GORTHITE	-2.072	-.120
LAUNONTITE	-25.098	-22.300	MICROCLINE	-15.362	-14.480	MAGNETITE	-24.678	-15.198
CA-MONTMOR.	-75.478	-58.249	K-MONTMOR.	-36.014	-30.043	MG-MONTMOR.	-76.855	-59.344
NA-MONTMOR.	-36.188	-28.870	MUSCOVITE	-18.643	-13.238	PREHNITE	-35.792	-33.787
PYRRHOTITE	-67.641	-42.726	PYRITE	-102.025	-54.965	QUARTZ	-2.587	-2.411
WAIKAITITE	-23.829	-22.300	WOLLASTONITE	9.153	6.715	ZOISITE	-35.503	-33.166
EPIDOTE	-38.915	-33.907	MARCASITE	-81.954	-54.965			

**APPENDIX 2.3 Computer Output for the Calibrated  
Downhole Sample**

UNU Geothermal Training Programme

REP.YBJ.004.A

YANGBAJING ZK-323

TIBET

PROGRAM WATCH2.

WATER SAMPLE (PPM)

STEAM SAMPLE

PH/DEG.C	6.64/****	GAS (VOL.%)	REFERENCE TEMP.	DEGREES C	.0 (CHA)
SiO2	235.68	CO2			
NA	422.30	H2S	SAMPLING PRESSURE	BARS ABS.	
K	48.78	H2	DISCHARGE ENTHALPY	MJ/UL/KG	
CA	13.20	O2	DISCHARGE	KG/SEC.	.0
MG	.377	CH4			
CO2	687.34	N2	MEASURED TEMPERATURE	DEGREES C	.0
SO4	32.38		RESISTIVITY/TEMP.	OHMM/DEG.C	.0/ .0
H2S	7.15		EH/TEMP.	MV/DEG.C	.000/ .0
CL	460.91				
F	10.18	LITERS GAS PER KG			
DISS.SOLIDS	.00	CONDENSATE/DEG.C	MEASURED DOWNHOLE TEMP.	FLUID INFLOW	
AL	1.8663		DEGREES C/METERS	DEPTH (METERS)	
B	55.5867				
FE	2.8563	CONDENSATE (PPM)	.0	.0	.0
NH3	.3400	PH/DEG.C	.0	.0	.0
Li	9.36	CO2	.0	.0	.0
Ba	0.39	H2S	.0	.0	.0
Br	1.44	NA	.0	.0	.0
			.0	.0	.0
			.0	.0	.0
			.0	.0	.0
		CONDENSATE WITH NAOH (PPM)	.0	.0	.0
		CO2	.0	.0	.0
		H2S	.0	.0	.0

IONIC STRENGTH = .02117      IONIC BALANCE :    CATIONS (MOL.EQ.) .02002347  
 ANIONS (MOL.EQ.) .02139542  
 DIFFERENCE (%)      -6.59

DEEP WATER (PPM)		DEEP STEAM (PPM)		GAS PRESSURES (BARS ABS.)	
SiO2	235.70	CO2	687.34	CO2	.116E+01
NA	422.30	H2S	7.15	H2S	.461E-02
K	48.78	H2	.00	H2	.000E+00
CA	13.20	O2	.00	O2	.000E+00
MG	.377	CH4	.00	CH4	.000E+00
SO4	32.38	N2	.00	N2	.000E+00
CL	460.87	NH3	.34	NH3	.138E-04
F	10.18			H2O	.676E+01
DISS.S.	.00			TOTAL	.792E+01
AL	1.8662				
B	55.5816			H2O (%)	.00
FE	2.8565			BOILING PORTION	.00

ACTIVITY COEFFICIENTS IN DEEP WATER

H+	.845	ES04-	.325	FE++	.475	FECL+	.816
OH-	.812	F-	.812	FE+++	.224	AL+++	.224
H3SIO4-	.816	CL-	.808	FE0H+	.823	ALOH++	.467
H2SIO4--	.467	NA+	.816	FE(OH)3-	.823	AL(OH)2+	.825
H2BO3-	.805	E+	.808	FE(OH)4--	.461	AL(OH)4-	.819
HCO3-	.816	CA++	.475	FROH++	.461	ALSO4+	.819
CO3--	.454	NG++	.502	FE(OH)2+	.825	AL(SO4)2-	.819
HS-	.812	CAHCO3+	.829	FE(OH)4-	.825	ALF++	.467
S--	.461	MGHCO3+	.816	FESO4+	.823	ALF2+	.825
H2SO4	.819	CAOH+	.829	FECL++	.461	ALF4-	.819
SO4--	.446	MGOH+	.832	FECL2+	.823	ALF5--	.454
NaSO4-	.825	NH4+	.805	FECL4-	.816	ALF6---	.169

CHEMICAL COMPONENTS IN DEEP WATER (PPM AND LOG MOLE)

H+ (ACT.)	.00	-6.645	NG++	.27	-4.958	FE(OH)3	.82	-5.118
OH-	.28	-4.777	NaCl	4.70	-4.095	FE(OH)4-	1.55	-4.903
H4SIO4	372.99	-2.411	KCl	.18	-5.621	FECL+	.18	-5.710
H3SIO4-	3.42	-4.444	NaSO4-	2.73	-4.640	FECL2	.00	-13.788
H2SIO4--	.00	-8.524	ES04-	1.07	-5.103	FECL++	.00	-18.304
NaH3SIO4	.70	-5.225	CASO4	1.30	-5.020	FECL2+	.00	-19.780
H3BO3	315.85	-2.292	MGSO4	.34	-5.555	FECL3	.00	-22.216
H2BO3-	2.02	-4.478	CACO3	.50	-5.299	FECL4-	.00	-25.107
H2CO3	514.65	-2.081	MGCO3	.00	-7.236	FESO4	.06	-6.432
HCO3-	435.82	-2.146	CAHCO3+	17.18	-3.770	FESO4+	.00	-18.000
CO3--	.13	-5.662	MGHCO3+	.13	-5.804	AL+++	.00	-17.378
H2S	3.48	-3.991	CAOH+	.01	-7.002	ALOH++	.00	-11.778
HS-	3.55	-3.968	MGOH+	.00	-7.044	AL(OH)2+	.01	-6.832
S--	.00	-12.581	NH4OH	.45	-4.896	AL(OH)3	4.80	-4.211
H2SO4	.00	-14.558	NH4+	.13	-5.139	AL(OH)4-	.71	-5.124
H2SO4-	.03	-6.520	FE++	.70	-4.900	ALSO4+	.00	-17.669
SO4--	28.17	-3.533	FE+++	.00	-20.266	AL(SO4)2-	.00	-19.168
HF	.06	-5.535	FROH+	1.10	-4.820	ALF++	.00	-12.844
F-	10.13	-3.273	FE(OH)2	.09	-6.017	ALF2+	.00	-9.813
CL-	457.87	-1.889	FE(OH)3-	.00	-8.175	ALF3	.00	-8.620
NA+	419.79	-1.739	FE(OH)4--	.00	-13.630	ALF4-	.00	-9.198
K+	48.38	-2.908	FE(OH)++	.00	-13.368	ALF5--	.00	-10.895
CA++	5.80	-3.839	FE(OH)2+	.00	-8.005	ALF6---	.00	-13.763

IONIC STRENGTH = .02117      IONIC BALANCE :      CATIONS (MOL.EQ.) .02002972  
 ANIONS (MOL.EQ.) .02139546  
 DIFFERENCE (%) -6.59

CHEMICAL GEOTHERMOMETERS DEGREES C      1000/T DEGREES KELVIN = 2.29

QUARTZ      184.4  
 CHALCEDONY      163.6  
 NAK      217.0

OXIDATION POTENTIAL (VOLTS) :      EH H2S= -.426      EH CH4= 99.999      EH H2= 99.999      EH NH3= 99.999

LOG SOLUBILITY PRODUCTS OF MINERALS IN DEEP WATER

	TEOR.	CALC.		TEOR.	CALC.		TEOR.	CALC.
ADULARIA	-15.364	-14.480	ALBITE LOW	-14.797	-13.307	ANALCINE	-11.982	-10.896
ANHYDRITE	-6.587	-8.046	CALCITE	-10.691	-10.168	CHALCEDONY	-2.411	-2.411
MG-CHLORITE	-80.320	-80.955	FLUORITE	-10.593	-10.890	GOETHITE	-2.072	-.120
LAUMONTITE	-25.098	-22.300	MICROCLINE	-16.362	-14.480	MAGNETITE	-24.677	-15.197
CA-MONTMOR.	-75.479	-58.252	K-MONTMOR.	-36.014	-30.045	MG-MONTMOR.	-76.856	-59.348
NA-MONTMOR.	-36.189	-28.872	MUSCOVITE	-18.643	-13.239	PREHNITE	-35.792	-33.786
PYRRHOTITE	-67.634	-42.723	PYRITE	-102.016	-54.964	QUARTZ	-2.587	-2.411
WAIBARITE	-23.829	-22.300	WOLLASTONITE	9.153	6.716	ZOISITE	-35.503	-33.166
EPIDOTE	-38.912	-33.906	MARCASITE	-81.946	-54.964			

**Table 2.1 Chemical Composition of Typical Geothermal Waters**

Source and reference*	Approx. temp. (°C)	Depth (m)	pH (25°)	Concentrations (mg/kg) for water collected at atmospheric pressure from discharge													
				Li	Na	K	Rb	Cs	Mg	Ca	Mn	Fe	F	Cl	Br	I	
Spring, Reykjavik, Iceland (a)	88	0	9.4	0.00	159	1.4	—	—	—	0.3	1.9	0.00	0.00	1.0	30	0.9	0.1
Drillhole, Reykjavik, Iceland (b)	100	600	8.6	<0.1	95	1.5	<0.02	0.02	—	—	0.5	—	—	—	31	—	—
Spring, Hveragerdi, Iceland (b)	100	0	9.3	—	—	—	—	—	—	0.8	2.5	—	—	1.1	186	—	—
Hole G-3, Hveragerdi, Iceland (b)	216	650	9.6	0.3	212	27	0.04	<0.02	—	0.0	1.5	0.00	0.1	1.9	197	0.45	0.0
Spring, Fuzubetsk, Kamchatka, USSR (c)	100	0	8.4	—	1010	88	—	—	—	10	64	—	0.0	0.8	1684	3.2	0.0
Fuzubetsk drill holes, Kamchatka, USSR (d)	170-195	300-400	8.9	—	Na + K 940	—	—	—	—	7	119	—	—	—	1470	—	—
Jubilee Bath, Ngawha, N.Z. (e)	50	0	6.5	11	870	79	0.3	0.5	—	2.5	8	—	—	0.3	1336	—	—
Drillhole 1, Ngawha, N.Z. (e)	230	585	7.4	12.2	950	80	0.8	0.4	—	Ca - Mg 28	—	0.02	0.1	0.8	1625	—	1.3
Ohaki Pool, Broadlands, N.Z. (e)	95	0	7.05	7.4	860	82	0.1	1.2	—	Ca - Mg 2.6	—	—	—	5.2	1060	3.0	0.6
Drill hole 2, Broadlands, N.Z. (e)	260	1000	8.3	11.7	1050	210	2.2	1.7	—	0.1	2.2	0.009	≈0.01	7.3	1763	5.7	0.8
Champagne Pool, Wairakei, N.Z. (f)	99	0	8.0	10.8	1070	182	1.1	2.7	—	0.4	26	—	—	6.6	1770	4.0	0.7
Drill hole 24, Wairakei, N.Z. (e)	250	800	8.3	13.2	1250	210	2.9	2.5	—	0.04	12	0.015	≈0.01	8.4	2210	5.5	0.3
Spring 6, Rotokaus, N.Z. (e)	65	0	2.5	7.8	990	102	—	—	—	11.3	11	—	—	<1	1433	—	—
Drill hole 2, Rotokaus, N.Z. (e)	220	800	7.8	10.2	1325	176	—	—	—	—	50	—	—	6.6	2675	—	0.2
Spring, Tahaungtsui, Tainan, Taiwan (f)	91	0	—	3.0	611	25.9	—	—	—	2.8	3.5	2.5	1.1	7.3	387	—	—
Hole E103, Tahaungtsui, Tainan, Taiwan (f)	200	1000	3.2	—	282	54	—	—	—	8 <sup>g</sup>	0	—	1368	—	1223	—	—
Shotaro Hotel, Matsubara, Japan (g)	78.5	0	3.1	—	40	8.6	—	—	—	8.2	31.8	—	8.6	—	3.0	—	—
Hole 1, Matsubara, Japan (g)	-300	415	4.9	—	264	144	—	—	—	8.7	22.9	—	508	—	12.4	—	—
Spring 22, Mexicali, Mexico (h)	—	0	—	11.6	4250	535	—	—	—	24	340	—	—	—	80.00	12.3	—
Hole 5, Mexicali, Mexico (h)*	340	1318	—	19	5820	1570	—	—	—	8	260	—	0.2	—	10.420	14.1	3.1
Water mudpots, Salton Sea, Calif. (i)	21	0	7.3	9.6	6470	486	—	—	—	325	79	0.9	0.8	14	8480	—	—
Hole 1, ID, Salton Sea, Calif. (i) <sup>g</sup>	340	1600	4.7	215	50,400	17,500	135	34	—	54	28,000	1400	2290	35	155,000	120	18
Spring, Makhchala, Dagestan, USSR	63	0	8.6	0.2	1137	5.4	—	—	—	2.4	16.4	—	—	0.4	335	1.6	—

\* References: (a) Bodvarsson (1963); (b) Chemistry Division, DSIR, N.Z. and pers. comm. from Dr. G. Bodvarsson, and Dr. G. E. Sigvaldason; (c) Ivanov (1958); (d) Averyer et al. (1981); (e) Chemistry Division, DSIR; (f) Y.-C. Liu (personal communication); (g) Naumova and Suami (1967); (h) Mercado (1966); (i) Muller and White (1969); (j) Ivanov and Nevraev (1984).

<sup>g</sup> Concentrations and pH in over aquifer.  
<sup>h</sup> Total CO<sub>2</sub>, SiO<sub>2</sub>, etc. is the total CO<sub>2</sub> + HCO<sub>3</sub><sup>-</sup> + CO<sub>3</sub><sup>2-</sup> expressed as CO<sub>2</sub>, silica = silicate as SiO<sub>2</sub>, etc.

**Table 2.2 Summary of the Chemical Equilibria Controlling the Composition of Geothermal Fluid**

Native copper	$8\text{Cu} + 8\text{H}^+ + \text{SO}_4^{2-} \rightleftharpoons 8\text{Cu}^+ + 4\text{H}_2\text{O} + \text{S}^{2-}$	Anglesite	$\text{PbSO}_4 \rightleftharpoons \text{Pb}^{2+} + \text{SO}_4^{2-}$
Pyrrhotite	$\text{FeS} \rightleftharpoons \text{Fe}^{2+} + \text{S}^{2-}$	Cerussite	$\text{PbCO}_3 \rightleftharpoons \text{Pb}^{2+} + \text{CO}_3^{2-}$
Sphalerite, Wurzite	$\text{ZnS} \rightleftharpoons \text{Zn}^{2+} + \text{S}^{2-}$	Tenorite	$\text{CuO} + 2\text{H}^+ \rightleftharpoons \text{Cu}^{2+} + \text{H}_2\text{O}$
Galena	$\text{PbS} \rightleftharpoons \text{Pb}^{2+} + \text{S}^{2-}$	Smithsonite	$\text{ZnCO}_3 \rightleftharpoons \text{Zn}^{2+} + \text{CO}_3^{2-}$
Covellite	$\text{CuS} \rightleftharpoons \text{Cu}^{2+} + \text{S}^{2-}$	Siderite	$\text{FeCO}_3 \rightleftharpoons \text{Fe}^{2+} + \text{CO}_3^{2-}$
Acanthite	$\text{Ag}_2\text{S} \rightleftharpoons 2\text{Ag}^{2+} + \text{S}^{2-}$	Dolomite	$\text{CaMg}(\text{CO}_3)_2 \rightleftharpoons \text{Ca}^{2+} + \text{Mg}^{2+} + 2\text{CO}_3^{2-}$
Chalcocite	$\text{Cu}_2\text{S} \rightleftharpoons 2\text{Cu}^+ + \text{S}^{2-}$	Anhydrite	$\text{CaSO}_4 \rightleftharpoons \text{Ca}^{2+} + \text{SO}_4^{2-}$
Pyrite	$\text{FeS}_2 + \text{H}_2\text{O} \rightleftharpoons \text{Fe}^{2+} + 1.75\text{S}^{2-} + 0.25\text{SO}_4^{2-} + 2\text{H}^+$	Gypsum	$\text{CaSO}_4 \cdot 2\text{H}_2\text{O} \rightleftharpoons \text{Ca}^{2+} + \text{SO}_4^{2-} + 2\text{H}_2\text{O}$
Chalcopyrite	$\text{CuFeS}_2 \rightleftharpoons \text{Cu}^{2+} + \text{Fe}^{2+} + 2\text{S}^{2-}$	Quartz	$\text{SiO}_2 + 2\text{H}_2\text{O} \rightleftharpoons \text{H}_4\text{SiO}_4$
Bornite	$\text{Cu}_5\text{FeS}_4 \rightleftharpoons 4\text{Cu}^+ + \text{Cu}^{2+} + \text{Fe}^{2+} + 4\text{S}^{2-}$	Microcline	$\text{KAlSi}_3\text{O}_8 + 4\text{H}^+ + 4\text{H}_2\text{O} \rightleftharpoons \text{K}^+ + 3\text{H}_4\text{SiO}_4 + \text{Al}^{3+}$
Cuprite	$\text{Cu}_2\text{O} + 2\text{H}^+ \rightleftharpoons 2\text{Cu}^+ + \text{H}_2\text{O}$	Low Albite	$\text{NaAlSi}_3\text{O}_8 + 4\text{H}^+ + 4\text{H}_2\text{O} \rightleftharpoons \text{Na}^+ + 3\text{H}_4\text{SiO}_4 + \text{Al}^{3+}$
Magnetite	$\text{Fe}_3\text{O}_4 + 8\text{H}^+ \rightleftharpoons \text{Fe}^{2+} + 2\text{Fe}^{3+} + 4\text{H}_2\text{O}$	Anorthite	$\text{CaAl}_2\text{Si}_2\text{O}_8 + 8\text{H}^+ \rightleftharpoons \text{Ca}^{2+} + 2\text{Al}^{3+} + 2\text{H}_4\text{SiO}_4$
Hematite	$\text{Fe}_2\text{O}_3 + 6\text{H}^+ \rightleftharpoons 2\text{Fe}^{3+} + 3\text{H}_2\text{O}$	Leucite	$\text{KAlSi}_2\text{O}_6 + 2\text{H}_2\text{O} + 4\text{H}^+ \rightleftharpoons \text{K}^+ + \text{Al}^{3+} + 2\text{H}_4\text{SiO}_4$
Brucite	$\text{Mg}(\text{OH})_2 \rightleftharpoons \text{Mg}^{2+} + 2\text{OH}^-$	Nepheline	$\text{NaAlSi}_3\text{O}_8 + 4\text{H}^+ \rightleftharpoons \text{Na}^+ + \text{Al}^{3+} + \text{H}_4\text{SiO}_4$
Gibbsite	$\text{Al}(\text{OH})_3 \rightleftharpoons \text{Al}^{3+} + 3\text{OH}^-$	Analcite	$\text{NaAlSi}_2\text{O}_6 \cdot \text{H}_2\text{O} + \text{H}_2\text{O} + 4\text{H}^+ \rightleftharpoons \text{Na}^+ + \text{Al}^{3+} + 2\text{H}_4\text{SiO}_4$
Calcite	$\text{CaCO}_3 \rightleftharpoons \text{Ca}^{2+} + \text{CO}_3^{2-}$	Kaolinite	$\text{Al}_2\text{Si}_2\text{O}_5(\text{OH})_4 + 6\text{H}^+ \rightleftharpoons \text{H}_2\text{O} + 2\text{Al}^{3+} + 2\text{H}_4\text{SiO}_4$
Na-Montmorillonite	$\text{Na}_{0.333}\text{Al}_{2.333}\text{Si}_{3.667}\text{O}_{10}(\text{OH})_2 + 7.332\text{H}^+ + 2.668\text{H}_2\text{O} \rightleftharpoons 0.333\text{Na}^+ + 2.333\text{Al}^{3+} + 3.667\text{H}_4\text{SiO}_4$		
K-Montmorillonite	$\text{K}_{0.333}\text{Al}_{2.333}\text{Si}_{3.667}\text{O}_{10}(\text{OH})_2 + 7.332\text{H}^+ + 2.668\text{H}_2\text{O} \rightleftharpoons 0.333\text{K}^+ + 2.333\text{Al}^{3+} + 3.667\text{H}_4\text{SiO}_4$		
Ca-Montmorillonite	$\text{Ca}_{0.1665}\text{Al}_{2.333}\text{Si}_{3.667}\text{O}_{10}(\text{OH})_2 + 7.332\text{H}^+ + 2.668\text{H}_2\text{O} \rightleftharpoons 0.1665\text{Ca}^{2+} + 2.333\text{Al}^{3+} + 3.667\text{H}_4\text{SiO}_4$		
Mg-Montmorillonite	$\text{Mg}_{0.1665}\text{Al}_{2.333}\text{Si}_{3.667}\text{O}_{10}(\text{OH})_2 + 7.332\text{H}^+ + 2.668\text{H}_2\text{O} \rightleftharpoons 0.1665\text{Mg}^{2+} + 2.333\text{Al}^{3+} + 3.667\text{H}_4\text{SiO}_4$		
Muscovite	$\text{KAl}_3\text{Si}_3\text{O}_{10}(\text{OH})_2 + 10\text{H}^+ \rightleftharpoons \text{K}^+ + 3\text{Al}^{3+} + 3\text{H}_4\text{SiO}_4$		
Illite	$\text{K}_{0.6}\text{Mg}_{0.25}\text{Al}_{2.70}\text{Si}_{3.60}\text{O}_{10}(\text{OH})_2 + 8\text{H}^+ + 2\text{H}_2\text{O} \rightleftharpoons 0.6\text{K}^+ + 0.25\text{Mg}^{2+} + 2.30\text{Al}^{3+} + 3.5\text{H}_4\text{SiO}_4$		
Biotite (Annite)	$\text{KFe}_3\text{AlSi}_3\text{O}_{10}(\text{OH})_2 + 10\text{H}^+ \rightleftharpoons \text{K}^+ + 3\text{Fe}^{2+} + \text{Al}^{3+} + 3\text{H}_4\text{SiO}_4$		

Source: From Helgeson, 1970, Copyright 1970 by the Mineralogical Society of America.

**Table 2.3 Equations Describing the Temperature Dependence of Cation/Proton Ratios and Un-dissociated Weak Acid Concentrations in Geothermal Well Discharge**

Weak acid/ ion ratio (moles/kg)	Temperature function				Mean deviation	Standard deviation
$\log \text{H}_4\text{SiO}_4$	-0.588	$-0.00441 \cdot T$	$-1515.21/T$	$+1.3470 \cdot \log T$	0.06	0.05
$\log \text{H}_2\text{CO}_3^*$	-1.794	$-0.00510 \cdot T$	$-4469.63/T$	$+4.1414 \cdot \log T$	0.30	0.26
$\log \text{H}_2\text{S}^0$	-1.678	$-0.00355 \cdot T$	$-5071.05/T$	$+3.8889 \cdot \log T$	0.36	0.33
$\log \text{H}_2\text{SO}_4^*$	-6.436	$-0.03906 \cdot T$	$-13335.68/T$	$+14.7958 \cdot \log T$	0.57	0.48
$\log \text{HF}^0$	-5.262	$-0.03511 \cdot T$	$-7964.11/T$	$+12.1022 \cdot \log T$	0.32	0.28
$\log \text{Na}^+/\text{H}^+$	2.694	$+0.02023 \cdot T$	$+4243.47/T$	$-6.2069 \cdot \log T$	0.14	0.12
$\log \text{K}^+/\text{H}^+$	2.505	$+0.01971 \cdot T$	$+3325.71/T$	$-5.7814 \cdot \log T$	0.12	0.09
$\log \text{Ca}^{+2}/\text{H}^+$	1.733	$+0.01117 \cdot T$	$+3890.51/T$	$-3.9977 \cdot \log T$	0.17	0.12
$\log \text{Mg}^{+2}/\text{H}^+$	1.816	$+0.01078 \cdot T$	$+3727.48/T$	$-4.1640 \cdot \log T$	0.34	0.27
$\log \text{Fe}^{+2}/\text{H}^+$	-4.696	$-0.04273 \cdot T$	$-1011.46/T$	$+10.8032 \cdot \log T$	0.18	0.17
$\log \text{Al}(\text{OH})_4^-/\text{OH}^-$	-3.407	$-0.02364 \cdot T$	$-3417.36/T$	$+7.8426 \cdot \log T$	0.21	0.12

Table 3.1 Analysis of Geothermal Waters with AAS

	Conc. Range (ppm)	Dilution <sup>a</sup>	Wave-length (Å)	Monochromator <sup>b</sup>				Lamp		Burner			Sam-pling height (mm)
				I	II	III	IV	Type <sup>d</sup>	Cur-rent (mA)	Slot length (mm)	Align-ment <sup>e</sup>	Flame <sup>c</sup>	
Li	0.5-30	(O)	6708	335	vis	in	3	HCL	10	70-100	⊥	C <sub>2</sub> H <sub>2</sub> -air (fuel lean)	8
	1-150	(D)	6708	335	vis	in	3	HCL	10	70-100		C <sub>2</sub> H <sub>2</sub> -air (fuel lean)	8
Na	100-1000	(D)	5890	295	vis	in	4	ODL	900	70-100	⊥	C <sub>2</sub> H <sub>2</sub> -air (fuel lean)	8
			5896										
K	4-400	(D)	7699	385	vis	in	4	ODL	400	70-100		H <sub>2</sub> -air (fuel rich)	8
Rb	0.1-10	(B)	7800	390	vis	in	4 <sup>f</sup>	ODL	250	70-100		H <sub>2</sub> -air (fuel rich)	8
Cs	0.2-20	(B)	8521	426	vis	in	5 <sup>f</sup>	ODL	400	70-100		H <sub>2</sub> -air (fuel rich)	8
Mg	0.001-1	(B)	2852	285	uv	out	4	HCL	6	70-100		C <sub>2</sub> H <sub>2</sub> -air (fuel lean)	8
	0.002-2	(O)	2852	285	uv	out	3	HCL	8	50-70		C <sub>2</sub> H <sub>2</sub> -N <sub>2</sub> O (RZ 3)	8
Ca	2-200	(D)	4227	211	vis	out	3	HCL	15	50-70		C <sub>2</sub> H <sub>2</sub> -N <sub>2</sub> O (RZ 5)	13
Mn	0.005-5	(B)	2795	279 <sup>g</sup>	uv	out	3	HCL	20	70-100		C <sub>2</sub> H <sub>2</sub> -air (fuel lean)	8
Al	0.04-50	(B)	3092.7	309	uv	out	3	HCL	25	50-70		C <sub>2</sub> H <sub>2</sub> -N <sub>2</sub> O (RZ 12)	8
			3092.8										
Fe	0.01-0.1	(B)	2483	248	uv	out	3	HCL	30	70-100		C <sub>2</sub> H <sub>2</sub> -air (fuel lean)	8
	0.1-20	(O)	2483	248	uv	out	3	HCL	30	50-70		C <sub>2</sub> H <sub>2</sub> -N <sub>2</sub> O (RZ 3)	8
SiO <sub>2</sub>	50-1000	(B)	2507	251	uv	out	3	HCL	40	50-70		C <sub>2</sub> H <sub>2</sub> -N <sub>2</sub> O (RZ 25)	7
B	20-1000	(B)	2497	250	uv	out	4	HCL	30	50-70		C <sub>2</sub> H <sub>2</sub> -N <sub>2</sub> O (RZ 25)	7

<sup>a</sup> Operating conditions are for models 303, 305, and 403; data are from Goguel, (1973).

<sup>b</sup> I, wavelength counter setting; II, grating; III, filter which excludes wavelengths shorter than 550 nm (5500 Å); IV, slit setting: (numbers correspond to spectral bandwidths) for the uv grating, 3 = 2.4 Å, 4 = 7 Å; for the visual grating, 3 = 5 Å, 4 = 14 Å, and 5 = 50 Å.

<sup>c</sup> RZ denotes height of the red zone in millimeters.

<sup>d</sup> HCL, hollow cathode lamp; ODL, Osram discharge lamp.

<sup>e</sup> Of the flame in the light path of the spectrophotometer: perpendicular alignment produces 0.1 or less of the sensitivity of the parallel alignment.

<sup>f</sup> An extra filter must be inserted into the light beam near the window of the spectrophotometer to the left of the flame in order to exclude modulated scattered Na light which reaches the photomultiplier via the reference beam. Filter holder 040-0251 (model 403) or 303-0828 (models 303-305) and a red filter Schott RG 5 or Corning 2-58 (Perkin-Elmer No. 290-1518) are required.

<sup>g</sup> Shortest wavelength of the triplet.

<sup>h</sup> Dilutions: (B) 1.1 fold. Add 5 ml of a buffer solution (2.5% recrystallized Sr(NO<sub>3</sub>)<sub>2</sub>, 4% KCl, 1 N HNO<sub>3</sub>) to 50 ml of each sample of standard. (D) 51 fold. Deliver 2 ml of sample or standard into 100 ml of a buffer solution (0.1% CsCl, 0.1N HNO<sub>3</sub>). (O) Undiluted water sample. Note: Sr(NO<sub>3</sub>)<sub>2</sub>, KCL, and CsCl are reagents of high purity (e.g., Merck "Suprapur").

Table 4.1 Equations Expressing the Temperature Dependence of Equilibrium Constants in CaO-CO<sub>2</sub>-H<sub>2</sub>O System

$$K_{H^*} = -7656970 - 3122.11449T + 1.092229T^2 + 1.880778E8 * T^{-1} + 3.1771246E6 * \log T$$

$$k = 108.875 + 0.174114604T - 1.9845113E(-4) * T^2 + 1.0131668E(-7) * T^3 - 58.867703 * \log T$$

$$\log K_1 = 124.4478 + 0.0056623T - 5.86972601E3 * T^{-1} - 45.589821 * \log T$$

$$\log K_2 = 143.4475 + 0.034559T - 1.9732326E(-5) * T^2 - 6.16187137E3 * T^{-1} - 57.248899 * \log T$$

$$\log K_e = -130.5593 - 0.0517898T + 2.6766438E(-5) * T^2 + 4.4176248E3 * T^{-1} + 51.47548 * \log T$$

$$\log K_c = 30.8131 - 0.1728295T + 3.271501E(-4) * T^2 - 2.5529153E(-7) * T^{-1} + 2.95989303 * \log T$$

$$A = -11092.1143 + 11.562984T + 0.01454757T^2 - 1.2064489E(-5) * T^3 + 4.4598806E(-9) * T^4 + 1.76312033E5 * T^{-1} + 5229.515 * \log T$$

$$B = 3.8096 + 0.01846467T + 4.8075571E(-5) * T^2 - 6.0838461E(-8) * T^3 + 3.0473184E(-11) * T^4 - 2.617130669E2 * T^{-1}$$

$$\log K_D = -1823.663 + 3.9000818T - 0.00412503T^2 + 1.75503E(-6) * T^3 + 4.2179661E5 * T^{-1} - 3.9002725E7 * T^{-2}$$

Table 4.2 Ionic Strength of Typical Geothermal Waters

Geothermal source	Ionic strength (molality)	Res. temp. (°C)	pH
Reykjahlól, Iceland	0.005	152	7.23
Námafjall, Iceland	0.007	252	7.48
Hveragerdi, Iceland	0.009	184	6.99
Leira, Iceland	0.014	127	6.73
Broadlands, N.Z. well 2	0.052	260	8.3
Wairakei, N.Z. hole No.24	0.062	250	8.3
Matsukawa, Japan hole No. 1	0.065	300	4.9
Sulphur Bank, CA Geyser spring	0.094	230	6.8
El Tatio, Chile geyser 238	0.230	220	7.32
Ahunchapan, El Salvador, ave.	0.312	230	6.3
Cerro Prieto, Mex. ave. 12 wells	0.431	388*	8.2
Matsao, Taiwan well 205	0.429	245	2.4
Sea water Std. Cl = 19‰	0.709	20	8.0
Halls Bayou, TX. FF No. 1	1.111	150	6.8
Chocolate Bayou, TX. Angle No. 3	1.348	118	5.9
Salton Sea Woolsey	3.434	176†	5.8
Salton Sea Magmax No.1	4.203	196†	5.5
Salton Sea hole I III	6.931	340	4.7

\*Max temp.

†Well head temp.

Table 4.3 Aqueous Species for Proton Mass Balance and Alkalinity Equations

Hydrogen ion mass balance species			Alkalinity species				
Coefficient		Coefficient		Coefficient			
1	H <sup>+</sup>	-1	Al(OH) <sup>2+</sup>	-2.875	Fe(OH) <sub>3</sub>	1	OH <sup>-</sup>
-1	OH <sup>-</sup>	-2	Al(OH) <sub>2</sub> <sup>+</sup>	1	PbH <sub>6</sub> S <sub>3</sub>	2	H <sub>2</sub> SiO <sub>4</sub> <sup>2-</sup>
-2	H <sub>2</sub> SiO <sub>4</sub> <sup>2-</sup>	-4	Al(OH) <sub>3</sub>	1.125	Cu <sup>2+</sup>	1	H <sub>3</sub> SiO <sub>4</sub> <sup>-</sup>
-1	H <sub>3</sub> SiO <sub>4</sub> <sup>-</sup>	-1	Hg(OH) <sup>+</sup>	1.125	CuCl <sup>+</sup>	1	HCO <sub>3</sub> <sup>-</sup>
1	HF	1	HgHCO <sub>3</sub>	1.125	CuCl <sub>2</sub>	2	CO <sub>3</sub> <sup>-</sup>
1	HF <sub>2</sub> <sup>-</sup>	-1	Fe(OH) <sup>+</sup>	1.125	CuCl <sub>2</sub> <sup>-</sup>	1	HS <sup>-</sup>
1	HCl	-3	Fe(OH) <sub>2</sub>	1.125	CuCl <sub>2</sub> <sup>2-</sup>	2	S <sup>2-</sup>
.5	O <sub>2</sub> aq	.25	Fe(OH) <sub>3</sub>	1.125	CuOH <sup>+</sup>	2	NaCO <sub>3</sub>
.25	H <sub>2</sub> aq	1.125	Fe <sup>3+</sup>	1.125	CuSO <sub>4</sub>	2	CaCO <sub>3</sub>
1	CH <sub>4</sub> aq	.125	FeOH <sup>2+</sup>	1.125	CuF <sup>+</sup>	1	CaOH
1	HCO <sub>3</sub> <sup>-</sup>	1.125	FeCl <sub>2</sub> <sup>+</sup>	-1	HnOH <sup>+</sup>	1	CaHCO <sub>3</sub>
2	H <sub>2</sub> CO <sub>3</sub>	1.125	FeCl <sub>2</sub> <sup>2+</sup>	-2	HgS <sub>2</sub> <sup>-</sup>	2	HgCO <sub>3</sub>
1	H <sub>2</sub> S	1.125	FeCl <sub>3</sub>	1	HgH <sub>2</sub> S <sub>3</sub>	1	HgOH <sup>+</sup>
-1	S <sup>2-</sup>	1.125	FeCl <sub>3</sub> <sup>-</sup>	-2.25	Hg <sub>2</sub> <sup>2+</sup>	1	HgHCO <sub>3</sub> <sup>+</sup>
1	HSO <sub>4</sub> <sup>-</sup>	1.125	FeF <sub>2</sub> <sup>+</sup>	-1	HgClOH	1	BaOH
-1	NnOH	1.125	FeF <sub>2</sub> <sup>2+</sup>	-1	HgOH <sup>+</sup>		
1	KHSO <sub>4</sub>	1.125	FeSO <sub>4</sub> <sup>+</sup>	-2	Hg(OH) <sub>2</sub>		
-1	CaOH <sup>+</sup>	.875	Fe(OH) <sub>2</sub>	2.25	AgCl <sub>2</sub> <sup>-</sup>		
-1	CaHCO <sub>3</sub> <sup>+</sup>	-1.875	Fe(OH) <sub>3</sub>	-1	Au <sub>2</sub> H <sub>2</sub> S <sub>3</sub> <sup>-</sup>		

**Table 5.1 Schematic Layout of the Function of WATCH Program**

GEOCHEMICAL MATERIAL	SELECTED PARAMETERS	COMPUTED PARAMETERS
1 Wet-steam well discharges (steam and water phases) 2 Boiling hot springs 3 Hot-water wells and non-boiled hot spring waters	1 Reference temperature a. measured b. chalcedony equilibrium c. quartz equilibrium d. Na-K feldspar equilibrium e. arbitrary 2 Degassing factor (only for geochemical material 1 and 2) 3 Discharge enthalpy (only for wet-steam wells)	1 Deep water composition 2 Species concentrations 3 Activity coefficients 4 $H^+$ activity 5 Redox potential 6 Gas partial pressures 7 Mineral solubilities
		<b>SPECIAL COMPUTATIONS</b>
		1 Speciation of variably boiled and cooled water

**Table 5.2 Input Data for WATCH Program**

---

**CHEMICAL DATA**

Water samples: pH/<sup>1</sup>°C, SiO<sub>2</sub>, B, Na, K, Ca, Mg, Fe, Al, Mn, CO<sub>2</sub>, SO<sub>4</sub>, H<sub>2</sub>S, Cl, F, dissolved solids, electric conductance<sup>¶</sup>.

Steam samples: (only for wet-steam wells) CO<sub>2</sub>, H<sub>2</sub>S, H<sub>2</sub>, N<sub>2</sub>, O<sub>2</sub>, H<sub>2</sub>, Cl<sub>2</sub>, and Na or Cl to check "dryness" of steam.

**PHYSICAL DATA**

Wet-steam wells: Sampling pressure, enthalpy of well discharge.

Hot springs and hot water wells: Discharge temperature.

**DATA WHICH ARE DESIRABLE**

Downhole temperature of wells.

Aquifer inflows of wells.

Discharge rates of wells and hot springs.

---

<sup>1</sup>Temperature at which the pH is measured. <sup>¶</sup>These data are not necessary for the programme calculations.

**Table 7.1 Effect of Process Parameters on Scale Formation**

Process Parameter	Equilibrium Effect on Potential Scale Species (a)			
	SiO <sub>2</sub>	CaCO <sub>3</sub>	Sulfide	Sulfate
Temperature decrease (as in plant cycle)	●	○	●	○ Ca ● Ba
Temperature increase (reheat during injection)	○	●	○	● Ca ○ Ba
Increased pH (as CO <sub>2</sub> is flashed)	● ○ pH >9	●	●	●
Decreased pH (acid addition)	○	○	○	○
Increased salinity (flashing; mixing)	●	○	○	○

(a) ● aggravates problem  
○ alleviates problem.

**Table 7.2 Factors affecting Silica Deposition Kinetics**

Factor	Impact	Comments
pH	Lowering pH slows kinetics by a factor of ~10 for every pH unit.	
Supersaturation ratio	Precipitation becomes rapid as the ratio exceeds 2.	Reduce pH and temperature
Temperature	Kinetics slows dramatically as temperature drops, which counteracts the increase in supersaturation ratio as a saturated solution cools.	The maximum silica deposition rate may occur 25 to 50°C below the temperature at which the cooled solution reaches amorphous silica solubility limits.
Salinity	Increased salinity increases kinetics of deposition	
F catalyst	This equilibrium (precipitation) accelerator may become the dominant controller of deposition in lower pH brines (pH 3?) where the normal precipitation mechanism is pH inhibited.	
Chemical inhibitors	Retards growth of silica particulates	Limited testing described in the Inhibitor Treatment section.

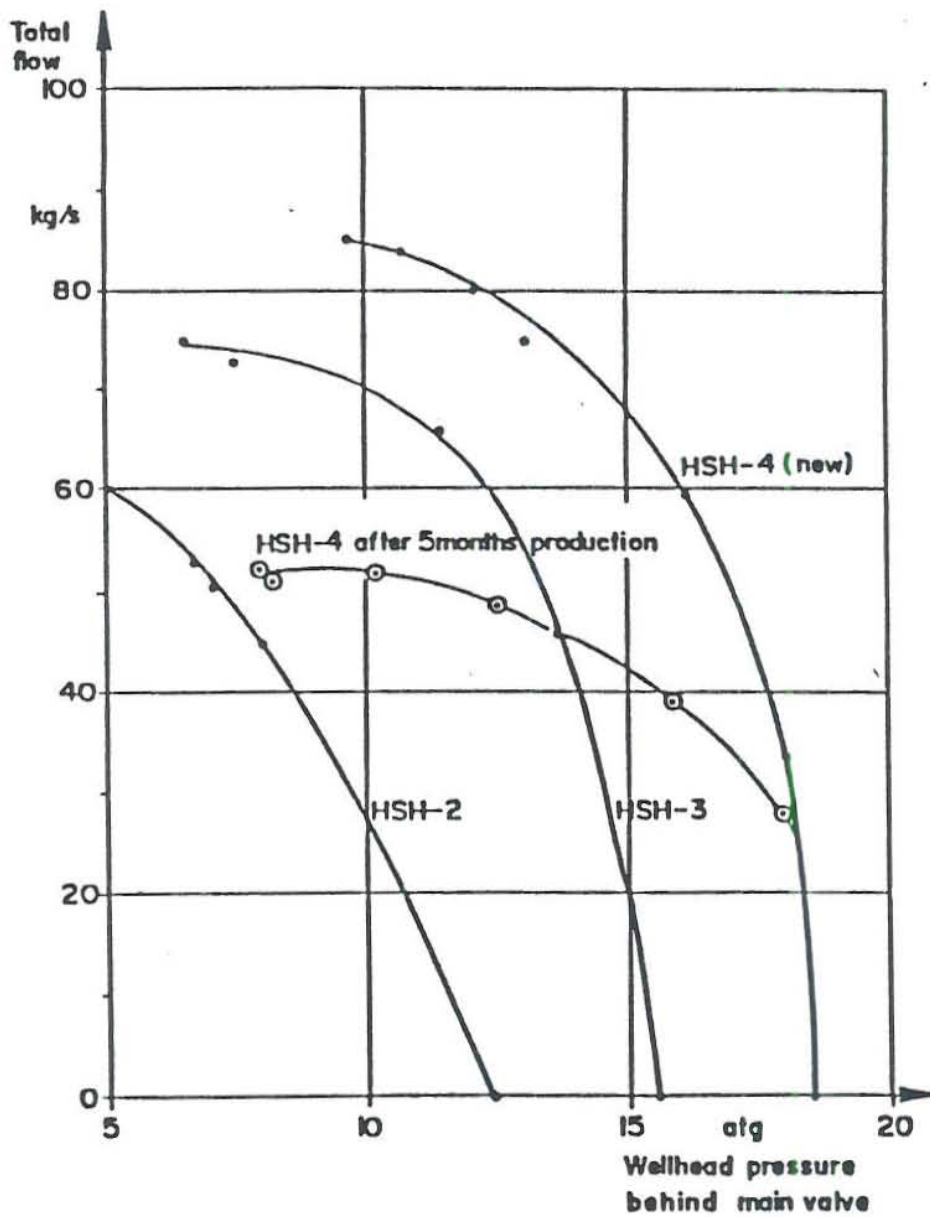
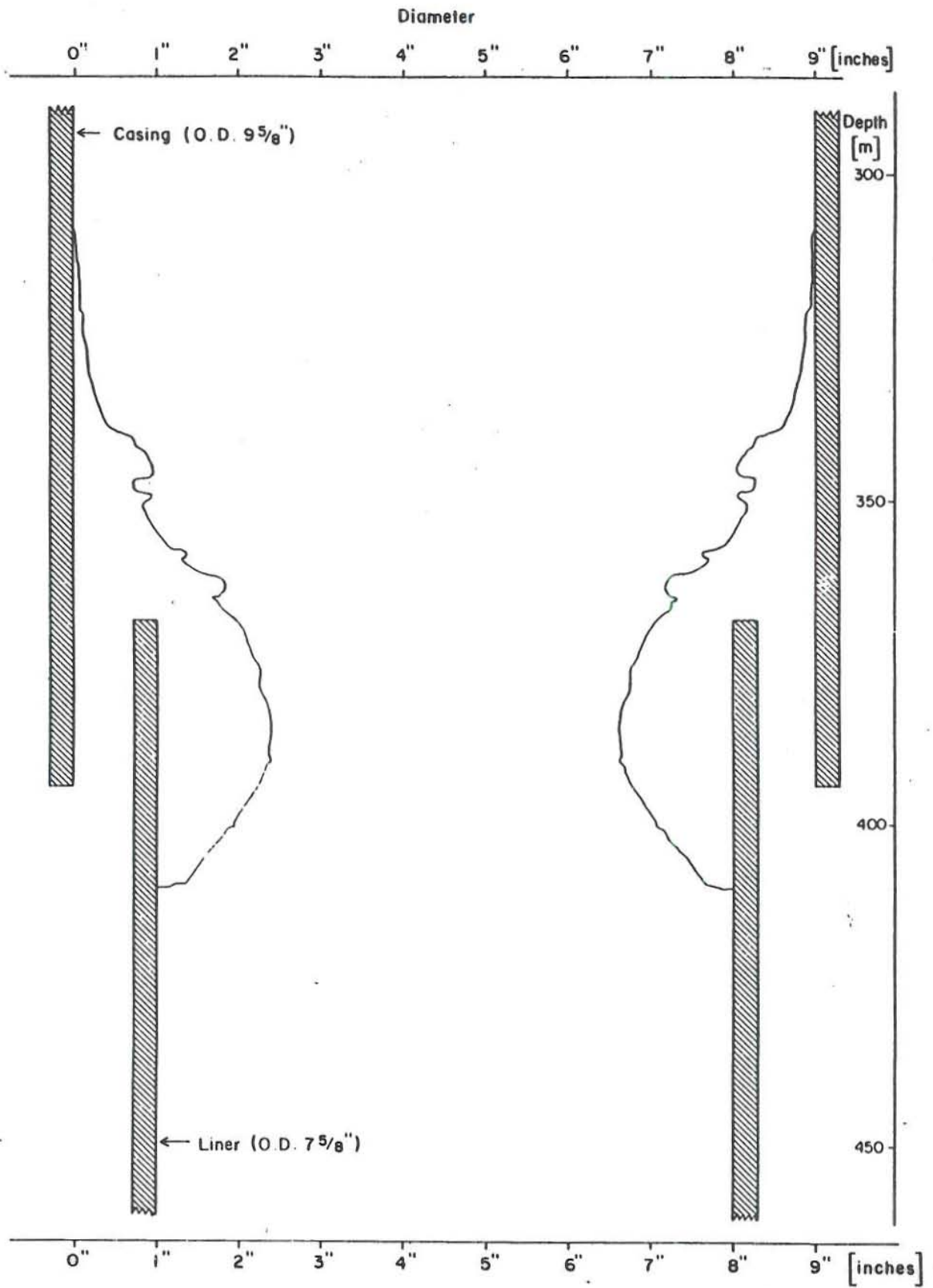


Figure 1.1 Output Decay due to Scaling in Well, Svartsengi



**Figure 1.2 Formation of Calcite Deposition in Well 4 in Svartsengi**

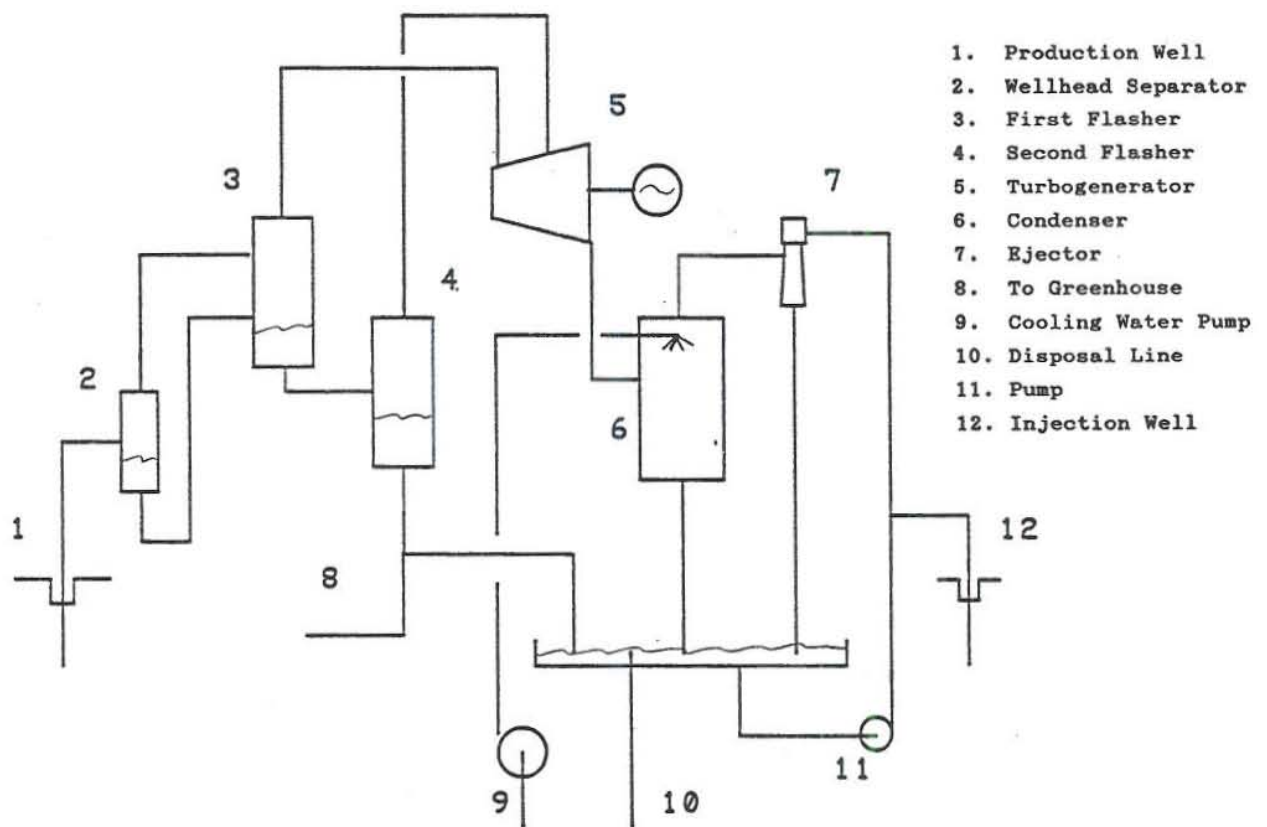


Figure 2.1 Schematic Flow Diagram of Double Flashing System in Yangbajing Power Plant

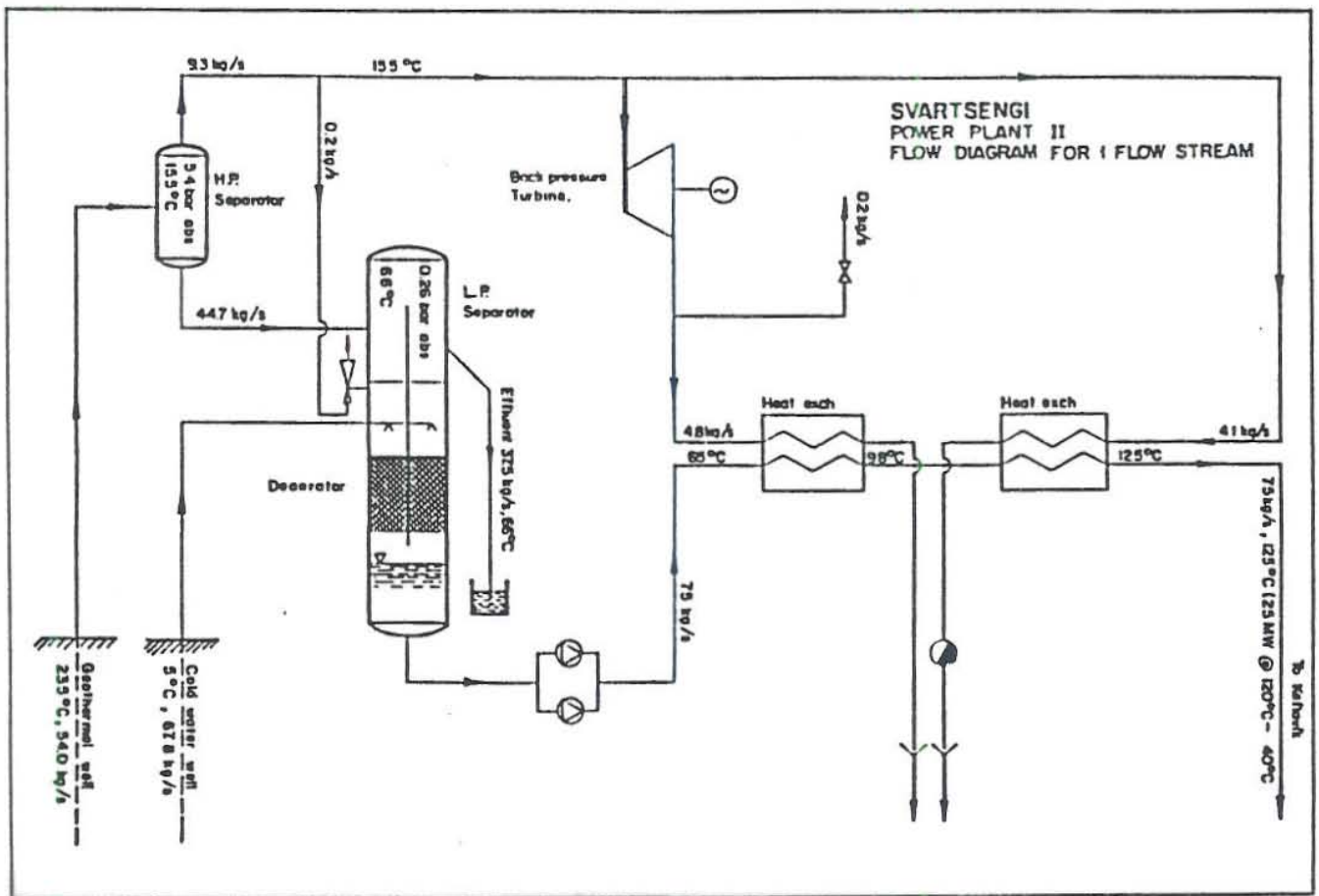
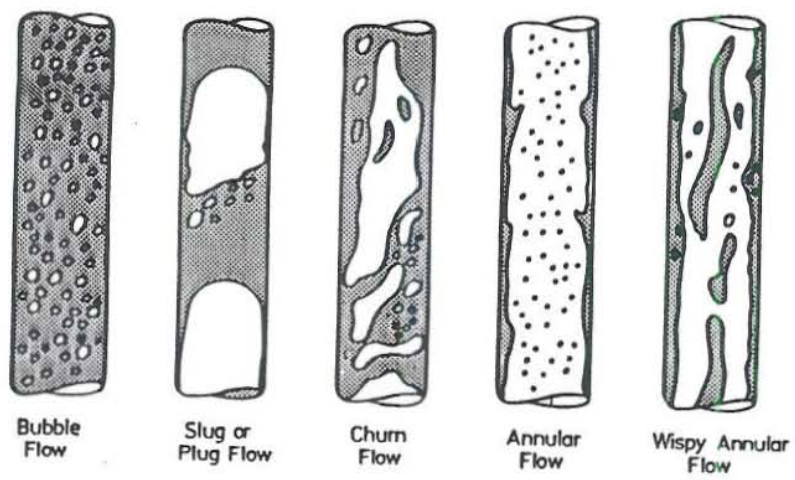


Figure 2.2 Flow Diagram of Svartsengi Power Plant (Björnsson and Albertsson, 1985)



**Figure 2.3 Flow Patterns of Vertical Two Phase Flow**

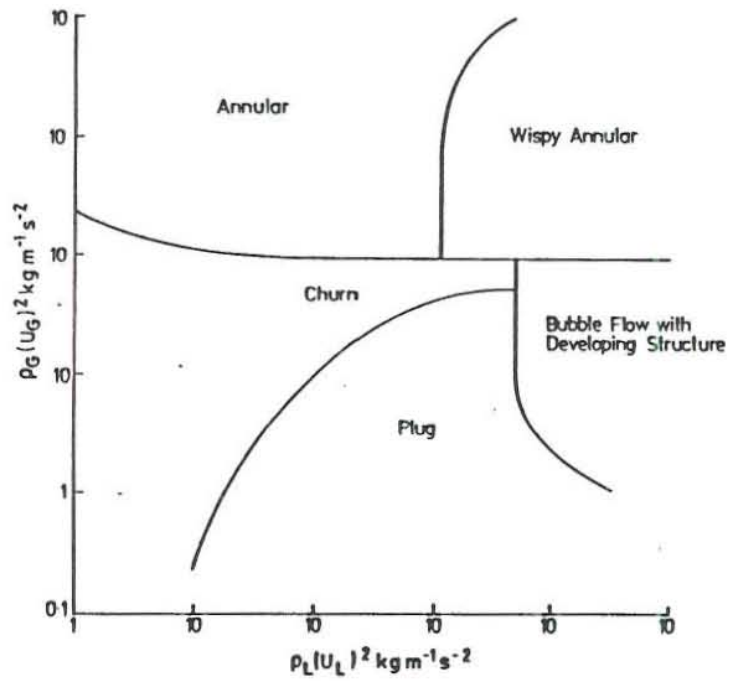
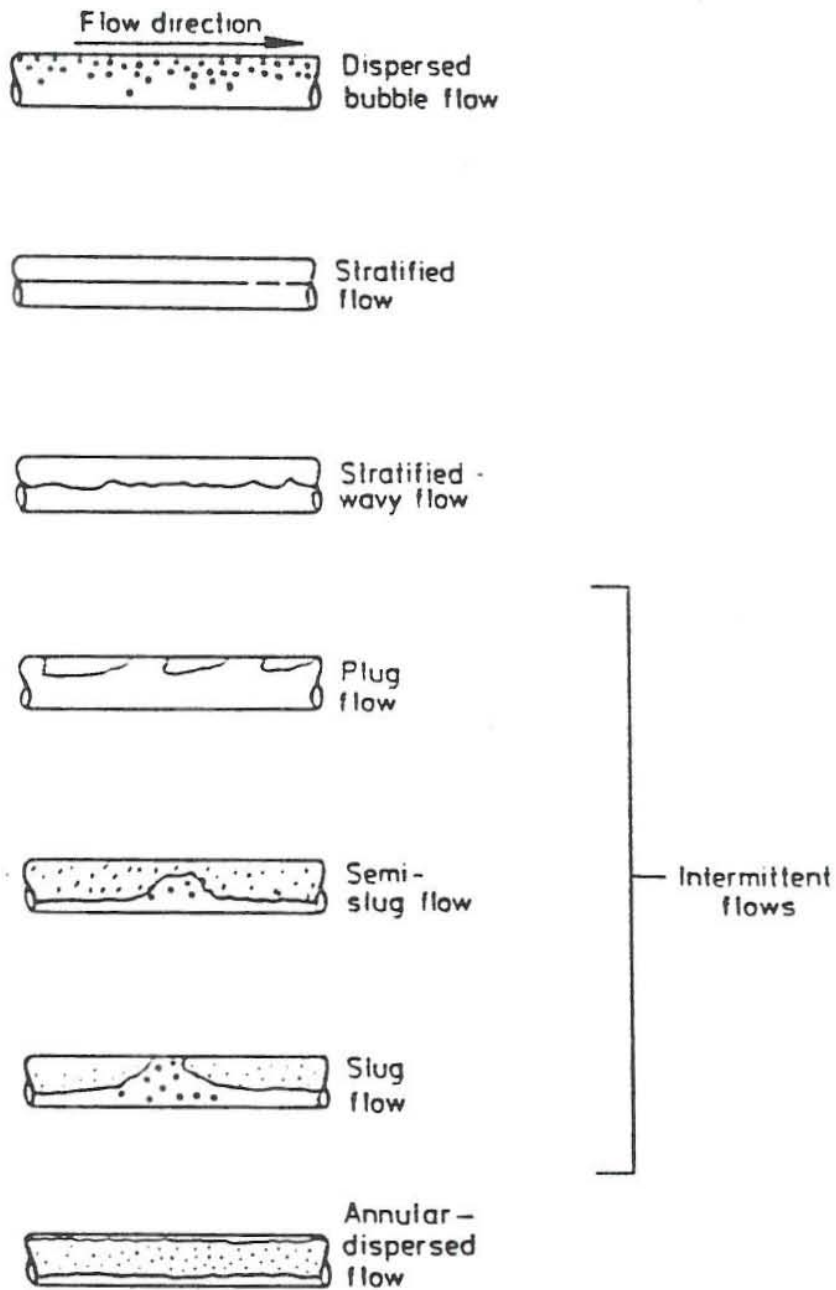


Figure 2.4 Flow Pattern Map for Vertical Two Phase Flow



**Figure 2.5 Flow Regimes in Horizontal Two Phase Flow**

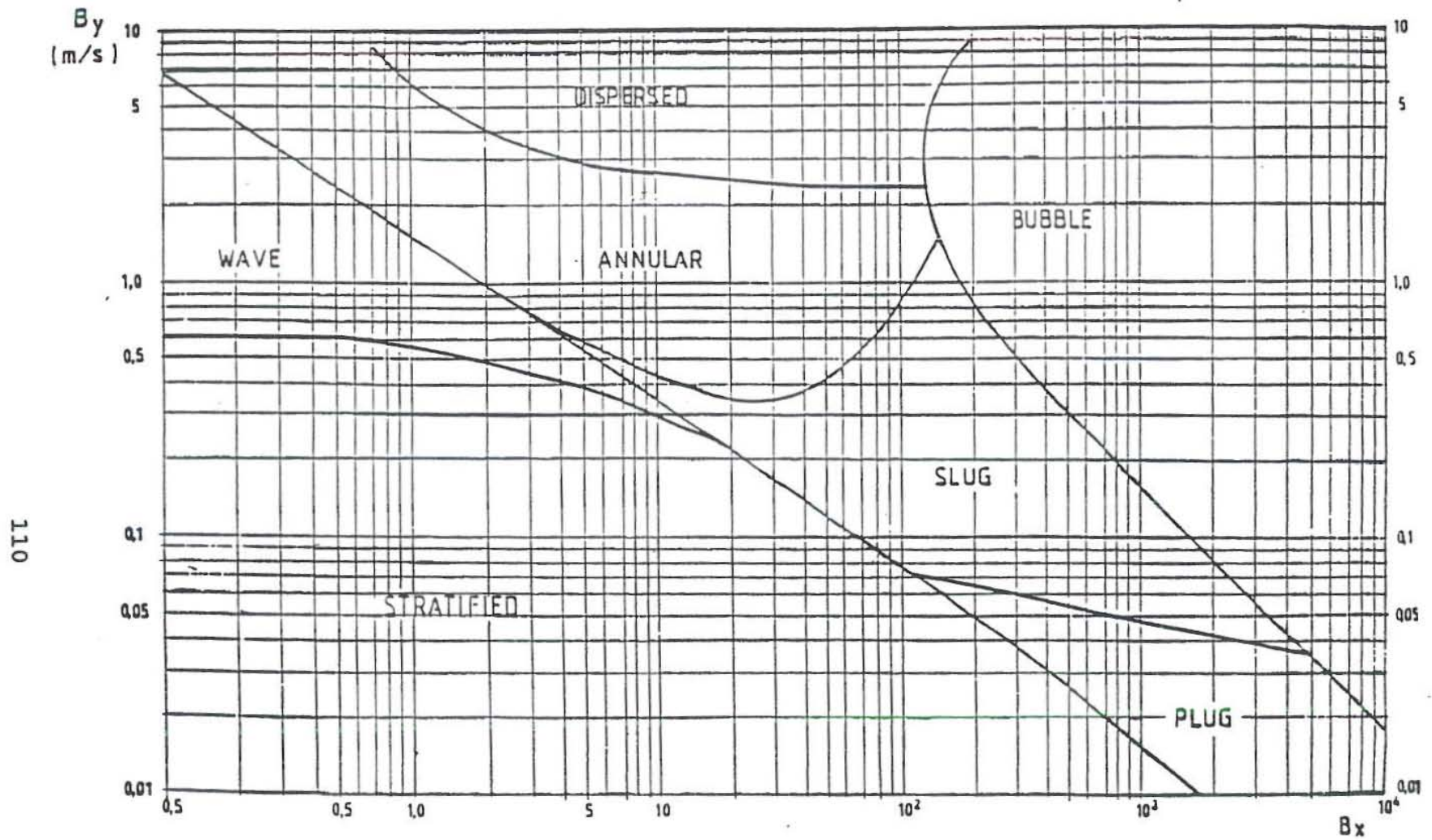
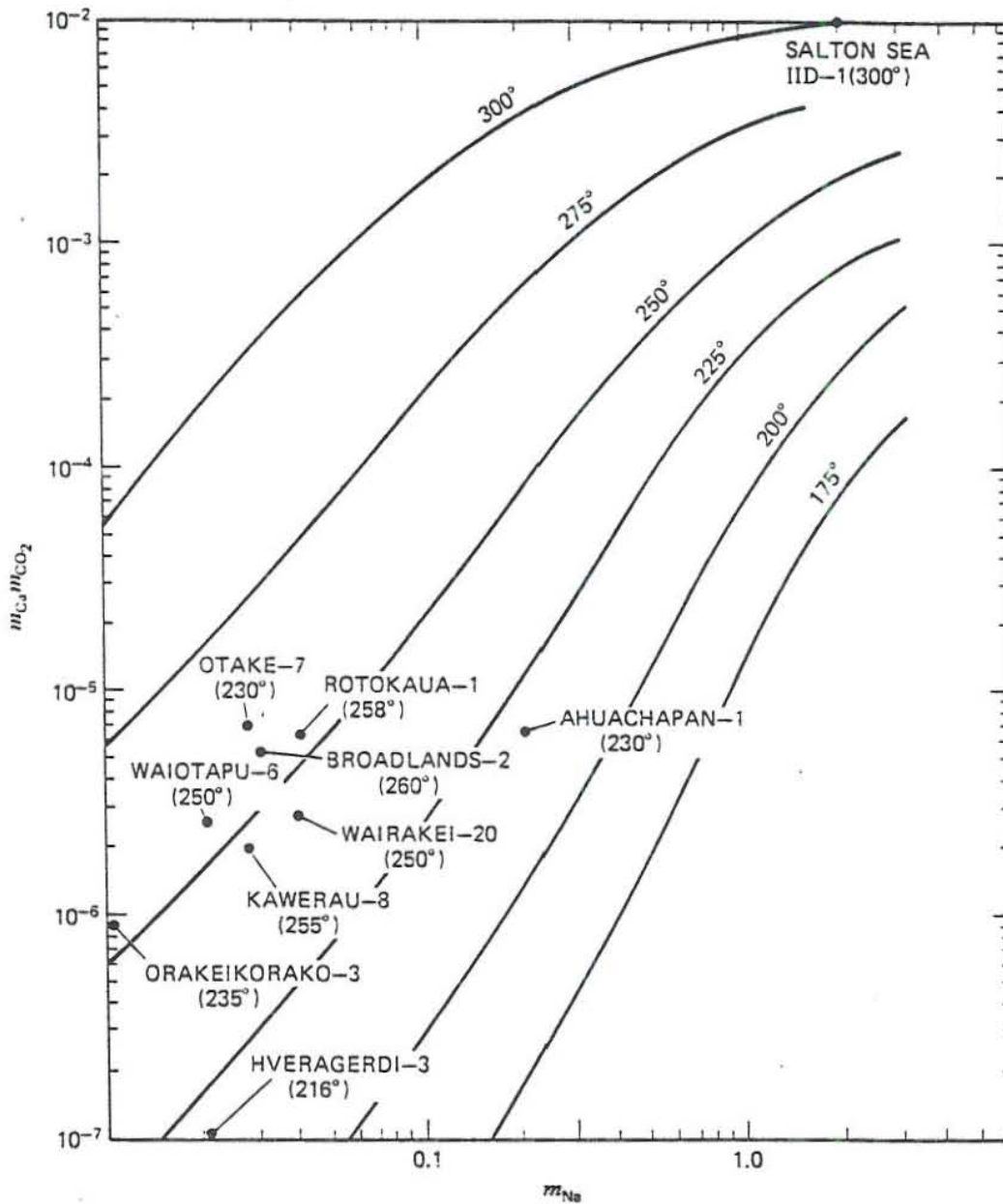


Figure 2.6 Flow Pattern Map of Baker as Modified by Scott



**Figure 2.7 Relationship of the Product of Calcium and Carbonate Ion Concentrations with Temperature and Sodium Concentration in Equilibrium Reservoir Conditions**

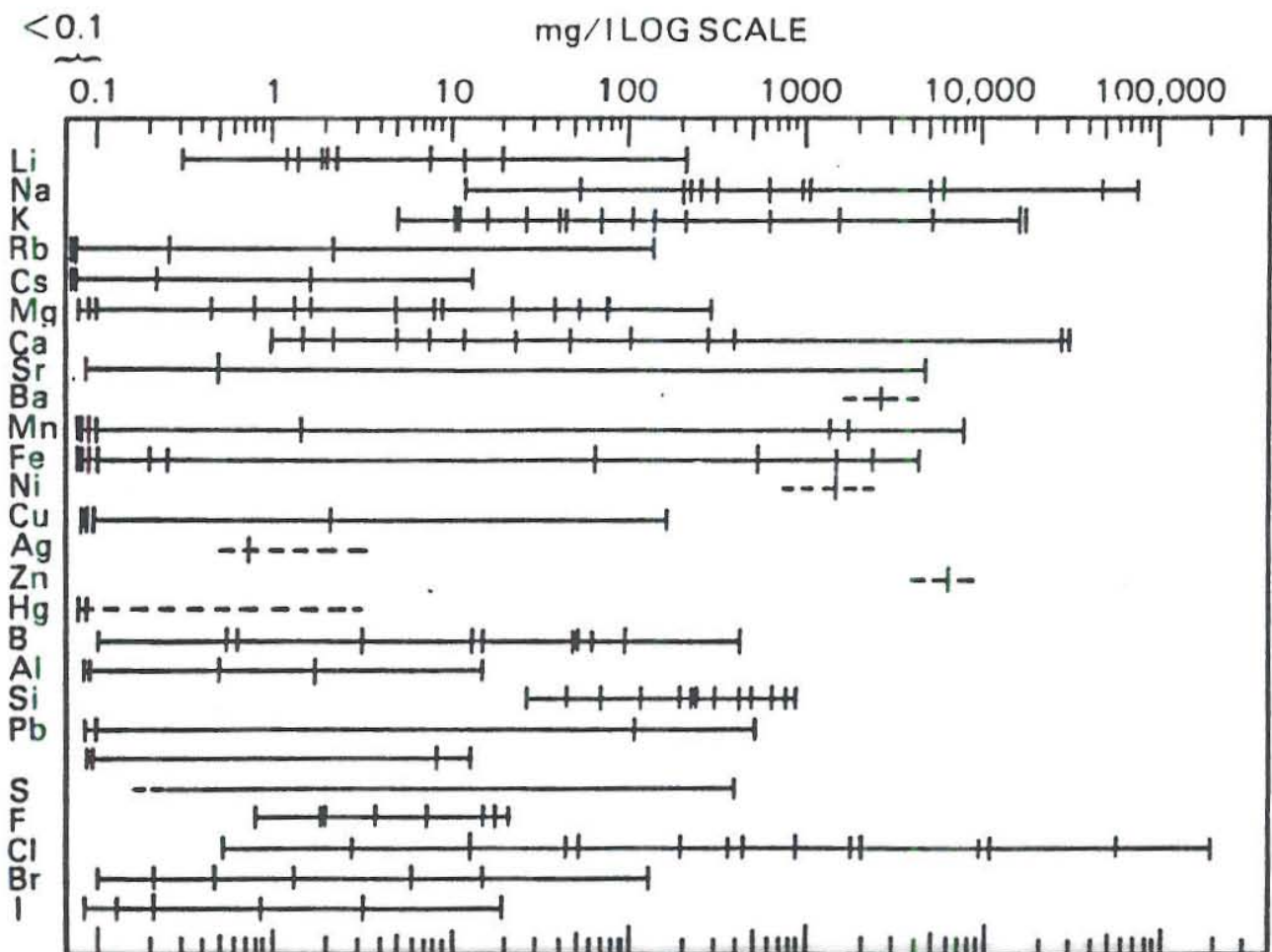


Figure 2.8 Concentration Ranges for Elements in Geothermal Water

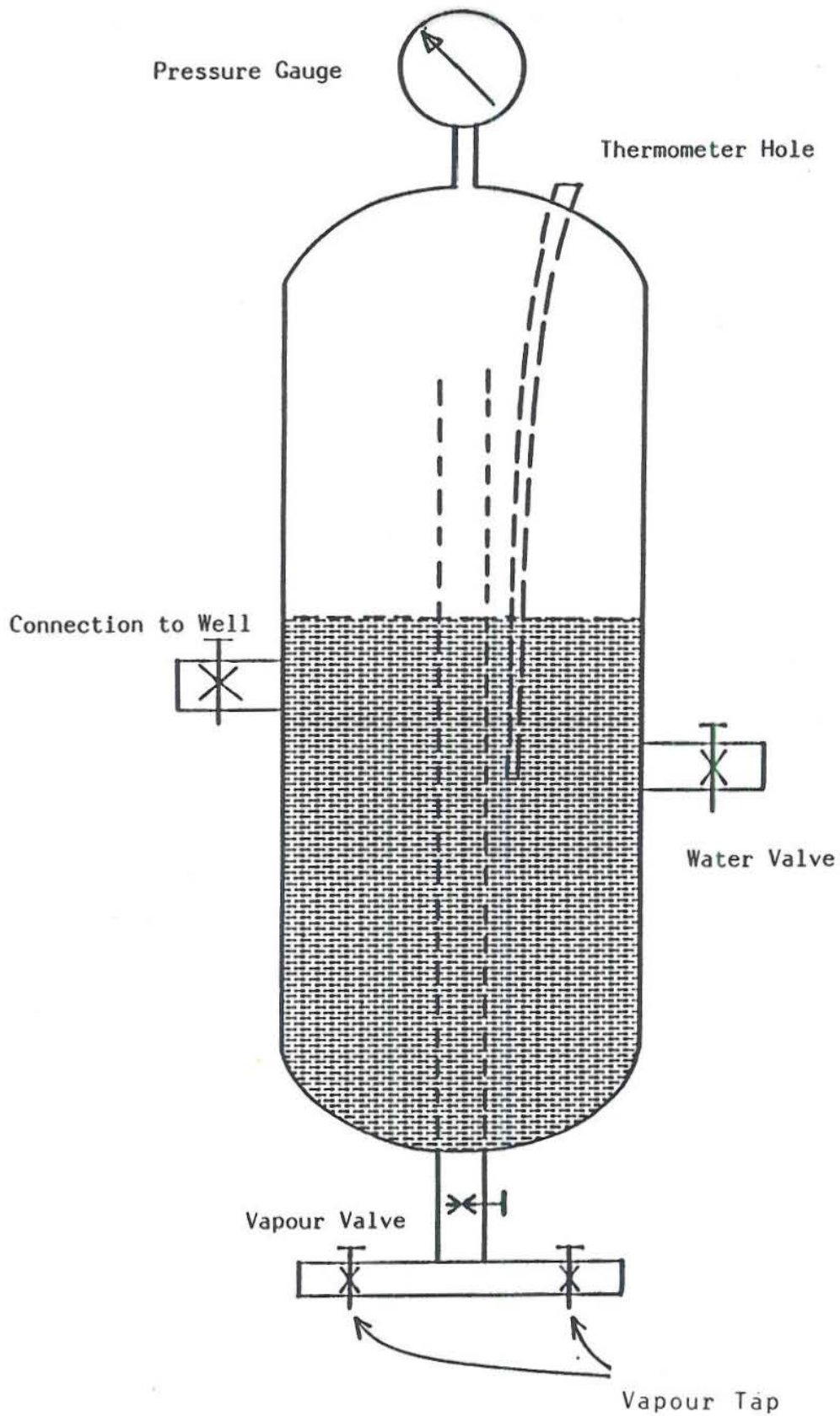


Figure 3.1 Small Separator for Sampling of Geothermal Well

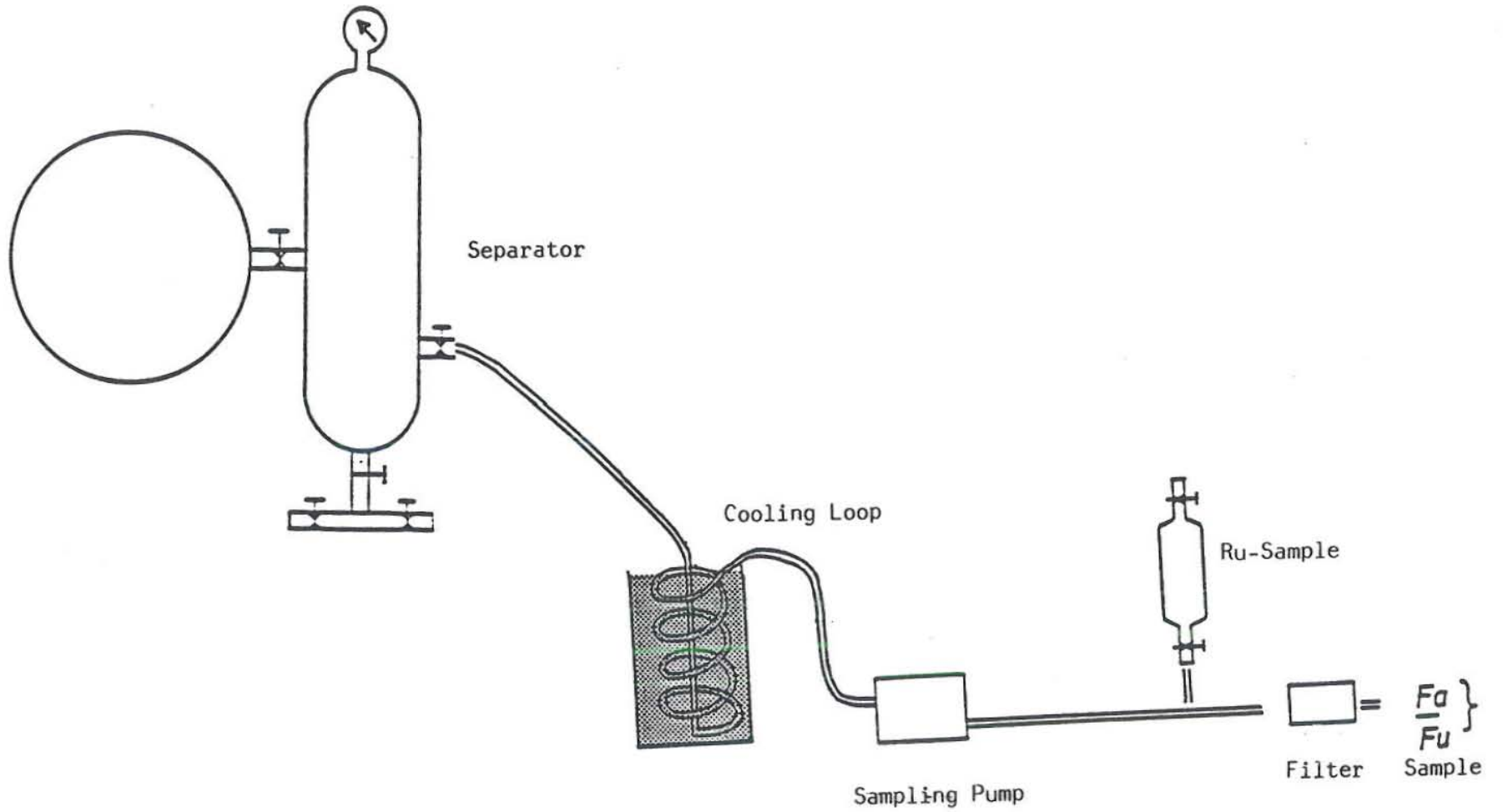


Figure 3.2 Collection of Water Phase

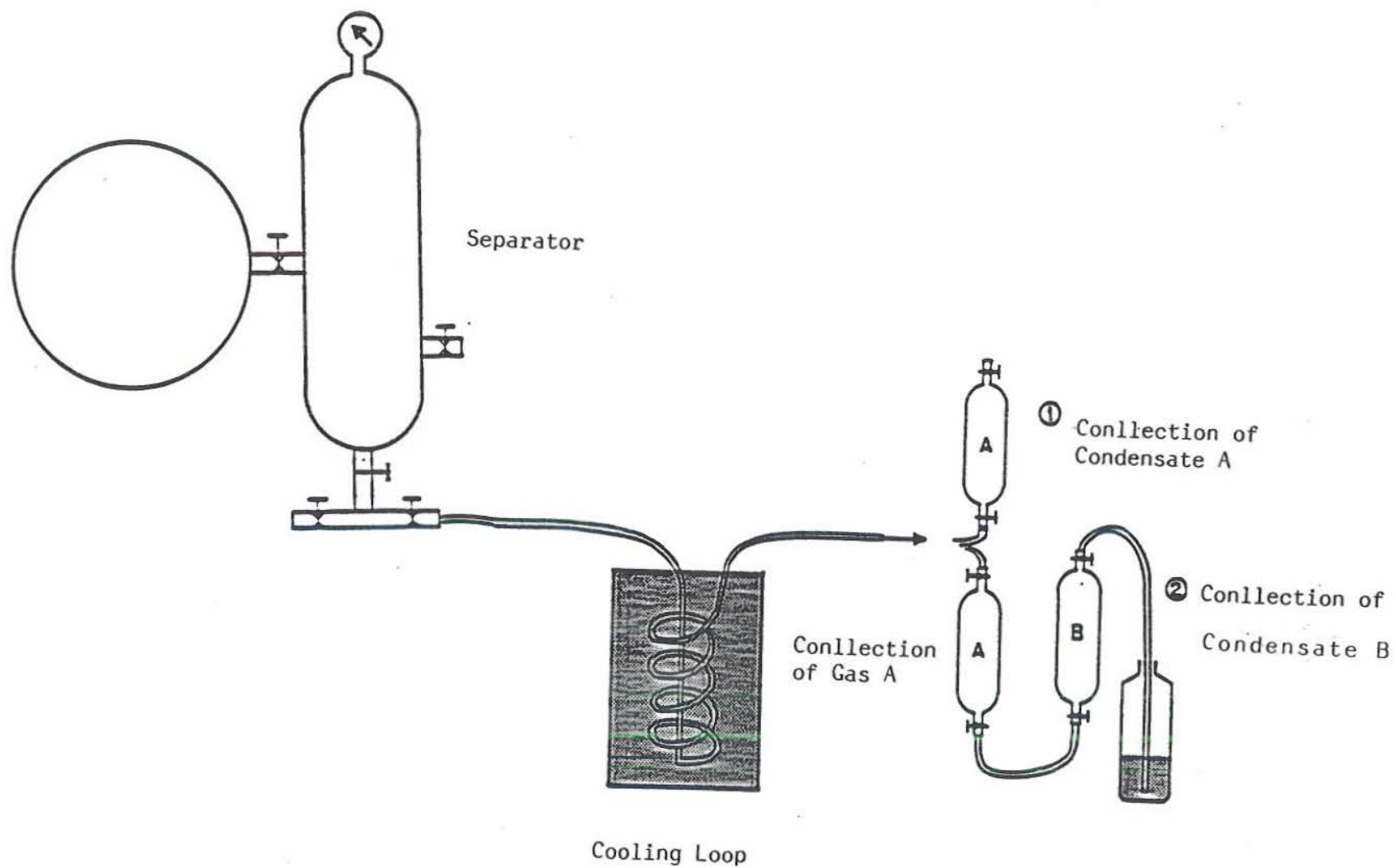


Figure 3.3 Collection of Condensate and Gases



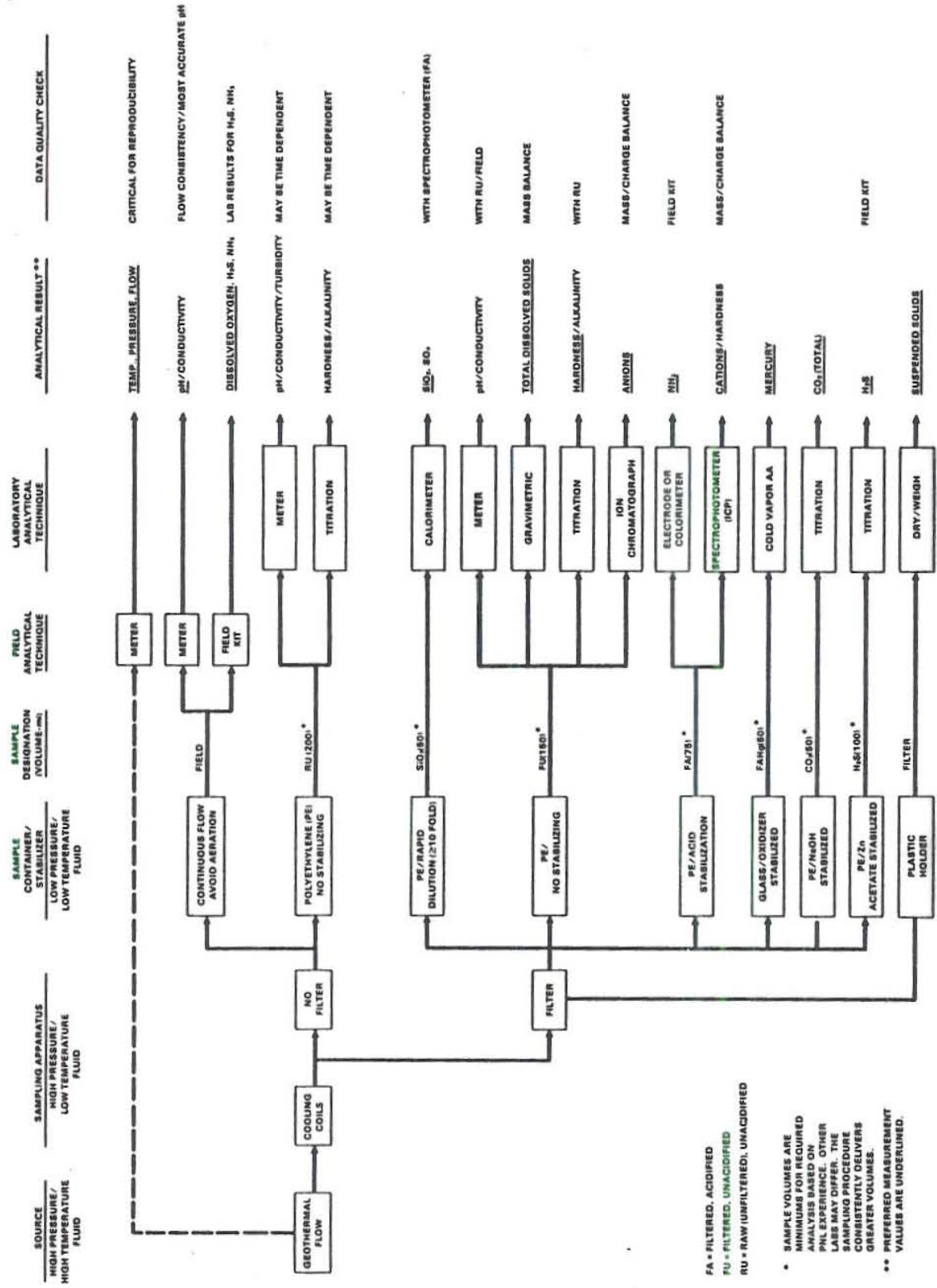


Figure 3.5 Flow Chart for Comprehensive Sampling and Analysis of Geothermal Fluid

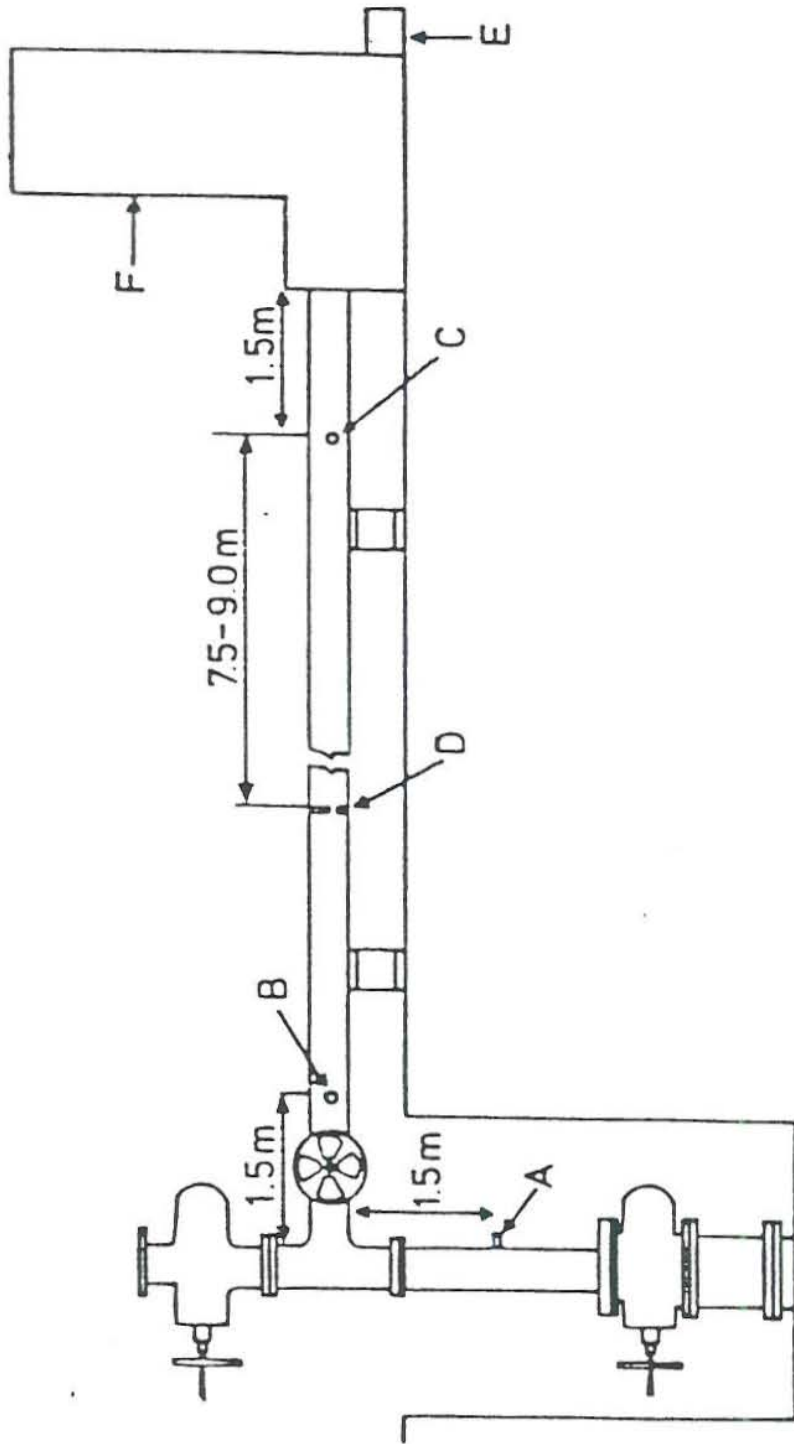


Figure 3.6 Positions of Sampling Points on Surface Piping

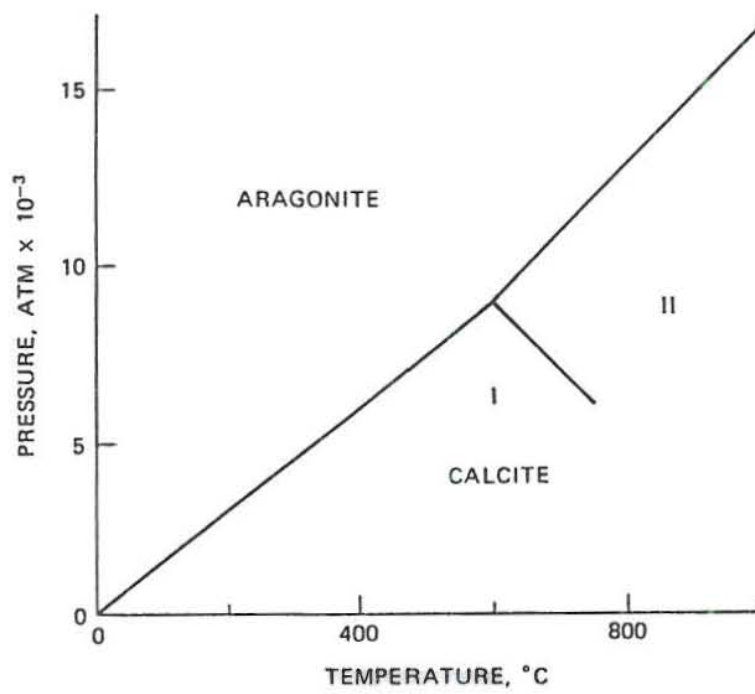


Figure 4.1 Aragonite-Calcite Phase Transition Diagram

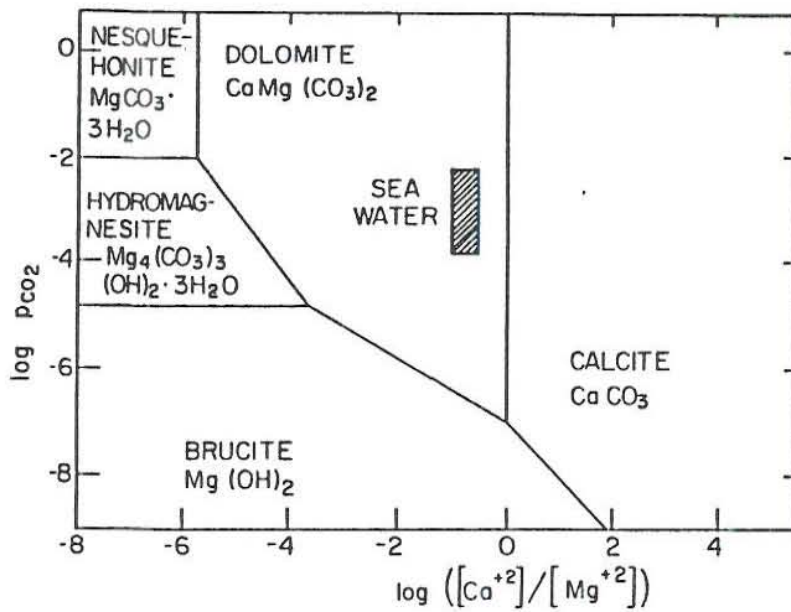
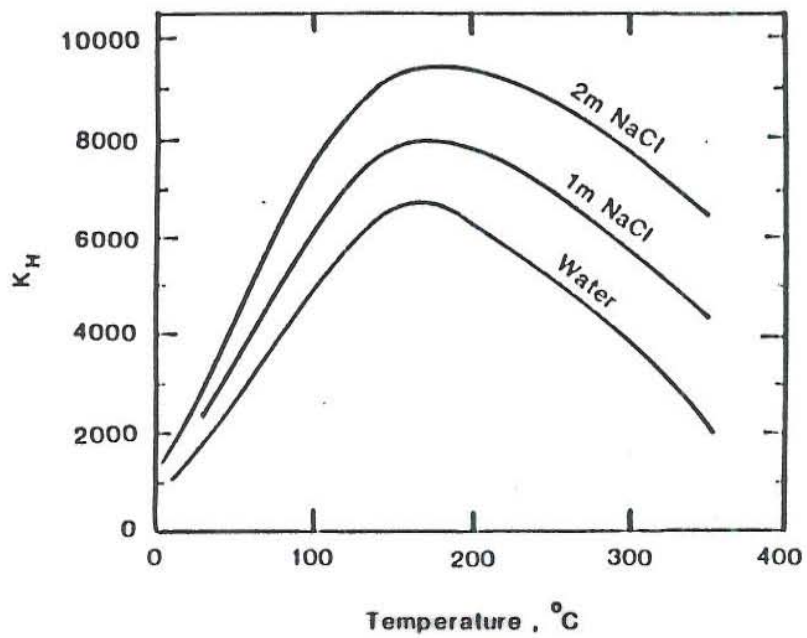
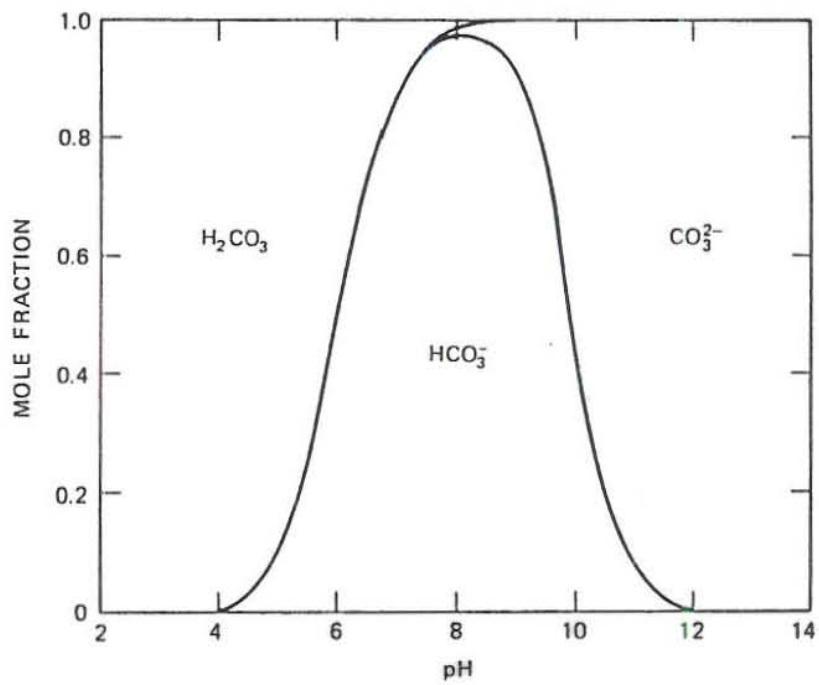


Figure 4.2 Stability Relations in  $\text{Ca}^{2+}$ - $\text{Mg}^{2+}$ - $\text{CO}_2$ - $\text{H}_2\text{O}$  System



**Figure 4.3** Effect of Salt Concentration on Henry's Law Constant



**Figure 4.4 Fraction of Carbonate, Bicarbonate, Carbonic Acid and  $\text{CO}_2$  Present as a Function of pH at 100°C**

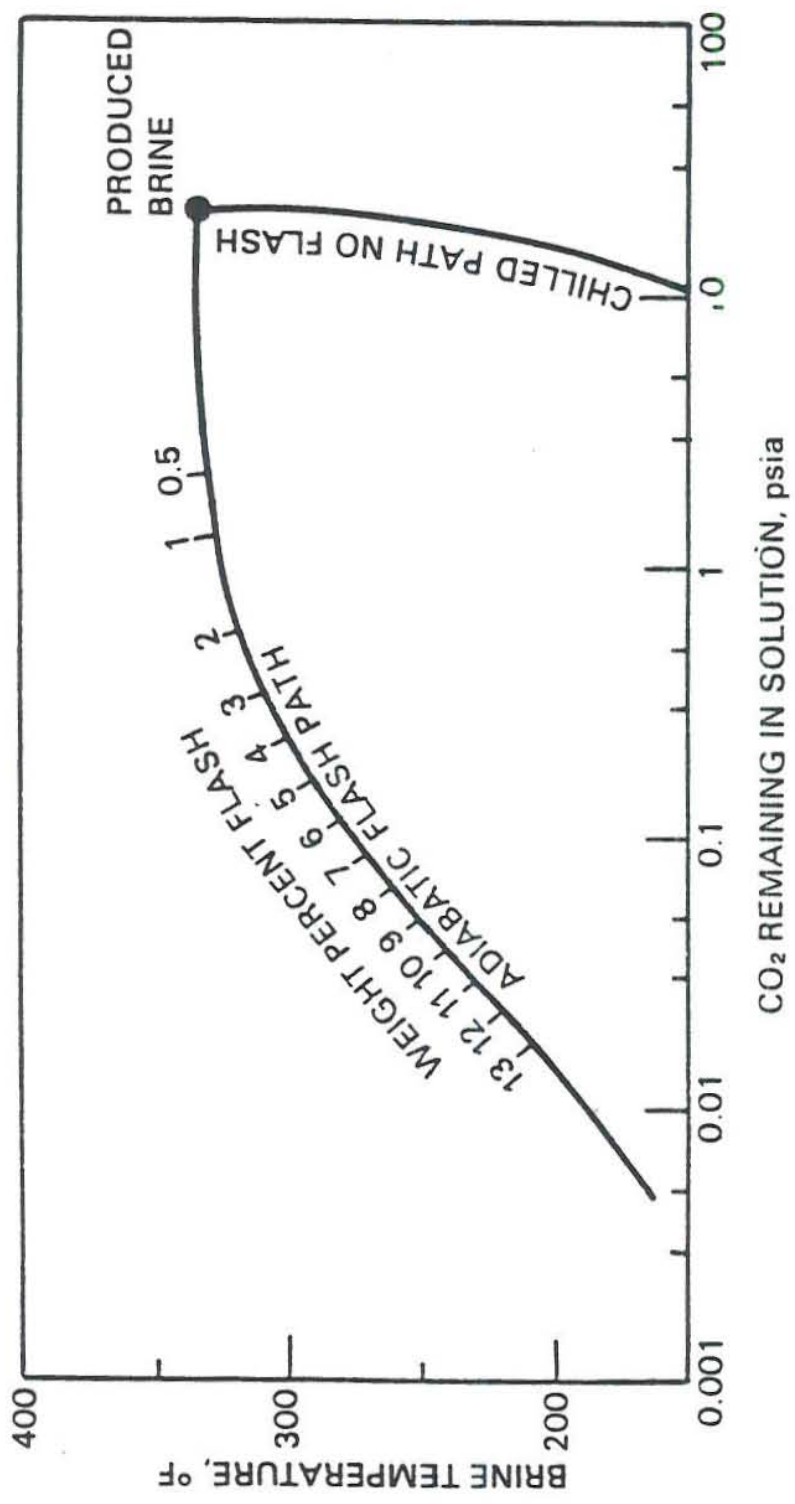
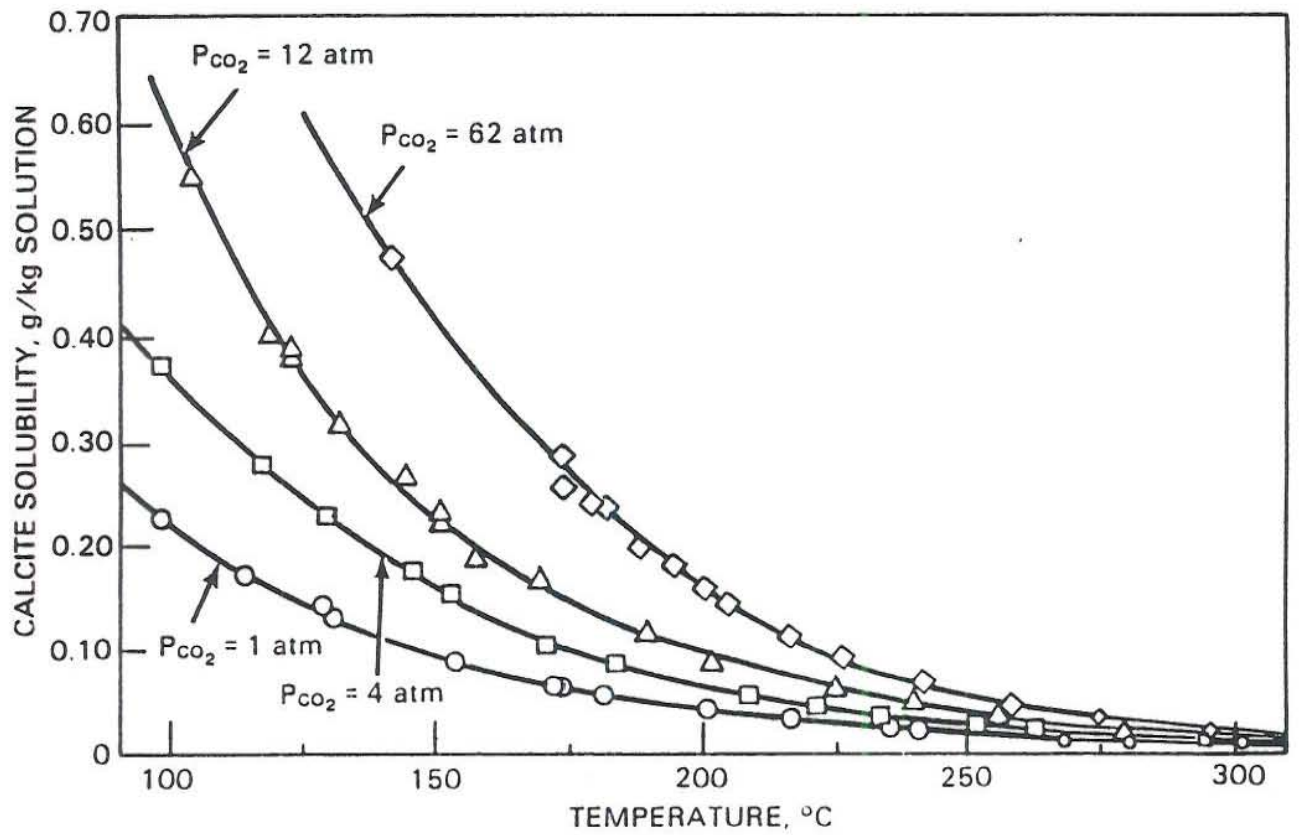
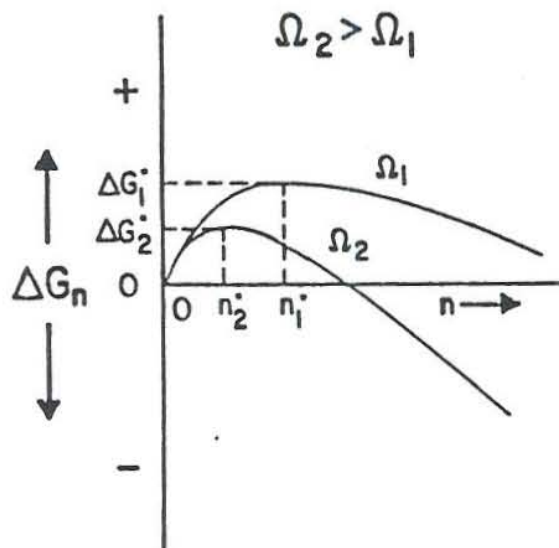


Figure 4.5 Loss of Carbon Dioxide as Flash Progresses



**Figure 4.6 Solubility of Calcite in Water up to 300°C at Various Partial Pressures of Carbon Dioxide**



**Figure 4.7 Plot of Free Energy of Precipitation vs Crystal Size Illustrating Nucleation and Growth**

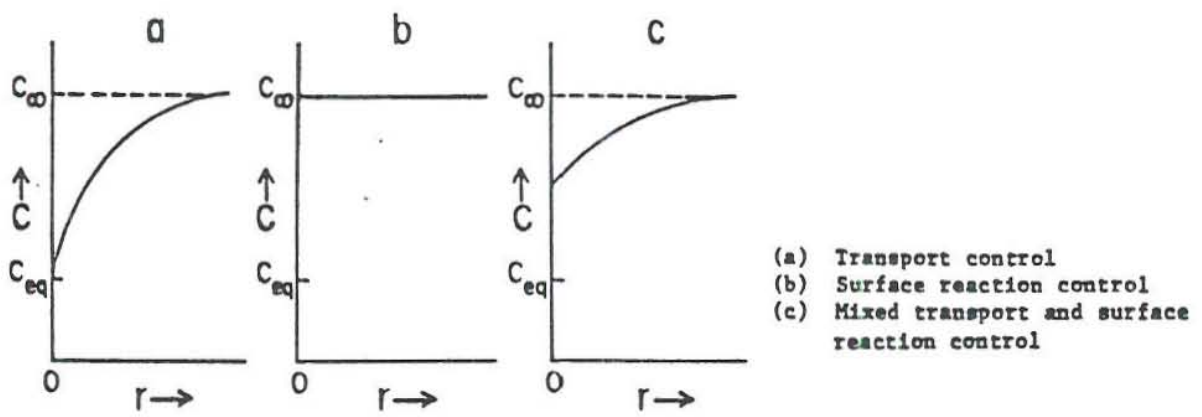


**Figure 4.8 Schematic Representation of Concentration in Solution as a Function of Radial Distance**

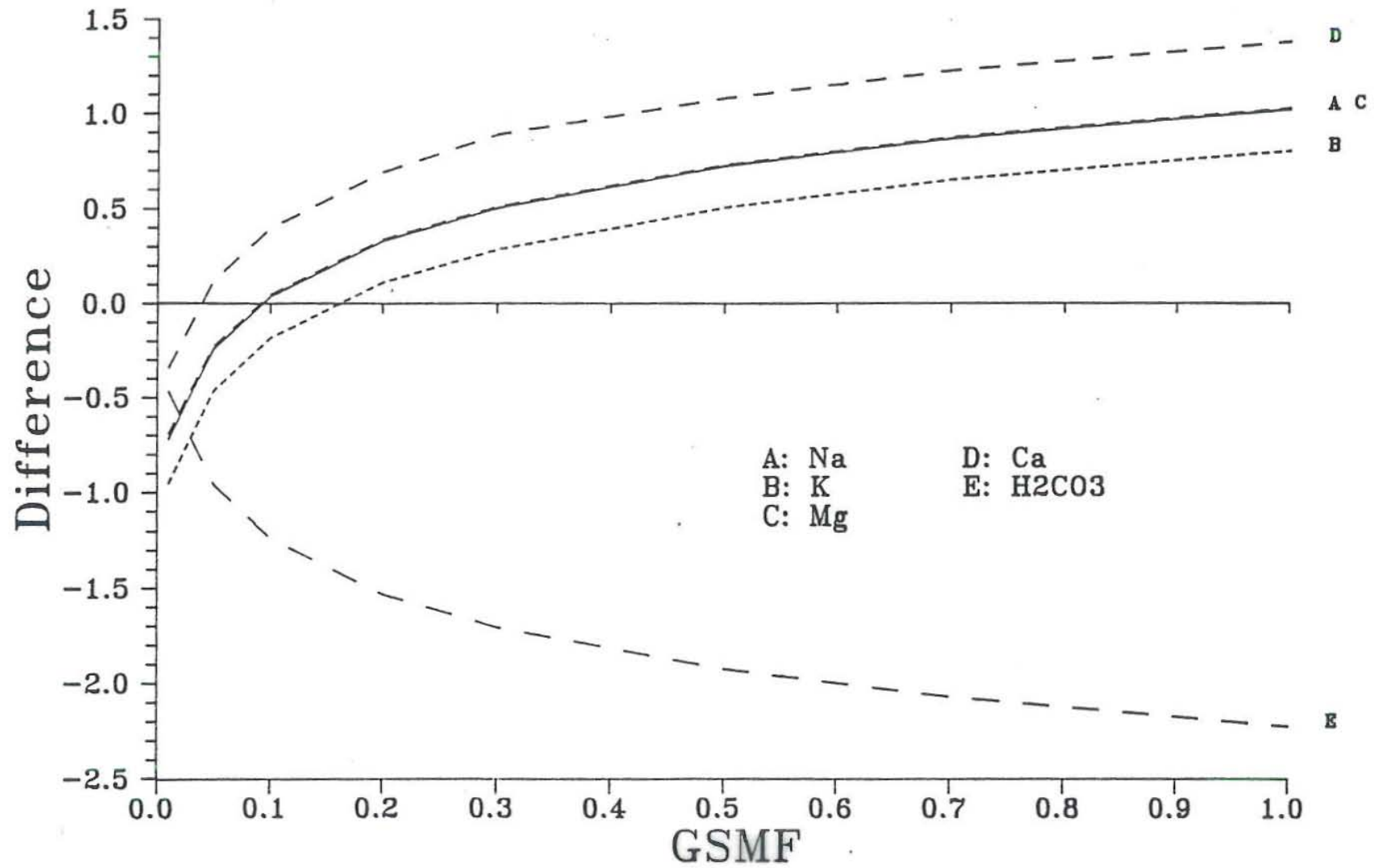


Figure 5.1 Difference Between Function and Output Values  
vs Gas Solubility Mutilplication Factor

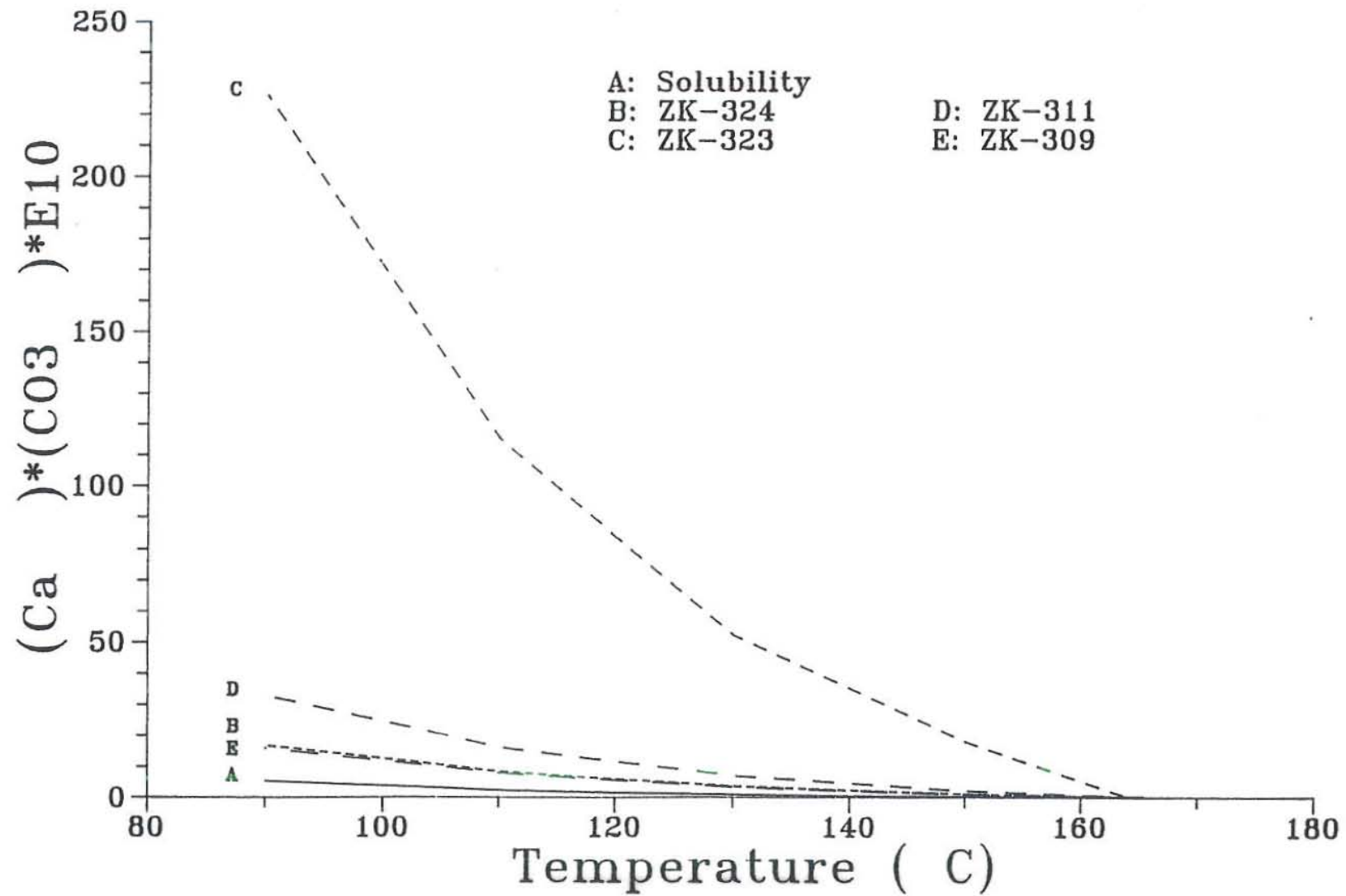


Figure 5.2 Calcite Activity Product for Samples from Yangbajing Geothermal Field

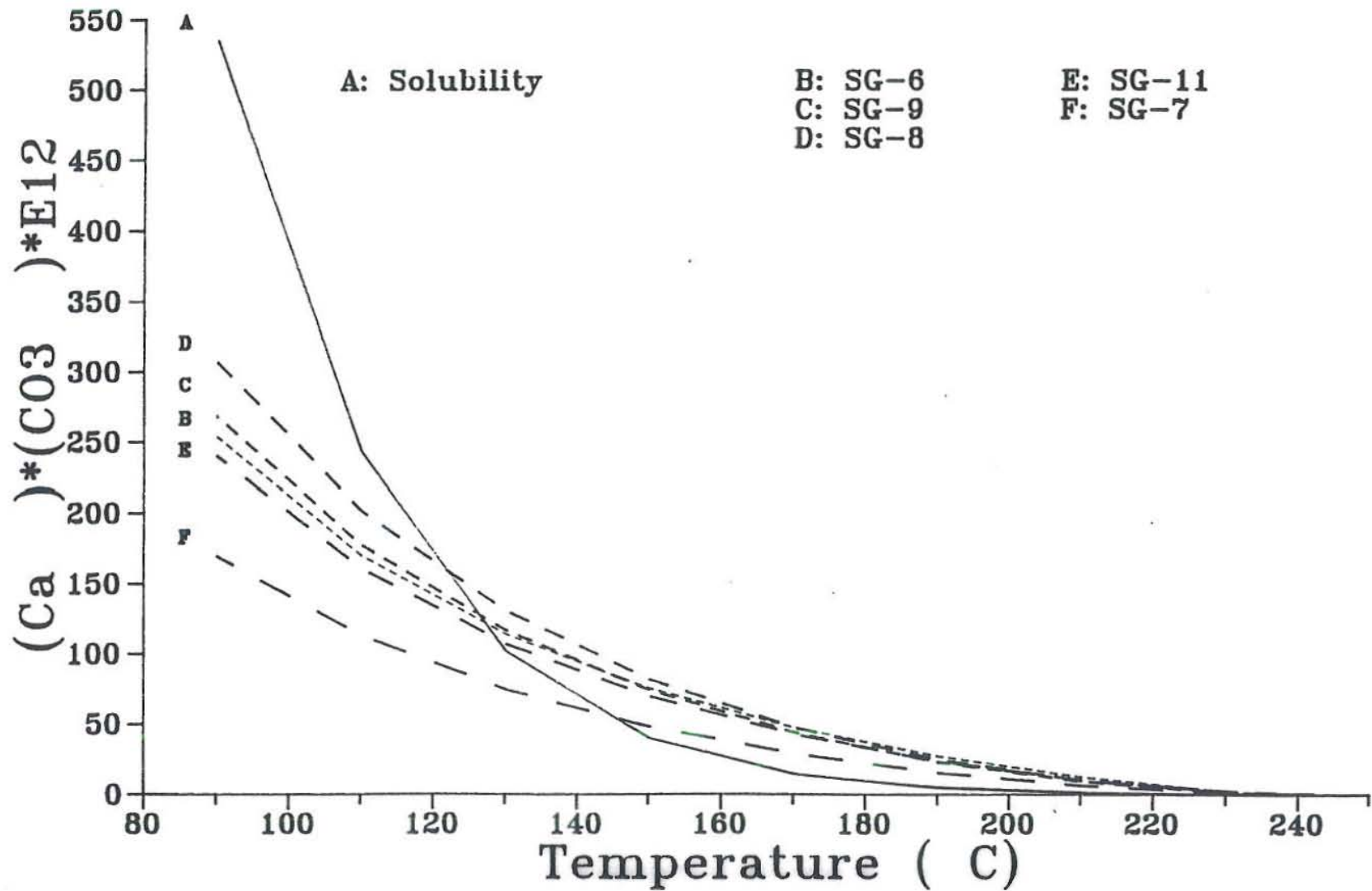


Figure 5.3 Calcite Activity Product for Samples from Svartsengi Geothermal Field

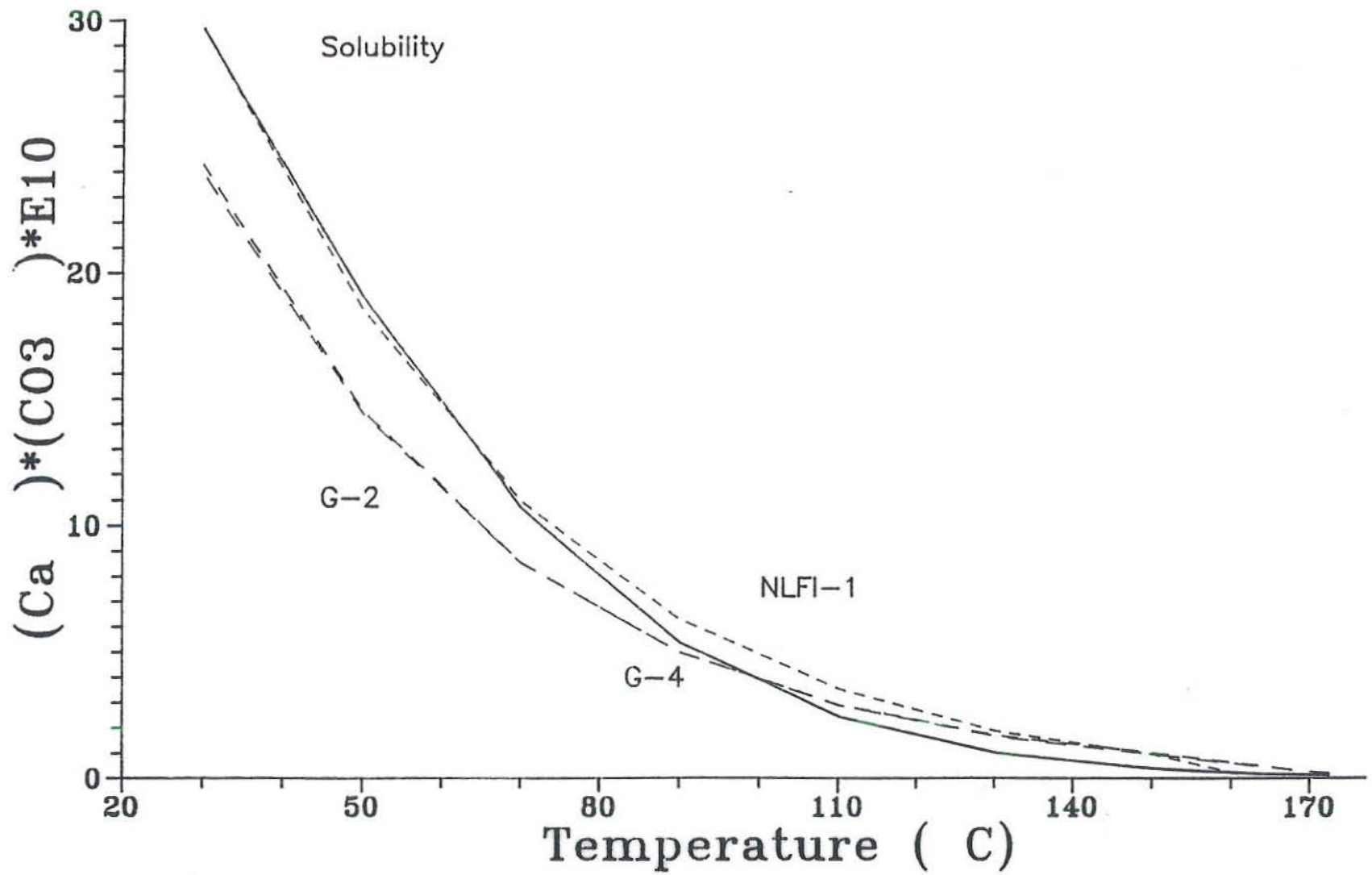


Figure 5.4 Calcite Activity Product for Samples from Hveragerði Geothermal Field

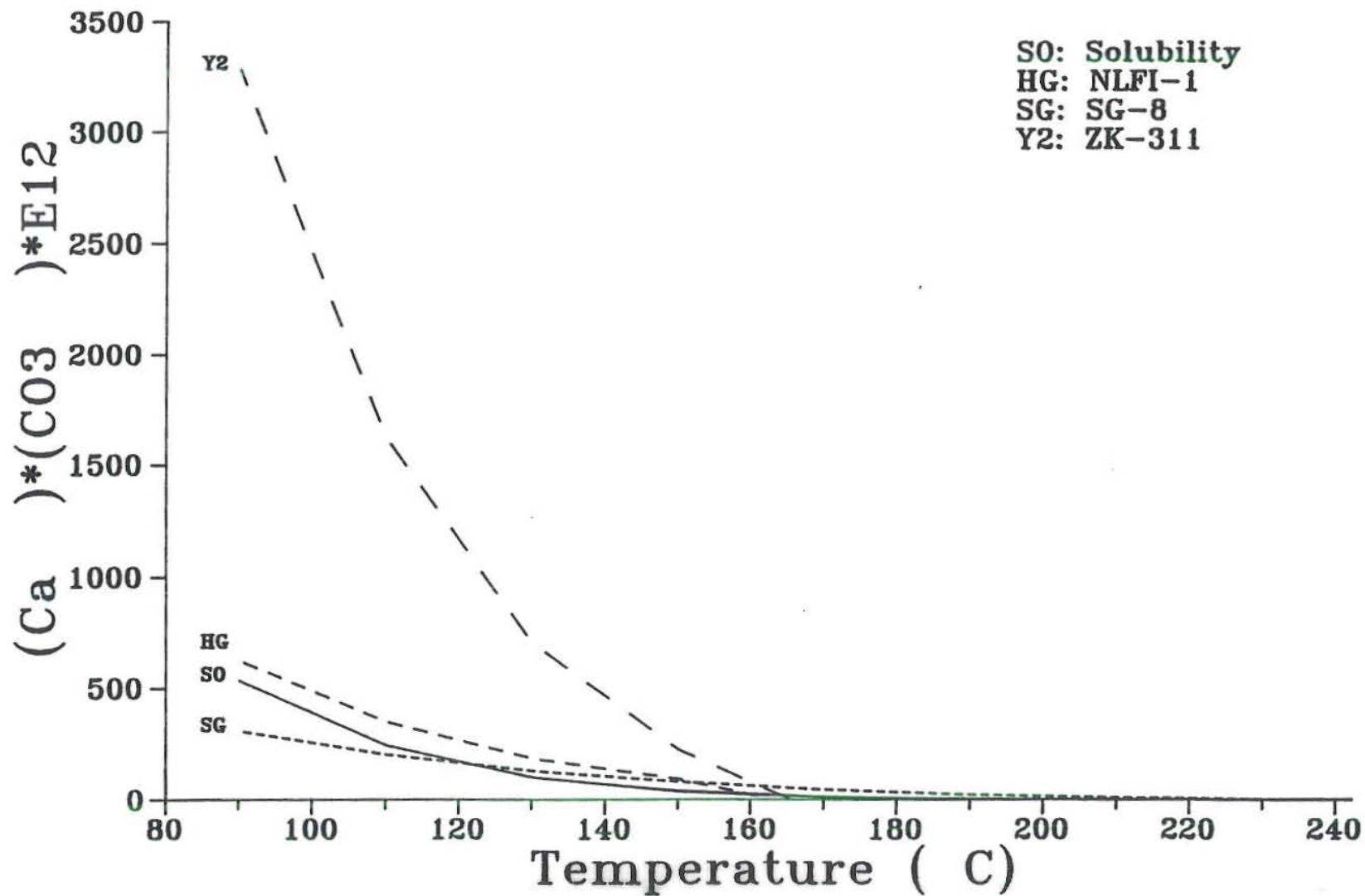


Figure 5.5 Comparison of Calcite Activity Product for  
 Samples from Yangbajing, Svartsengi and Hveragerði Geothermal  
 Fields

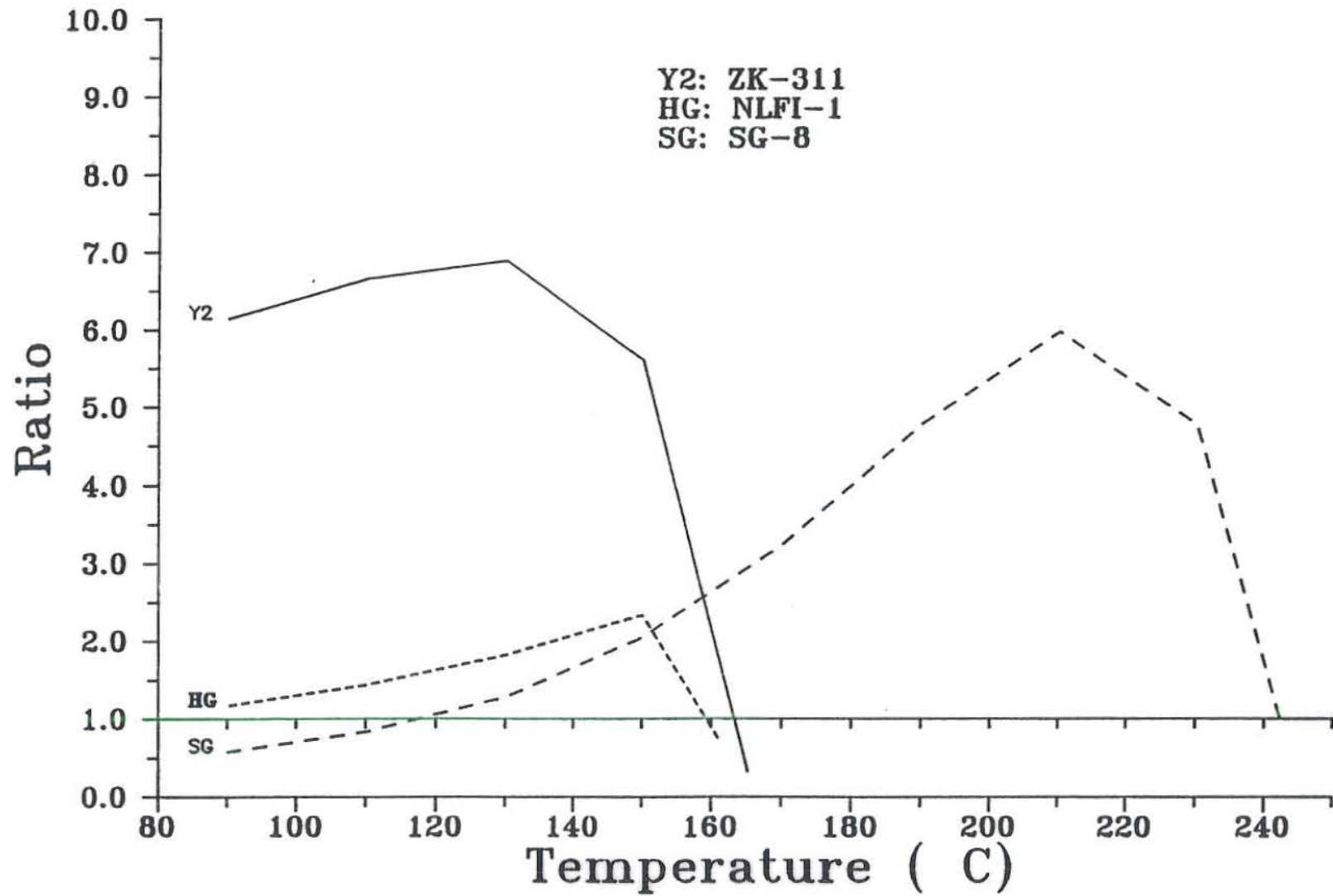


Figure 5.6 Ratio of Calcite Activity and Solubility Products for Samples from Yangbajing, Svartsengi and Hveragerði Geothermal Fields

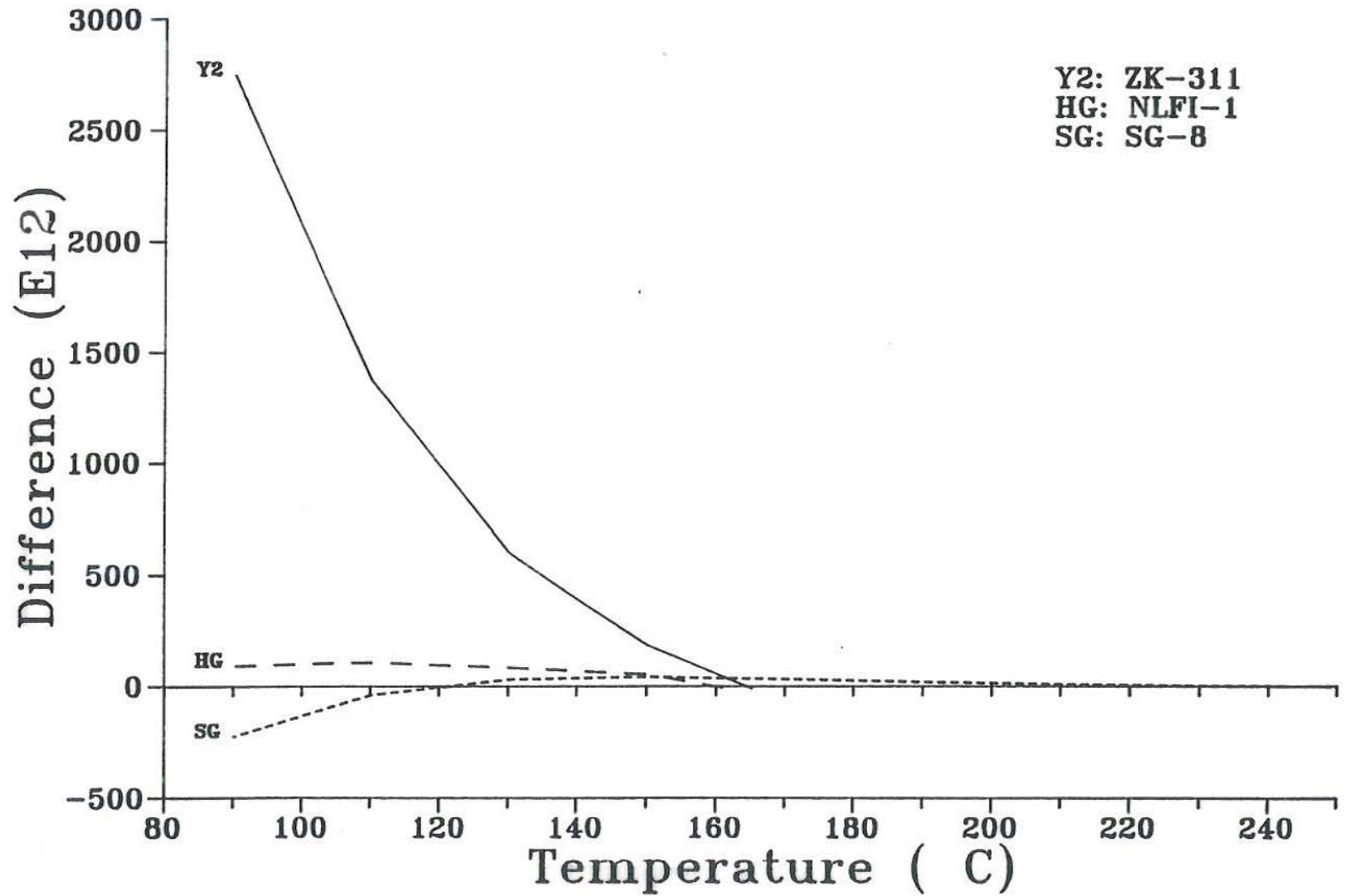


Figure 5.7 Difference of Calcite Solubility and Activity Products for Samples from Yangbajing, Svartsengi and Hveragerði Geothermal Fields

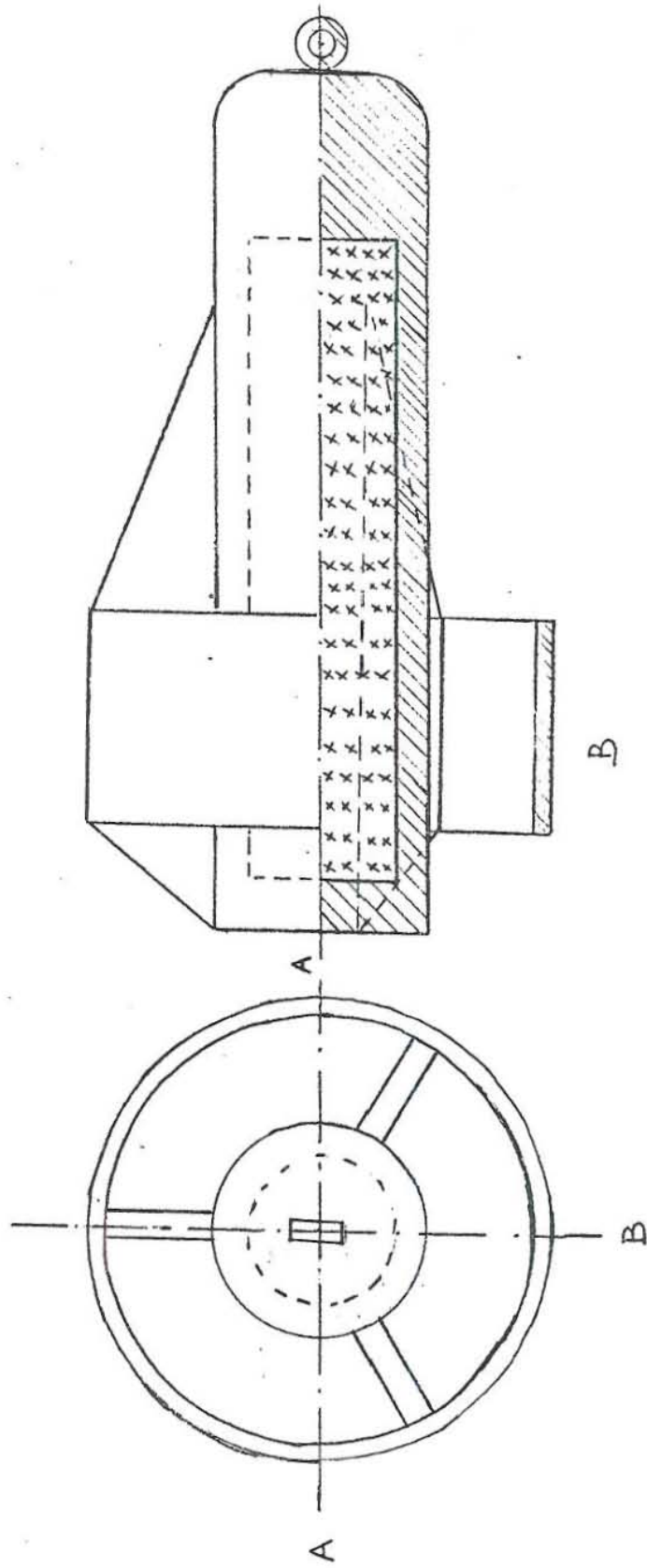


Figure 6.1 Mechanical Cleaning Equipment in Yangbajing

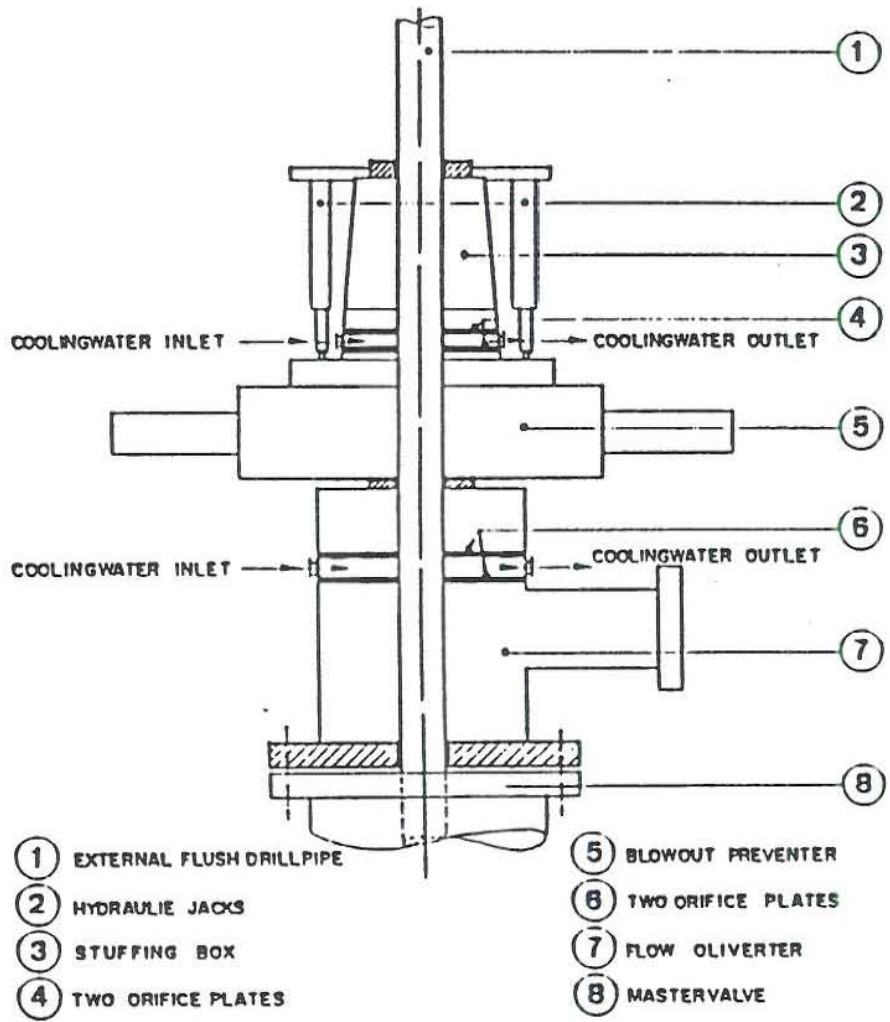


Figure 6.2 Reaming of Scale in Svartsengi

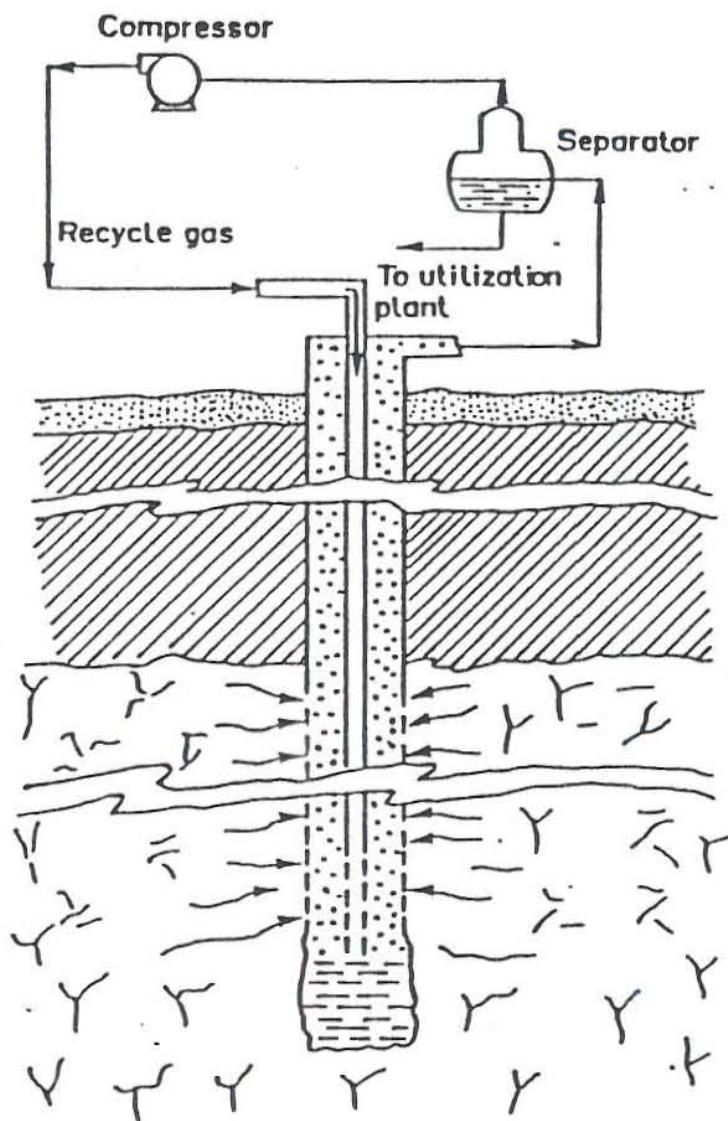
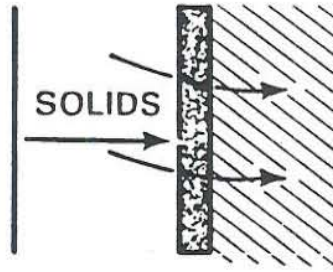
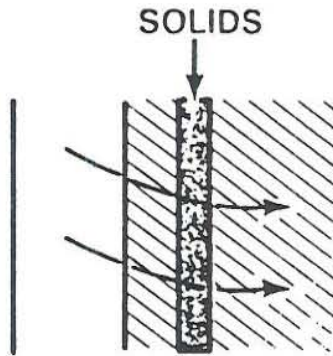


Figure 6.3 Sketch of a Plant for  $\text{PCO}_2$  Control

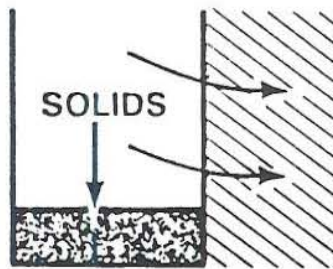
WELLBORE NARROWING  
(FILTER CAKE)



INVASION



WELLBORE FILLING



PERFORATION PLUGGING

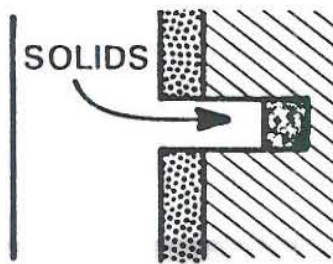


**Figure 7.1** Types of Wellbore Impairment Caused by Suspended Solids

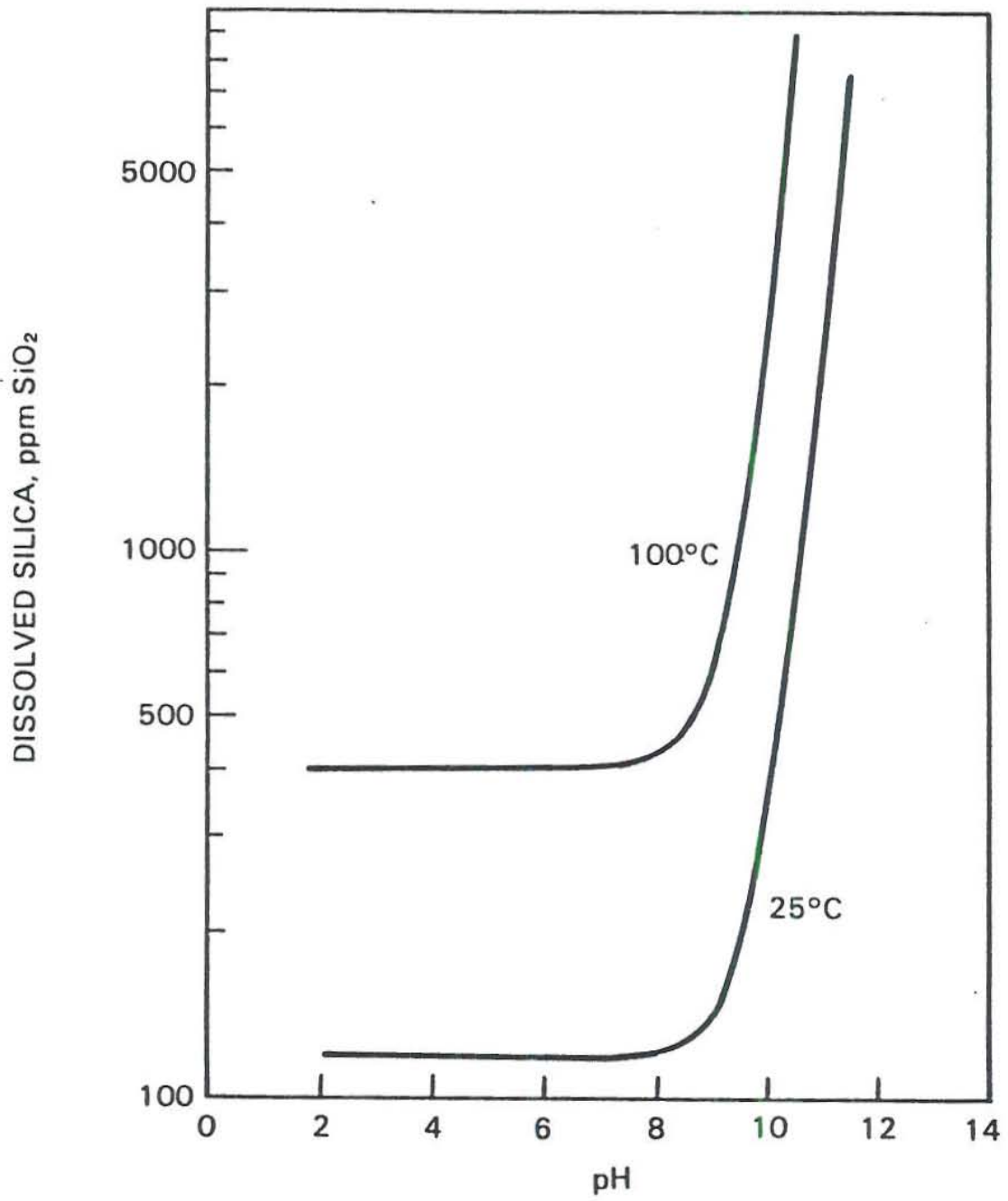


Figure 7.2 Silica Solubility as a Function of pH

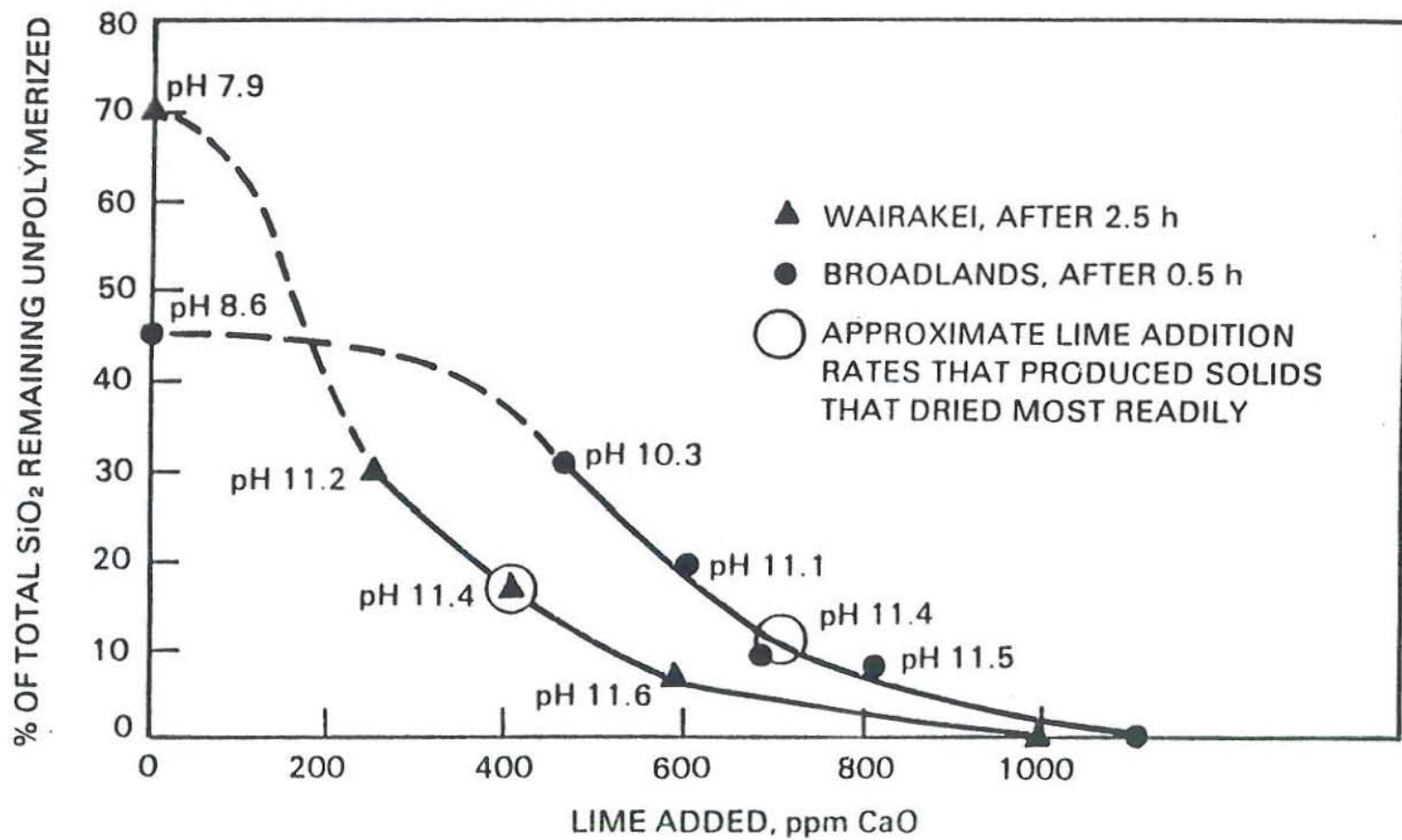
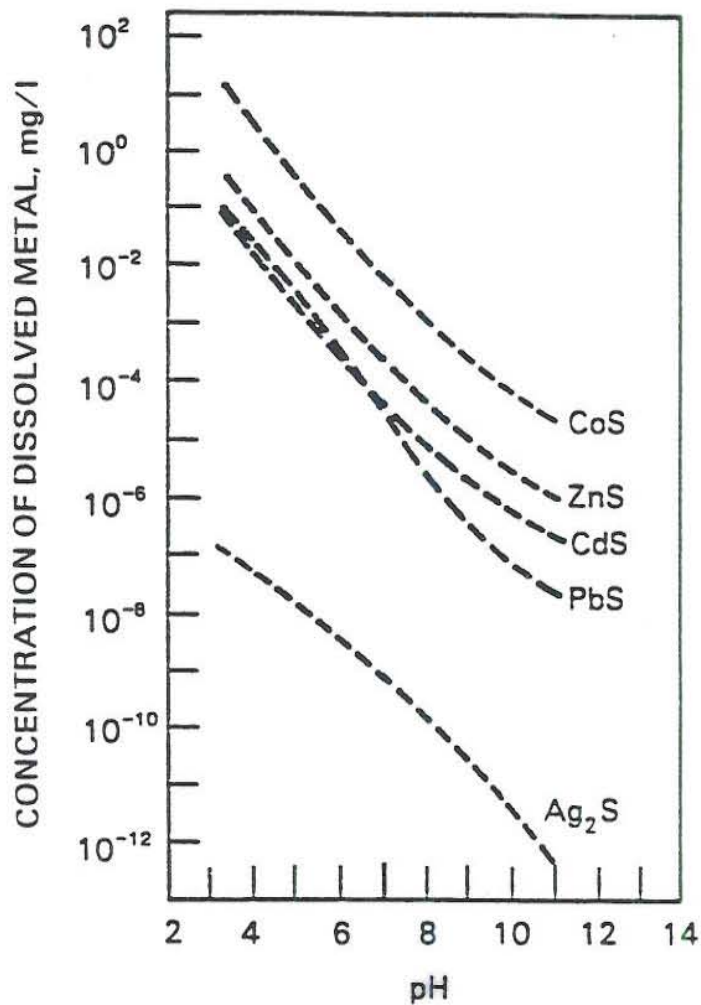
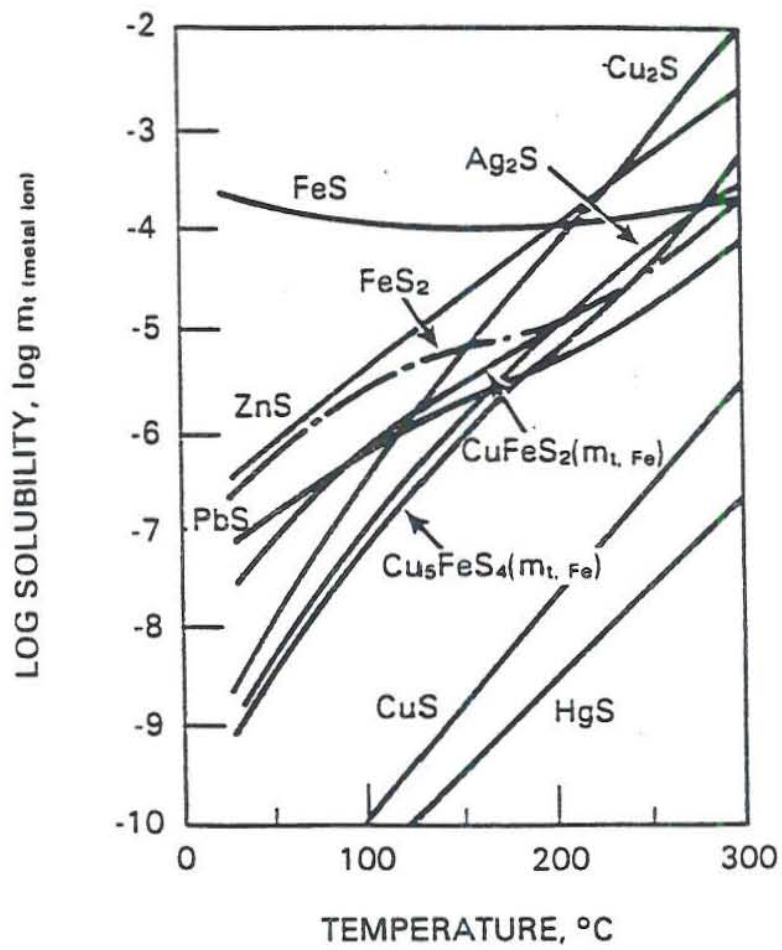


Figure 7.3 Effect of Lime Treatment on Silica



**Figure 7.4 Metal Sulfides Solubility in Water as a Function of pH**



**Figure 7.5 Solubility of Sulfides in Solution as a Function of Temperature**

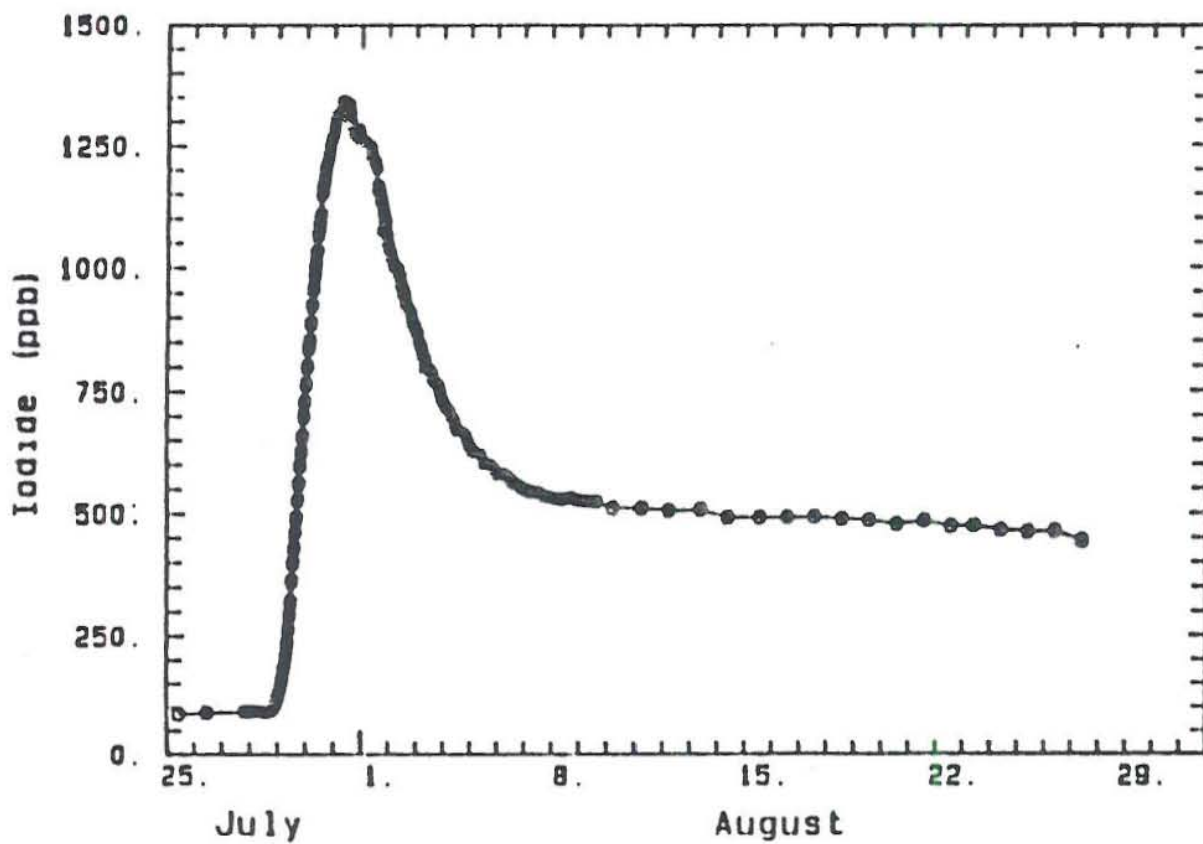


Figure 7.6 Iodide Breakthrough Curve in Well 6, Svartsengi